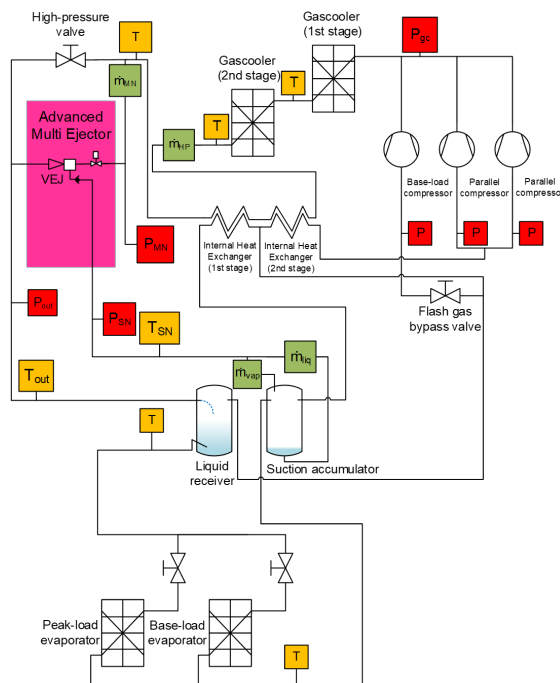


Merethe Leksen Selnes

# Experimental analysis of an advanced R744 multi-ejector

Master's thesis in Energy and Environmental Engineering  
 Supervisor: Armin Hafner  
 August 2020





Merethe Leksen Selnes

# **Experimental analysis of an advanced R744 multi-ejector**

Master's thesis in Energy and Environmental Engineering  
Supervisor: Armin Hafner  
August 2020

Norwegian University of Science and Technology  
Department of Energy and Process Engineering





EPT-M-2020

**MASTER THESIS**for  
student Merethe Leksen Selnes  
Spring 2020**Experimental analysis of an advanced R744 multi-ejector***Analyse av en avansert R744 multiejektor***Background and objective**

The increasing interest in energy efficient solutions and working towards a more sustainable future, give rise to the importance of saving energy. Present supermarket refrigeration systems, with carbon dioxide, have a large potential to limit power consumption. Multi-ejectors are a part of the solution and have already been installed in throughout Europe, but further improvements are necessary.

The next generation of a multi-ejector prototype developed by Danfoss will be investigated in a CO<sub>2</sub> test facility at Varmeteknisk at NTNU Trondheim. Experimental investigations are based on parameters and boundary conditions given by Danfoss. Mass flow rates, pressures and temperatures on the motive, suction (only vapour) and outlet side of the multi-ejector will be measured.

The objective of the master is to analyse the measured data and perform an uncertainty analysis of the results.

**The following tasks are to be considered:**

1. Literature review on R744 ejector technology
2. Perform an HSE evaluation of the laboratory work.
3. Plan and perform test campaign.
4. Data processing and analysis of results.
5. Final report including conclusion and proposal for further work.
6. Make a draft scientific paper based on the main results.

The master thesis comprises 30 ECTS credits.

-- " --

Within 14 days of receiving the written text on the master thesis, the candidate shall submit a research plan for his project your supervisor.

When the thesis is evaluated, emphasis is put on processing of the results, and that they are presented in tabular and/or graphic form in a clear manner, and that they are analysed carefully.

The thesis should be formulated as a research report with summary both in English, conclusion, literature references, table of contents etc. During the preparation of the text, the candidate should make an effort to produce a well-structured and easily readable report. In order to ease the evaluation of the thesis, it is important that the cross-references are correct. In the making of the report, strong emphasis should be placed on both a thorough discussion of the results and an orderly presentation.

The candidate is requested to initiate and keep close contact with his/her academic supervisor(s) throughout the working period. The candidate must follow the rules and regulations of NTNU as well as passive directions given by the Department of Energy and Process Engineering.

Risk assessment of the candidate's work shall be carried out, in cooperation with your supervisor, according to the department's procedures. The risk assessment must be documented and included as part of the final report. Events related to the candidate's work adversely affecting the health, safety or security, must be documented and included as part of the final report. If the documentation on risk assessment represents a large number of pages, the full version is to be submitted electronically to the supervisor and an excerpt is included in the report.

Pursuant to "Regulations concerning the supplementary provisions to the technology study program/Master of Science" at NTNU §20, the Department reserves the permission to utilize all the results and data for teaching and research purposes as well as in future publications.

The final report is to be submitted digitally in INSPERA. An executive summary of the thesis including title, student's name, supervisor's name, year, department name, and NTNU's logo and name, shall be submitted to the department as a separate pdf file. Based on an agreement with the supervisor, the final report and other material and documents may be given to the supervisor in digital format.

Submission deadline: 28. August 2020

- Work to be done in lab (Water power lab, Fluids engineering lab, Thermal engineering lab)  
 Field work

Department for Energy and Process Engineering, 15<sup>th</sup> of February 2020



---

Prof. Dr. ing Armin Hafner  
Academic Supervisor

Co-Supervisor: Associate Prof. Krzysztof Banasiak (NTNU and SINTEF)

---

# Preface

This thesis represents the final work of my Master's degree, carried out spring 2020, and concludes my degree in Energy and Environmental Engineering at the Norwegian University of Science and Technology (NTNU), Department of Energy and Process Engineering.

This thesis evaluates the performance and uncertainty of a multi-ejector prototype from the Danish company Danfoss. Additionally, a comparison with other multi-ejector blocks from Danfoss serves the purpose of analysing the associated performance of the multi-ejector block prototype.

A project work, serving as a feasibility study for this Master Thesis carried out during autumn 2019, granted me with important knowledge of the present multi-ejector technologies and hence been a supportive toolbox through this final work.

I will like to thank my main supervisor, Professor Dr.ing. Armin Hafner at NTNU, for offering good discussions and great knowledge of ejectors in R744 systems. My co-supervisor Krzysztof Banasiak at SINTEF has been an essential asset in the test facility. I will also like to express my gratitude for their availability during this semester.

Trondheim, 28.08.2020

Merethe Leksen Selnes

Merethe Leksen Selnes, MSc. student

---



---

# Abstract

The increasing interest in energy efficient solutions and working towards a more sustainable future, give rise to the importance of saving energy. Present supermarket refrigeration systems with carbon dioxide have a large potential to limit power consumption. The multi-ejector has been developed as a part of the solution, but further improvements are necessary. The aim of this Master's Thesis is to carry out a campaign of experimental tests at performance mapping of a new advanced multi-ejector.

A prototype of an advanced multi-ejector designed by the Danish company Danfoss was experimentally investigated at a R744 parallel-compression system. The test facility at NTNU Trondheim was utilized to evaluate the performance of the multi-ejector. Based on the patent situation of the prototype, the dimensions and number of ejector cartridges are confidential and are therefore not revealed in this Master's Thesis.

The ejector performance was investigated for inlet motive nozzle pressures from 59.3 bar to 90.3 bar with a motive temperature between 18.4°C and 35.2°C. The suction side pressures were between 25.2 bar to 28.3 bar, while the ejector outlet/receiver pressures ranged from 27.8 bar to 35.5 bar. This resulted in a pressure lift between 2 bar and 8 bar. The overall ejector efficiencies recorded were between 5% and 23%. The entrainment ratios varied between 0.06 and 0.53.

In addition, an uncertainty analysis was performed for the test results of the advanced multi-ejector. It was determined that the pressure transmitters in the test facility have a relative high uncertainty compared with the mass flow meters. This indicates that new pressure transmitters in the test facility must be installed.

Moreover, a comparison analysis was performed between the advanced multi-ejector and commercial multi-ejectors from Danfoss. The experimental results were implemented into the selection tool Coolselector. Here, transcritical low pressure and high pressure multi-ejectors from Danfoss were recommended under the same operational conditions as the advanced multi-ejector. Three cases were investigated based on the difference in suction mass flow rate, receiver pressure (ejector outlet pressure) and motive nozzle mass flow rate.

Additionally, for the three cases, the corresponding entrainment ratios, ejector efficiencies and pressure lifts were compared. The conducted simulations confirmed that the advanced multi-ejector has low efficiencies for higher motive nozzle pressures around 90 bar. The simulations also indicated that the multi-ejector is more similar to a low pressure multi-ejector than a high pressure multi-ejector.

---

---

# Sammendrag

Den økende interessen for energieffektive løsninger, samt å arbeide mot en mer bærekraftig framtid, viser til viktigheten av å spare energi. Dagens butikkjøleanlegg med karbondioksid har et stort potensial for å redusere primærenergiforbruket. Multiejektoren har blitt utviklet som en del av løsningen, men videre forbedringer er nødvendig. Formålet med masteroppgaven er å gjennomføre en rekke eksperimentelle tester ved å kartlegge den avanserte multiejektoren.

En prototype av en avansert multiejektor utviklet av Danfoss ble eksperimentelt undersøkt i et R744 parallellkompresjonssystem. Testanlegget hos NTNU Trondheim ble brukt for å evaluere ytelsen til multiejektoren. Grunnet prototypens patentsituasjon, avsløres ikke dimensjoner og antall ejektorpatroner i denne masteroppgaven.

Ejektorens ytelse ble undersøkt for ejektorinnløpet på høytrykksiden fra 59,3 bar til 90,3 bar med en temperatur mellom 18,4°C og 35,2°C. Trykkene på sugesiden var mellom 25,2 og 28,3 bar, mens ejektorutløpstrykkene økte fra 27,8 bar til 35,5 bar underveis i målingene. Dette resulterte i et trykkløft fra 2 bar til 8 bar. Ejektorvirkningsgraden varierte mellom 5% og 23%. Massestrømsforholdet varierte fra 0,06 til 0,53.

En usikkerhetsanalyse ble gjennomført for resultatene fra den avanserte multiejektoren. Det ble fastsatt at trykksensorene i testanlegget hadde en relativt høy usikkerhet sammenlignet med massestrømsmålerne. Dette viser at nye trykksensorer i testanlegget må installeres.

Videre ble det utført en sammenligningsanalyse mellom den avanserte multiejektoren og kommersielle multiejektorer fra Danfoss. De eksperimentelle resultatene ble lagt inn i beregningsverktøyet Coolselector. Her ble transkritiske lavtrykk og høytrykkmultiejektorer fra Danfoss anbefalt med de samme driftsbetingelser som den avanserte multiejektoren. Tre tilfeller ble undersøkt basert på forskjellen i massestrøm på sugesiden, beholdertrykket (utløpstrykket i ejektor) og massestrøm på høytrykksiden.

I tillegg, for de tre tilfellene ble de tilhørende massestrømforholdene, ejektoreffektivitetene og trykkløftene sammenlignet. De gjennomførte simuleringene bekreftet at den avanserte multiejektoren har lav virkningsgrad for høyere trykk rundt 90 bar. Simuleringene antydte også at multiejektoren ligner mer på en lavtrykkmultiejektor enn en høytrykkmultiejektor.

---

# Table of Contents

<b>Thesis assignment</b>	<b>i</b>
<b>Preface</b>	<b>iii</b>
<b>Abstract</b>	<b>v</b>
<b>Sammendrag</b>	<b>vii</b>
<b>Table of Contents</b>	<b>x</b>
<b>List of Tables</b>	<b>xi</b>
<b>List of Figures</b>	<b>xv</b>
<b>Nomenclature</b>	<b>xvi</b>
<b>1 Introduction</b>	<b>1</b>
<b>2 Literature review</b>	<b>3</b>
2.1 CO <sub>2</sub> . . . . .	3
2.2 Ejector . . . . .	5
2.2.1 Function behind an ejector . . . . .	5
2.2.2 Simple two-phase ejector process . . . . .	9
2.2.3 Various ejector designs . . . . .	11
2.3 Multi-ejector . . . . .	14
2.4 Supermarket refrigeration systems . . . . .	18
2.4.1 Development of R744 booster systems in supermarkets . . . . .	18
2.4.2 R744 Transcritical supermarkets locations . . . . .	23
<b>3 Methodology</b>	<b>25</b>
3.1 Ejector performance parameters . . . . .	25
3.2 Test facility . . . . .	28

---

3.2.1	Component description and MiniLog . . . . .	32
3.2.2	Test conditions . . . . .	34
3.3	Uncertainty analysis . . . . .	35
3.3.1	Type A and Type B evaluation of standard uncertainty . . . . .	35
3.3.2	Uncertainty of the ejector efficiency . . . . .	38
3.3.3	Uncertainty of the superheat . . . . .	40
3.4	Coolselector <sup>®</sup> 2 calculation and selection software from Danfoss . . . . .	42
3.4.1	LP multi-ejector . . . . .	43
3.4.2	HP multi-ejector . . . . .	47
3.4.3	Ejector efficiency calculation from Coolselector . . . . .	49
<b>4</b>	<b>Results</b>	<b>51</b>
4.1	Laboratory tests with the advanced multi-ejector . . . . .	51
4.2	Comparing laboratory tests with Coolselector <sup>®</sup> 2 . . . . .	64
4.2.1	Advanced multi-ejector compared to LP multi-ejector from Coolselector . . . . .	66
4.2.2	Advanced multi-ejector compared to LP multi-ejector – efficiency, entrainment ratio and pressure lift . . . . .	70
4.2.3	Advanced multi-ejector compared to HP multi-ejector from Coolselector . . . . .	74
4.2.4	Advanced multi-ejector compared to HP multi-ejector – entrainment ratio, ejector efficiency and pressure lift . . . . .	78
<b>5</b>	<b>Discussion</b>	<b>83</b>
5.1	Laboratory measurements . . . . .	83
5.2	Uncertainty analysis . . . . .	84
5.2.1	Change of temperature and pressure uncertainties . . . . .	84
5.2.2	Change of differential pressure uncertainties . . . . .	87
5.3	Coolselector . . . . .	88
5.3.1	Refrigeration conditions outside the ejectors envelope in Coolse- lector . . . . .	88
5.3.2	Is the advanced multi-ejector prototype a LP or a HP multi-ejector?	90
<b>6</b>	<b>Conclusion</b>	<b>91</b>
<b>7</b>	<b>Suggestions for further work</b>	<b>93</b>
	<b>Bibliography</b>	<b>95</b>
	<b>Appendix</b>	<b>101</b>
	Appendix A Draft for scientific paper . . . . .	A1
	Appendix B Risk assessment . . . . .	B1
	Appendix C Ejector performance data with uncertainty . . . . .	C1

---

# List of Tables

3.1	Set of main components in the R744 multi-ejector test rig. . . . .	32
3.2	Sensor specifications at the test facility. FS means full scale (range). . . .	33
3.3	Multi-ejector test conditions from Danfoss. . . . .	34
3.4	Three cases for comparison in Coolselector. . . . .	44
4.1	Overview over the measurements with overall uncertainty for the advanced multi-ejector. . . . .	53
4.2	Results from the advanced multi-ejector that are inserted into Coolselector. The motive- and the suction nozzle mass flow rate and the receiver pressure is compared with the multi-ejectors suggested in Coolselector. . .	64
4.3	Test conditions from the advanced multi-ejector that are compared with multi-ejectors suggested from Coolselector. . . . .	64
4.4	Three cases for comparison in Coolselector. . . . .	65

---



# List of Figures

2.1	A pressure and temperature diagram presenting the phases for CO <sub>2</sub> (Adapted from Eikevik (2017)). . . . .	4
2.2	Ejector with the function of Bernoulli's equation; When the speed of a fluid increases its pressure decreases and vice versa. . . . .	7
2.3	Mach number over 1 and under 1 for nozzle and diffuser. Velocity fluid change, where $du < 0$ is acceleration and $du > 0$ is deceleration. Cross-sectional area (A), where $dA < 0$ is converging area and $dA > 0$ is diverging area. . . . .	8
2.4	Basic R744 ejector cycle with components. . . . .	10
2.5	Pressure – enthalpy diagram for a basic R744 ejector cycle. . . . .	10
2.6	Needle ejector . . . . .	11
2.7	Vortex ejector . . . . .	12
2.8	Multi-ejector adopted and modified from Danfoss (2018a) . . . . .	15
2.9	Ejector efficiency as defined in Equation 3.7 as a function of the motive nozzle inlet conditions and pressure ratios for VEJ1. The measurement uncertainties for ejector efficiency are $\pm 0.008$ (Adopted from Banasiak et al. (2015a)). . . . .	17
2.10	Motive nozzle mass flow rate as a function of the motive inlet conditions for VEJ1 (Adopted from Banasiak et al. (2015a)). . . . .	17
2.11	First generation of "CO <sub>2</sub> only" refrigeration system . . . . .	19
2.12	Second generation of "CO <sub>2</sub> only" refrigeration system with parallel compression. . . . .	20
2.13	A booster system with multi-ejector, parallel compression and AC in a supermarket. . . . .	21
2.14	Transcritical CO <sub>2</sub> supermarkets globally in 2020. Adopted from Shecco (2020). . . . .	23
3.1	Pressure and specific enthalpy diagram to recognize the enthalpies $h_A, h_B, h_C, h_D$ that are included in the equation of the ejector efficiency of a two-phase ejector. . . . .	27

---

3.2	Experimental test facility with pressure gauges and compressors in front. The advanced multi-ejector is censored behind a pink shaped rectangle on the left side of the rig. . . . .	28
3.3	Illustrates the pipeline and instrumental diagram of the CO <sub>2</sub> test rig, where all main components are included. The water loop and glycol loop are excluded. . . . .	29
3.4	A closer look at the censored advanced multi-ejector developed by Danfoss. . . . .	31
3.5	A illustration of the rectangle distribution in Type B. The accuracy from data sheets is symbolised as <i>a</i> . . . . .	37
3.6	Example on a calculation of a LP multi-ejector system in Coolselector. . .	43
3.7	System sketch for the LP multi-ejector system in Coolselector . . . . .	45
3.8	Pressure-specific enthalpy (ph) diagram for the LP multi-ejector system in Coolselector . . . . .	46
3.9	Example on a calculation of a HP multi-ejector system in Coolselector . .	47
3.10	System sketch for the HP multi-ejector in Coolselector . . . . .	48
3.11	Pressure-specific enthalpy diagram for the HP multi-ejector system in Coolselector . . . . .	49
4.1	Ejector efficiency and pressure lift for all the measurements in Table 4.1. The coloured dots represent the divided sections/groups outlined in the table successively in the same order. For instance, dark grey is Test 1-3 in the table. . . . .	55
4.2	The ejector efficiency for the advanced multi-ejector as a function of suction nozzle mass flow rate. . . . .	56
4.3	Ejector efficiency and superheat as a function of pressure lift (Test 21-30 in Table 4.1) Triangles show the tests with a low superheat. . . . .	57
4.4	Entrainment ratio and pressure lift for all the measurements in Table 4.1. The coloured dots represent the divided sections/groups outlined in the table successively in the same order. For instance, dark grey is Test 1-3 in the table. . . . .	59
4.5	Inlet motive nozzle pressure as a function of enthalpy for all the the measurements in Table 4.1. The coloured dots represent the groups in the table, respectively. This is inlet motive point in ejector efficiency Figure 3.1. . .	61
4.6	Inlet suction nozzle pressure as a function of enthalpy for all the the tests in Table 4.1. The coloured points represent the same order as grouped in the overview Table 4.1. This presents the inlet suction nozzle point in the ph-diagram Figure 3.1. . . . .	63
4.7	Suction nozzle mass flow rate for low pressure lift ejector performance comparison at equal motive nozzle mass flow rate and receiver pressure (Case 1, Test A and B). . . . .	67
4.8	Receiver pressure level for low pressure lift ejector performance comparison at equal motive- and suction nozzle mass flow rate (Case 2). . . . .	68
4.9	Motive nozzle mass flow rate for low pressure lift ejector performance comparison at equal suction nozzle mass flow rate and receiver pressure (Case 3, Test A and B). . . . .	69

---

---

4.10	Entrainment ratio and ejector efficiency for lower pressure ejector performance comparison at equal motive nozzle pressure and pressure lift (Case 1 like Figure 4.7). . . . .	71
4.11	Pressure lift and ejector efficiency for lower pressure lift ejector performance comparison at equal motive nozzle pressure and entrainment ratio (Case 2 like Figure 4.8). . . . .	72
4.12	Entrainment ratio and ejector efficiency for lower pressure ejector performance comparison at equal motive nozzle pressure and pressure lift (Case 3 like Figure 4.9). . . . .	73
4.13	Suction nozzle mass flow rate for high pressure lift ejector performance comparison at equal motive nozzle mass flow rate and receiver pressure (Case 1). . . . .	75
4.14	Receiver pressure level for higher pressure lift ejector performance comparison at equal motive- and suction nozzle mass flow rate (Case 2). . . .	76
4.15	Motive nozzle mass flow rate for higher pressure lift ejector performance comparison at equal suction mass flow rate and pressure lift (Case 3). . . .	77
4.16	Entrainment ratio and ejector efficiency for higher pressure lift ejector performance comparison at equal motive nozzle pressure and pressure lift (Case 1 like Figure 4.13). . . . .	79
4.17	Pressure lift and ejector efficiency for higher pressure lift ejector performance comparison at equal motive nozzle pressure and entrainment ratio (Case 2 like Figure 4.14). . . . .	80
4.18	Entrainment ratio and ejector efficiency for higher pressure lift ejector performance comparison at equal motive nozzle pressure and pressure lift (Case 3 like Figure 4.15). . . . .	81
5.1	Type A versus Type B uncertainty as a function of ejector efficiency. . . .	84
5.2	Type B uncertainty as a function of ejector efficiency with original (blue) and new improved (green) temperature and pressure sensors. The accuracies for pressure (p) and temperature (t) sensors used in the uncertainty calculations are found in the upper left corner. Full scale (FS) is 160 bar. . .	86
5.3	Motive envelope for HP 1875 adapted from Coolselector . . . . .	89
5.4	Suction/receiver envelope for HP 1875 adapted from Coolselector . . . . .	89

---

---

# Nomenclature

## List of abbreviations

AC	=	Air conditioning unit
CFC	=	Chlorofluorocarbons
gc	=	Gas cooler
FS	=	Full scale
GWP	=	Global warming potential
HFC	=	Hydrofluorocarbons
HP	=	High pressure lift
HPV	=	High pressure electronic expansion valve
IT	=	Intermediate temperature
LEJ	=	Liquid ejector cartridge
LP	=	Low pressure lift
LT	=	Low temperature
MN	=	Ejector inlet motive nozzle flow
MT	=	Medium temperature
out	=	Ejector flow outlet
SN	=	Ejector inlet suction nozzle flow
VEJ	=	Vapour ejector cartridge

---

## List of symbols

$C_P$	=	Heat capacity	[kJ/K]
$ER$	=	Entrainment ratio	[-]
$h$	=	Specific enthalpy	[kJ/kg]
$\eta$	=	Efficiency	[%]
$\dot{m}$	=	Mass flow rate	[kg/h]
$p$	=	Pressure	[bar]
$\Delta p$	=	Pressure lift	[bar]
$t$	=	Temperature	[°C]
$T$	=	Temperature	[K]
$s$	=	Specific entropy	[kJ/kgK]
$u$	=	uncertainty	[-]
$q$	=	vapour mass fraction	[-]

---

# Introduction

Global warming and climate change have led researchers to search for sustainable solutions to reduce emission of greenhouse gases. The implementation of the EU F-Gas regulation 517/2014 on HFC gases has made the industry substitute harmful refrigerants by environmental friendly alternatives. The goal is to decrease HFC emissions by 79% by 2030, which will favour low GWP refrigerants as CO<sub>2</sub> in the refrigeration sector (Commission (2014)).

Supermarkets are energy-intensive users, accounting for between 3% and 4% of the annual electricity consumption in industrialized countries. Refrigeration systems account for 30-60 percent of the total energy use in supermarkets, making them the highest consuming system in the store. The energy use varies due to non-technical barriers such as climate and social habits (Tassou et al. (2011)). Hence, supermarkets has also one of the highest specific energy consumption per m<sup>2</sup> of all commercial buildings. The specific energy demand, regards the refrigeration system, is between 300 kWh/m<sup>2</sup> and 600 kWh/m<sup>2</sup>. Meanwhile, an office building consumes between 150 kWh/m<sup>2</sup> and 200 kWh/m<sup>2</sup> (Nordtvedt and Hafner (2012)).

Today, there are more than 35 500 transcritical CO<sub>2</sub> installations globally. In May 2020 there was 29 000 transcritical CO<sub>2</sub> installations in Europe, which is a growth of 81% since 2018, when there were approximately 16 000 installations. Gullo et al. (2019) estimated for new supermarkets in 2020 the market share of ejector supported parallel systems is supposed to be in the range from 50% to 80%. Moreover, the commercial refrigeration applications can go HFC-free all over Europe, due to the great energy efficiency in any European climate context by adapting the system layout for R744. The “CO<sub>2</sub> only” concept can be installed world-wide (Gullo et al. (2018)).

The multi-ejector concept in supermarkets is commercialized in cold ambient temperatures, but also the later years in high ambient temperatures. According to Gullo et al. (2017b) the multi-ejector concept leads to a reduction in energy consumption by 37.1% in

the cold climate of Oslo and 19.9% in the warm climate in Athens over a R404A unit.

Further development of the multi-ejector solution is important for decreasing the energy consumption in supermarkets. Therefore, the objective of this Master's Thesis is to carry out a campaign of experimental tests at performance mapping of a prototype of an advanced multi-ejector developed by Danfoss. An evaluation of the performance of the advanced multi-ejector is carried out by comparison with other transcritical R744 multi-ejectors and is performed by employing a selection tool.



# Literature review

## 2.1 CO<sub>2</sub>

Carbon dioxide, also known as CO<sub>2</sub> and R744, is a natural working fluid. It has a global warming potential (GWP) of 1 and a ozone depletion potential (ODP) of 0, which means it neither contributes to global warming nor ozone depletion. CO<sub>2</sub> is often preferred over other natural refrigerant (ammonia, propane, isobutane etc.), because it is the only natural refrigerant that is non-toxic and non-flammable with a safety classification of A1. CO<sub>2</sub> is also inexpensive and readily available working fluid (Kim et al. (2004)).

In 1989 Professor Gustav Lorentzen from NTNU reintroduced CO<sub>2</sub> as a working fluid, after years of use of chlorofluorocarbons (CFC). He patented a transcritical CO<sub>2</sub> cycle system, where the throttling valve controlled the high pressure (Kim et al. (2004)). Today, CO<sub>2</sub> is widely used in supermarkets and is a rising star of the commercial food retail industry, especially since the refinement of the transcritical system (Shecco (2020)).

CO<sub>2</sub> has a high operating pressure of 73.8 bar, a low critical temperature of 31.1°C and a triple point at 5.18 bar and -56.57°C as shown in Figure 2.1. CO<sub>2</sub> has favourable thermo-physical properties. These include higher specific heat, density, latent heat, thermal conductivity and volumetric cooling capacity than HFC refrigerants. Since CO<sub>2</sub> has a relatively low viscosity in the liquid phase, this leads to a lower pumping performance for systems with large pipelines. Together with the low surface tension, CO<sub>2</sub> has excellent heat transfer properties especially in the nucleate boiling regime (Eikevik (2017)).

Another advantage is the high system pressure with CO<sub>2</sub>. A high operating pressure leads to a steeper saturation pressure curve, which results in a lower saturation temperature difference due to pressure loss. In terms of system efficiency, this results in a significant advantage. At 0°C, the temperature change of CO<sub>2</sub> for 1 kPa pressure drop is about 0.01 K. The same pressure drop with R410a and R134a is about 4-10 times higher, which gives a temperature change of 0.04 and 0.10 K, respectively (Kim et al. (2004)). Additionally,

the critical pressure gives CO<sub>2</sub> an advantage in low temperature applications.

Due to the properties of CO<sub>2</sub>, the main components has to be adapted both with respect to safety and energy efficiency. For example, CO<sub>2</sub> has a high specific volume capacity, which means that the compressors and the diameter of the piping are small and must withstand high pressures.

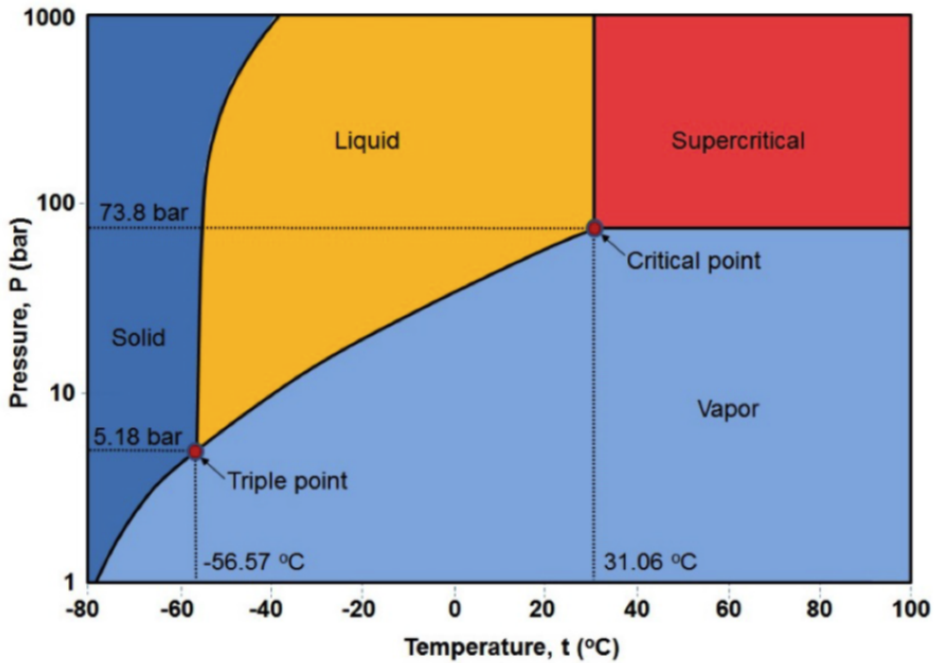


**Figure 2.1:** A pressure and temperature diagram presenting the phases for CO<sub>2</sub> (Adapted from Eikevik (2017)).

## 2.2 Ejector

The ejector can be traced all the way back to 1858, when Henry Giffard (1860) invented the component that would pump water inside steam boilers in stationary locomotives. Later Norman Gay (1931) patented the two-phase ejector, in which he described how it improved the performance of refrigeration systems by reducing the inherent throttling losses of the expansion valve.

However, it was not until the 1980's that energy efficiency of the ejector gained momentum and the CO<sub>2</sub> air conditioner for cars was seriously considered. About 10 years ago the first commercial tap water heat pumps in Japan came on the market. Some of these heat pumps use ejector technology today (Hafner and Eikevik (2019)).

The purpose of an ejector is to combine a high pressure stream with a entrained low pressure stream which thereby exit at an intermediate pressure. An advantage of the ejector is that it has no movable parts, which make it resilient. The use of ejectors in R744 refrigeration and heat pump systems is one of the best ways to reduce the throttling loss and increase the energy efficiency of the system (Banasiak et al. (2015b))

### 2.2.1 Function behind an ejector

An ejector consists of four main components and is schematised in Figure 2.2. The first component is the motive chest, followed by the motive converging-diverging nozzle attached to the suction chamber (mixing area), which is connected to the fourth component, the diffuser.

The ejector's function is based on the connection between pressure and velocity expressed through the Bernoulli's equation Haukås (2016), see Figure 2.2. An ejector uses the properties of compressible fluids to initially develop supersonic speed. This works by converting the pressure energy of the motive fluid, otherwise known as potential energy, into velocity energy or kinetic energy through a converging surface of the nozzle. Here the motive fluid is in subsonic state, which means the Mach number below 1, see Equation 2.1. In the narrowest area of the motive nozzle the critical Mach number 1 is achieved. Then velocity of the motive fluid continues to accelerate in the diverging section of the motive nozzle. This is achieved by adiabatic expansion from the motive fluid pressure to the suction load pressure. The design of the motive nozzle is set by the manufacturer for specific operating conditions and plays an accentual part in ejector performance. A well designed converging-diverging nozzle leads to a Mach number greater than 1 and thus a supersonic flow, see Figure 2.3. The Mach number is a dimensionless quantity, which describes the ratio of the local flow velocity to the local speed of sound of the medium (Schröder (2014)). It is a key figure to characterize the flow and its equation can be found in Equation 2.1:

$$M_a = \frac{u_{\text{local flow velocity}}}{u_{\text{speed of sound in the medium}}} \quad (2.1)$$

The connection between cross-sectional area (A), velocity (u) and pressure (p) relationship

can be calculated out of the continuity equation, where no friction and isentropic nozzle flow are assumed.

The velocity relationship is shown in Equation 2.2:

$$\frac{du_{\text{local flow velocity}}}{u_{\text{local flow velocity}}} = -\frac{dA}{A} \frac{1}{1 - M_a^2} \quad (2.2)$$

and the pressure relationship is shown in Equation 2.3:

$$\frac{dp}{u_{\text{local flow velocity}}} = \frac{dA}{A} \frac{1}{1 - M_a^2} \quad (2.3)$$

The fluid behaviour in a converging-diverging cross-sectional area according to the Mach number can be explained by Figure 2.3.

Motive fluid enters the motive chest having a high pressure (point A, Figure 2.2). The motive fluid can be vapour. However, it can be any fluid that is at a higher pressure than the ejector is trying to compress to.

At point B, the suction fluid, which can be a mixture of vapour and liquid, enters the ejector. At point C, the high velocity motive fluid expands to a pressure slightly less than the suction load pressure. That creates a localized low pressure region, which draws in the suction load vapour.

The suction chamber is the bridge between the nozzle and the rest of the ejector. The high velocity motive stream, coming from the outlet of the motive nozzle at point C, mixes and entrains the suction fluid in the suction chamber. With the conservation of the momentum, the high velocity of the motive stream is transferred to the suction load gases, which accelerates the suction fluid and consequently decelerating the motive gas to a new mixture fluid speed. The high velocity of the motive stream is high enough that the combined velocity with the suction fluid is still above Mach number 1. This causes a deceleration of the mixture fluid velocity due to the converging cross-sectional area of the diffuser.

The diffuser consists of three sections, the inlet converging section, throat section with constant area and outlet diverging section. The mixture fluid velocity is decreased and pressure is increased as the cross-sectional area is reduced. In the throat section the work of the compression occurs. In this section the cross-sectional area is constant.

The diffuser throat is sized to achieve an optimal transonic shock system. To accomplish that, the Mach number of the mixture fluid is above 1 and a shock wave occurs. After the shock wave the Mach number dramatically drops below 1. Hence, the transition from supersonic to subsonic flow across the shock system produces a dramatic increase in pressure. Slightly more than half of the total compression achieved in an ejector is obtained in this section. The static pressure temperature and the density increase across the shock

system whereas the velocity decreases.

The pressure increases further in the outlet diverging section where the subsonic velocity of the mixture reduces as the cross sectional area increases from the throat diameter to the discharge diameter. Slightly less than half of the total compression achieved in an ejector is obtained in the outlet diffuser section through deceleration of the subsonic flow (Daneshmand et al. (2009), Graham Corporation (2017), Ma et al. (2017)).

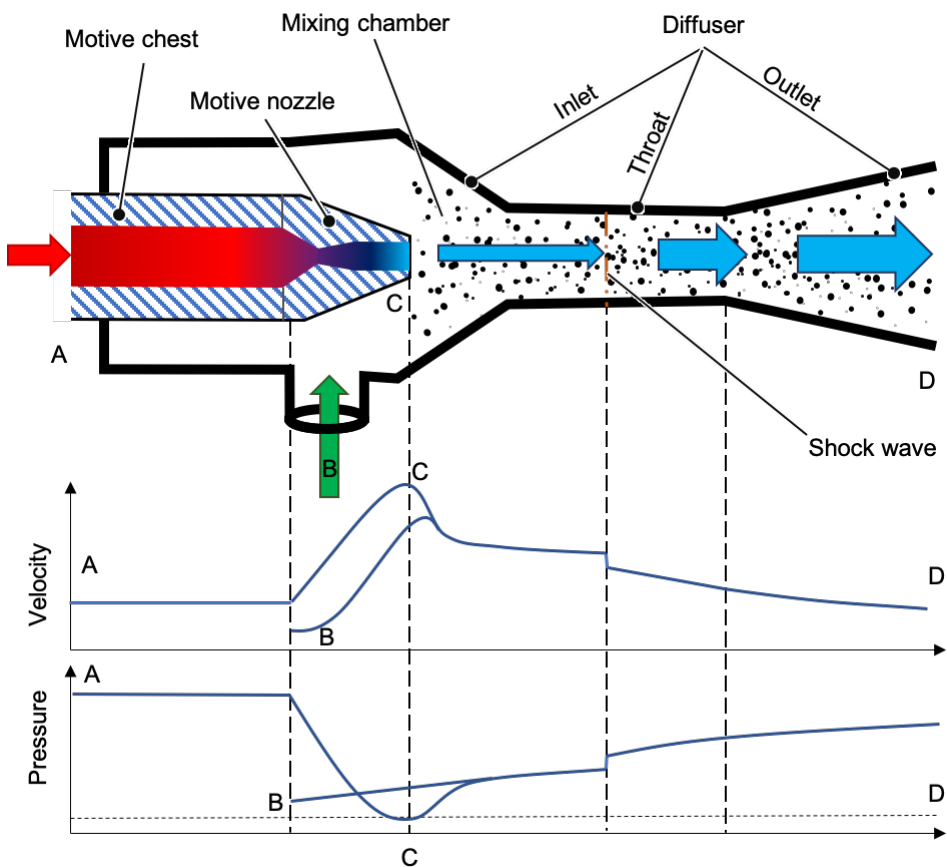


**Figure 2.2:** Ejector with the function of Bernoulli's equation; When the speed of a fluid increases its pressure decreases and vice versa.

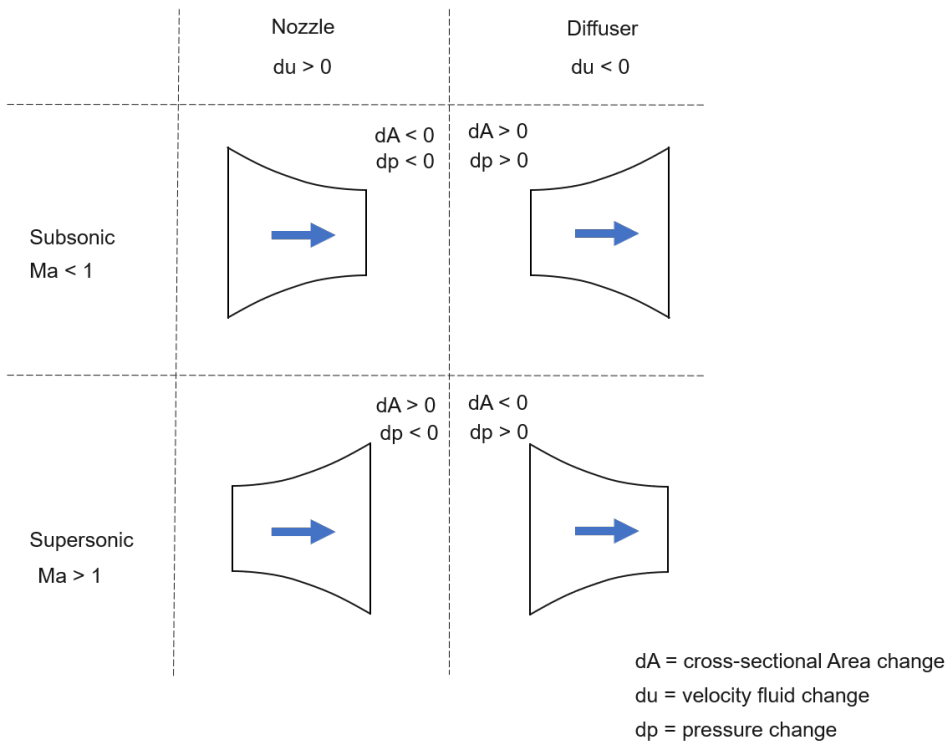


**Figure 2.3:** Mach number over 1 and under 1 for nozzle and diffuser. Velocity fluid change, where  $du < 0$  is acceleration and  $du > 0$  is deceleration. Cross-sectional area ( $A$ ), where  $dA < 0$  is converging area and  $dA > 0$  is diverging area.

### 2.2.2 Simple two-phase ejector process

A simple transcritical R744 vapor-compression unit employing an two-phase ejector aimed at expansion work recovery is shown in Figure 2.4. The corresponding pressure and specific enthalpy diagram sketched in Figure 2.5. The difference from a simple vapour compression cycle with the main components: a compressor, a condenser, an expansion valve and an evaporator, is that the expansion valve is changed with an ejector. The condenser is subcritical and the gas cooler is transcritical. The latter means that the CO<sub>2</sub> is cooled, but not condensed at the outlet of the gas cooler, staying above the critical temperature. The purpose of a refrigeration system, is that the condensation process will release heat and the evaporation will absorb heat.

When approaching the compressor in thermodynamic state 1, the refrigerant is in vapour phase and is compressed through the compressor. In the gas cooler releases heat to the surroundings, as the ambient temperature is lower than than the refrigerant. At the gas cooler outlet, the high pressure flow is expanded into the motive nozzle of the ejector is the two-phase area. The ejector process is shown in the thermodynamic states 4, 5, 6 and 7. The high pressure motive flow (4) from the gas cooler and the low pressure suction flow (5) from the evaporator mixes together (6). An intermediate pressure flow (7) streams out of the ejector and further into the receiver. From the receiver the vapour flows into the compressor and the liquid into the expansion valve and further into the evaporator. The evaporator absorbs heat, as the surrounding temperature is higher than the temperature of the refrigerant (Eikevik (2017)).

By replacing the high pressure expansion valve with an ejector, two main advantages occurs. Firstly, the refrigeration effect increases as the evaporator enters at a lower vapour enthalpy and quality. Secondly, the the refrigerant is pre-compressed by the ejector from the evaporator pressure to the intermediate pressure, causing a decrease in compressor power input (Gullo et al. (2019)).

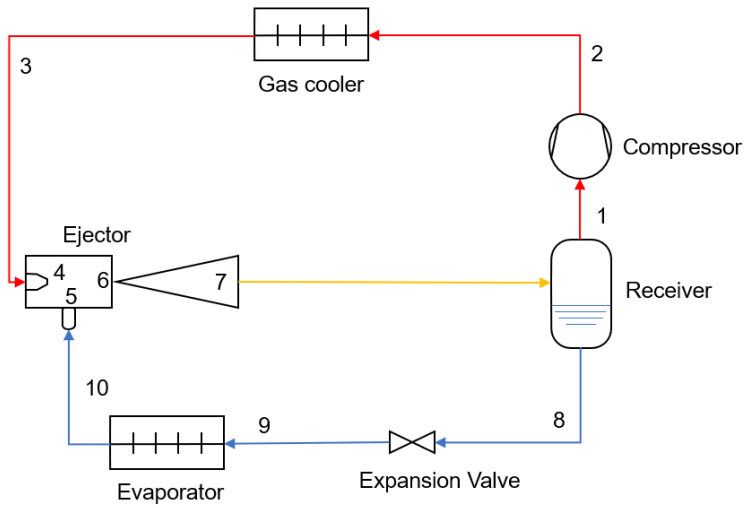


**Figure 2.4:** Basic R744 ejector cycle with components.

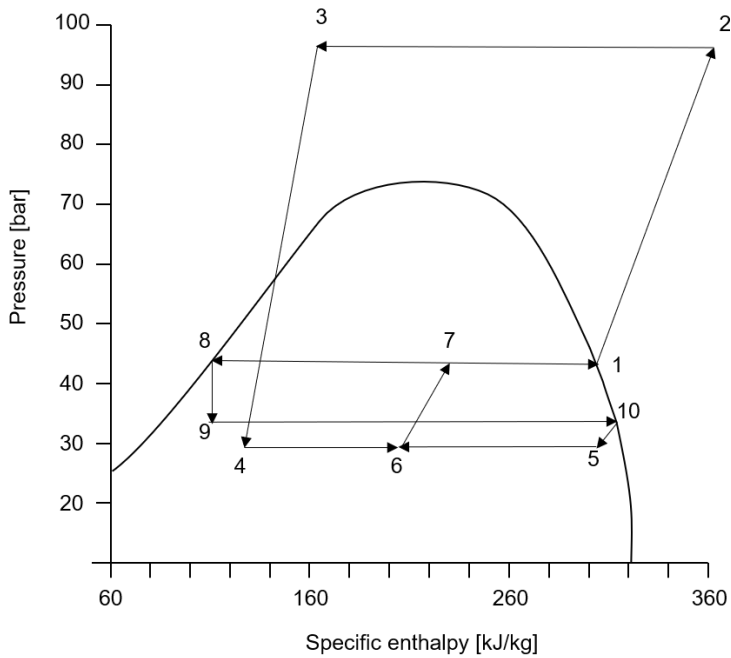


**Figure 2.5:** Pressure – enthalpy diagram for a basic R744 ejector cycle.



### 2.2.3 Various ejector designs

Ejector cycle performance is usually sensitive to working condition changes, that is why ejector geometry is very important. One of the key dimensions affecting the ejector cycle coefficient of performance (COP) is the ejector motive nozzle throat diameter, which has a direct impact on the motive mass flow rate. The ejector efficiency and COP get affected by the motive nozzle position mixing chamber constant area diameter and the converging angle of the suction chamber (Sarkar (2012)). The two-phase ejector has to be permanently suited to the operating conditions in addition to implementation of appropriate capacity control along with an effective expansion work recovery (Liu et al. (2012)).

#### Needle motive

Elbel and Hrnjak (2008) were the first researchers to publish experimental results on installing a needle in the motive nozzle in a two-phase ejector to control the motive nozzle throat diameter using R744 as a refrigerant. An advantage using the needle mechanism is that it can control the gas cooler high-side pressure and thereby reach a optimum performance of the transcritical cycle. In other words the ejector capacity modulation can be implemented. However, according to Boccardi et al. (2017) moving parts in an ejector can be unreliable and untrustworthy. Besides, the design is also expensive and complicated in terms of optimisation of the geometry. It can also be mentioned that additional frictional losses can affect the ejector efficiency negatively.

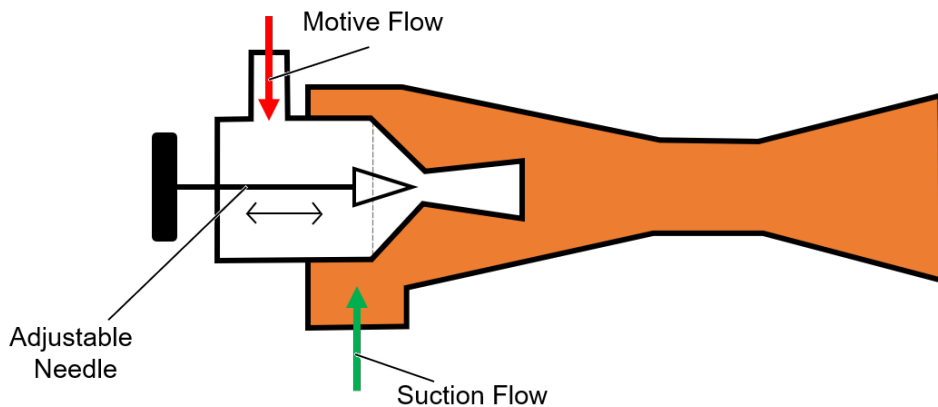


Figure 2.6: Needle ejector

## Vortex

The adjustable vortex based capacity control strategy is together with the multi-ejector concept (see Section 2.3), the two capacity control methods requiring no geometry change (Gullo et al. (2020)). The vortex strategy was developed by Zhu and Elbel (2016).

A vortex ejector illustrated in Figure 2.7 differs from a conventional ejector, in which an adjustable vortex is generated at the ejector motive inlet. The injecting part on the tangential inlet creates the motive inlet vortex. The tangential flow mixes together with the axial flow. The valve installed at the motive tangential inlet adjusts the ratio of mass flow rates through the two inlets. Thereby the valve changes the vortex strength (Zhu and Elbel (2016)).

The advantage of the vortex is that it is less vulnerable to clogging than the needle, it is simple and potentially less expensive. The work of Zhu and Elbel (2016) with R134a has shown that the nozzle throttling of the two-phase flow can be adjusted over a wide range without changing the nozzle geometry. Applying the same inlet and outlet configurations, the mass flow rate through the nozzle can be throttled by 36% of the full load. For future application of the ejector in mobile or stationary systems under changing operating conditions, this feature could be of considerable benefit.

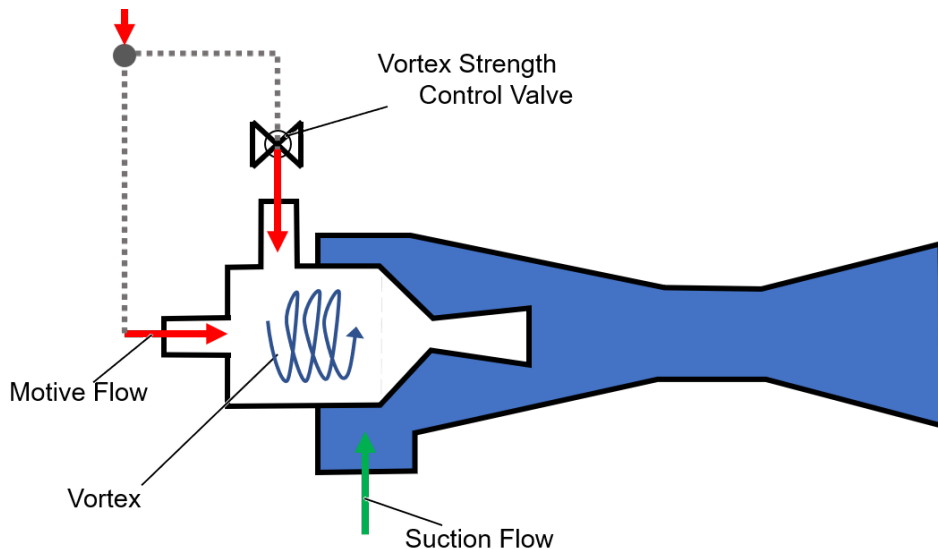


**Figure 2.7:** Vortex ejector

Bodys et al. (2016) revealed that a swirl (vortex) in the motive nozzle in a R744 multi-ejector block corresponded to an mass entrainment ratio improvement of 3%, when compared to an ejector without swirl. The entrainment ratio and hence the ejector efficiency was higher for larger inlet diameter in the motive nozzle. The rotational speed in the motive nozzle was 4000 rotations per minute (rpm). In addition, it was concluded that the

swirl should not be installed in the suction nozzle due to bad efficiencies, which resulted in an installation only in the motive nozzle. Compared to an ejector, the entrainment ratio and hence the ejector efficiency for a vortex-ejector was higher for larger inlet diameters in the motive nozzle at moderate motive pressures.

### **Current status of capacity control**

According to the latest publication Gullo et al. (2020) on current status of capacity control of two-phase ejectors, the large and medium scale vapour compression units can be properly controlled by two-phase ejectors. However, the small scale vapour compression solutions still requires suitable capacity control mechanism. Further development in this regard is needed and is intensively discussed among experts in the field.

Multi-ejector capacity control compared to needle based ejector and vortex based ejector used in medium and large applications are too complicated and expensive (Zhu and Elbel (2020)). The multi-ejector concept dominates the large- and medium-scale transcritical R744 applications. According to Gullo et al. (2020), the vortex- and the needle-based ejectors are not limited in terms of size, which means that it is still unknown whether they can be competitive or not. The vortex ejectors are still under investigation on a laboratory scale. The needle-based ejector is found in the literature, but no field measurements from real applications are available. According to Zhu and Elbel (2020), the ejector performance is better for the needle than the vortex, but the vortex is still early in the development.

## 2.3 Multi-ejector

The multi-ejector consist of multiple fixed-geometry ejectors together in a block, which can provide significant energy savings. The multi-ejector is used in high energy-demanding buildings (e.g., gyms, hotels, spas) as well as commercial supermarkets (Gullo et al. (2019)). The conception of the multi-ejector introduced by Hafner et al. (2014) has positively influenced the knock-on effect on the commercial "CO<sub>2</sub> only" refrigeration systems.

It can be a challenge to regulate the suction capacity without losing efficiency in a basic ejector solution. In other words, it is difficult to have an effective control of the heat rejection pressure and at the same time implementing the recovery expansion work in an ejector with constant geometry. Due to this disadvantage, the multi-ejector concept was developed. The multi-ejector arrangement is constructed to operate under various temperature and operating conditions (Banasiak et al. (2015a)).

Figure 2.8 shows how the inside content of a typical multi-ejector looks like on the commercial market today. A multi-ejector block consists of several fixed ejector cartridges of various size. The present multi-ejectors on the commercial market for food retails are delivered with 4 to 6 vapour ejectors (VEJ) and 2 liquid ejectors (LEJ). A built-in non-return valve is a part of every individual ejector preventing backflow, which removes the need for external check valves in the suction line. The ejectors in the block are all placed parallel to each other. There is a linearly variable capacity between the vapour ejectors, to ensure maximum system flexibility. The capacity is higher for the VEJ4 than the VEJ1 in a multi-ejector from Danfoss (Danfoss (2018b)). The capacity is controlled by selecting which of the cartridges should be switched on or off.

In Figure 2.8 only one VEJ on the left side is schematized as an active cartridge. The pressure levels are measured by the pressure transmitters on the left side of the block and on the top are the solenoid valves. By following the white arrows, it can be seen that the red motive stream mixes with the blue suction stream which flows upwards into the vertical ejector cartridge. Both streams mix together, coloured in yellow, and flow out of the ejector cartridge and onto the receiver pressure outlet.

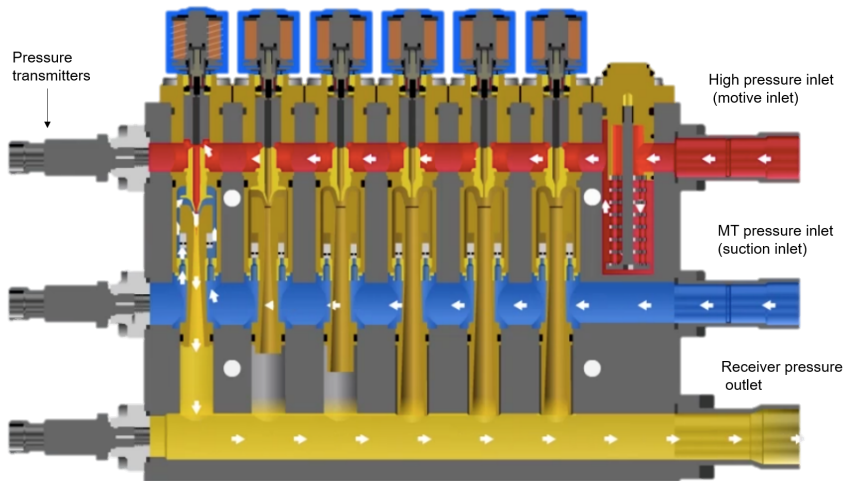


**Figure 2.8:** Multi-ejector adopted and modified from Danfoss (2018a)

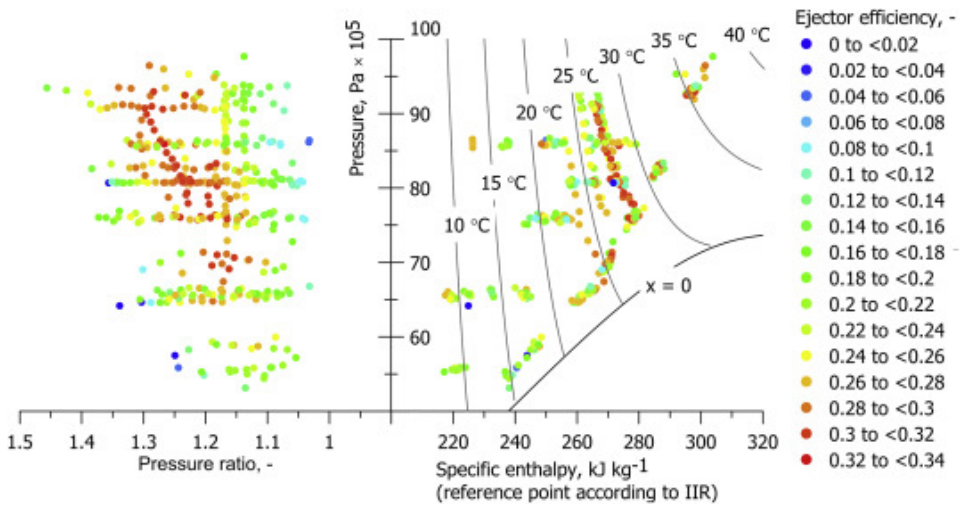
Banasiak et al. (2015a) recorded ejector efficiencies over 30% for all four vapour cartridges in the multi-ejector having a wide operation range. In the research from 2015, the highest measured efficiencies were 33.0% for VEJ1, 36.8% for VEJ2, 36.2% for VEJ3, and 33.6% for VEJ4. To the best of the authors knowledge, 36.8% is still today the highest recorded efficiency for an ejector cartridge in a R744 system. Before 2015 the highest reported ejector efficiency for R744 was 30.8% (Banasiak et al. (2012)). However, the highest ever recorded ejector cartridge efficiency was 42% and was reached with a R134a ejector system (Sag et al. (2015)).

According to Lawrence and Elbel (2015), the work recovery efficiency for CO<sub>2</sub> ejectors reported from studies in the open literature, generally achieves 20% to 30%, meanwhile R134a achieves generally less than 20%. The latter is a low pressure refrigerant, which has a greater sensitivity of low pressure fluids to pressure losses in the ejector and therefore a possible lower ejector efficiency. It is worth mentioning that a better ejector performance does not necessarily mean a higher cycle COP. The impact of properly controlled super-heat or high-side pressure can increase the cycle COP, but it can have a negative effect in which the highest ejector efficiency is not achieved.

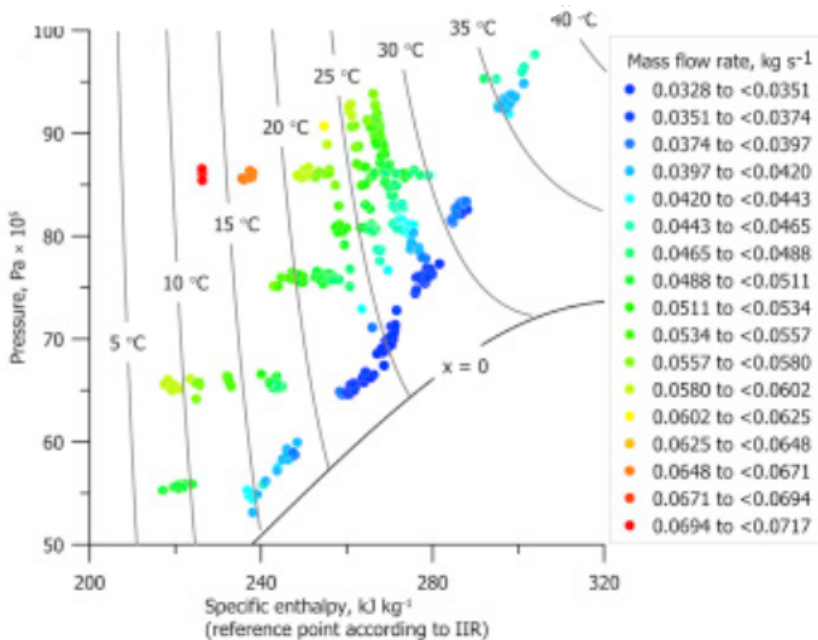
Taking a further look into the laboratory experiment of Banasiak et al. (2015a), the overall multi-ejector efficiency was 22.8% with the utilization of VEJ1, VEJ2 and VEJ3. The entrainment ratio was 0.16. The overall ejector uncertainty is lower than the individual ejector cartridges, due to the influence by the imperfect mixing of the outlet flows of the individual ejectors. It was discovered that the overall uncertainty was heavily influenced by the compressor efficiency with respect to the selected combination of ejector cartridges.

Figure 2.9 shows the ejector efficiency as a function of the motive nozzle inlet conditions and pressure ratios for VEJ1. The highest ejector efficiencies around 30% was found at the motive nozzle pressure between 70 bar and 90 bar with motive temperatures from 25°C and 35°C. The corresponding pressure ratio was between 1.15 and 1.18 for the highest ejector efficiencies under the motive pressure of 75 bar, meanwhile the motive nozzle pressures around 90 bar reached higher pressure ratios from 1.22 to 1.31.

Figure 2.10 illustrates the motive nozzle mass flow rate depending on the inlet density and inlet pressure. The lowest mass flow rates occurred in the switching point between the subcritical and supercritical operation mode, whereas the highest was recorded for the heat recovery operation mode.



**Figure 2.9:** Ejector efficiency as defined in Equation 3.7 as a function of the motive nozzle inlet conditions and pressure ratios for VEJ1. The measurement uncertainties for ejector efficiency are  $\pm 0.008$  (Adopted from Banasiak et al. (2015a)).



**Figure 2.10:** Motive nozzle mass flow rate as a function of the motive inlet conditions for VEJ1 (Adopted from Banasiak et al. (2015a)).

## 2.4 Supermarket refrigeration systems

Annually, leakages of working fluids stands for 3% to 22% of the total charge. In Europe the refrigerant R404A ( $GWP_{100 \text{ years}} = 3942 \text{ kg}_{\text{CO}_2} / \text{kg}_{\text{refrigerant}}$ ) is a widely utilized refrigerant (Karampour et al. (2016)). It is estimated, that the average annual leakage rate is between 15% and 20% of the total charge (Hafner et al. (2014)). Since 1st of January 2020 the refrigerant R404a is banned in new commercial refrigeration applications in Europe and only recycled refrigerants can be used for servicing (Commission (2014)). With  $\text{CO}_2$ , a natural refrigerant, the environmental influence of a leakage is zero. That is one of many reasons for installing R744 supermarket refrigeration systems (Ciconkov (2018)).

An arrangement for a supermarket refrigeration system typically consists of medium temperature circuit (MT) and a low temperature circuit (LT). The medium temperature circuit is used for chilled food, while the low temperature circuit is used for frozen food.

The three main solutions for  $\text{CO}_2$  applied in supermarket refrigeration are the indirect, cascade and the transcritical systems (Sawalha (2008)).

In the indirect system  $\text{CO}_2$  is used as a two-phase secondary fluid for low temperature applications. The primary refrigerant in the system is often HFC. This system is used for freezing applications (Sawalha (2013)).

The standard two-stage cascade refrigeration system consists of two separated vapour compression cycles of different refrigerants. Due to excellent thermo-physical properties,  $\text{CO}_2$  is used as a low temperature refrigerant, whereas ammonia or other synthetic refrigerants as R404A are used as typical high-pressure refrigerants. The cascade heat exchanger condenses the  $\text{CO}_2$  against the other refrigerant that has a higher temperature. The higher temperature refrigerant must reduce the evaporation temperature, to ensure a heat transfer between the two refrigerants (Ge and Tassou (2011)).

For  $\text{CO}_2$  transcritical systems, booster configurations are commonly used in supermarkets. The transcritical system is most significant for this thesis which concerns multi-ejectors and is therefore described further in the next subsection.

### 2.4.1 Development of R744 booster systems in supermarkets

The design of "CO<sub>2</sub> only" supermarket refrigeration has undergone a remarkable development from the 1st to the 3rd generation within the last 11 years. There has been a technological development especially for units located in warm climates (Gullo et al. (2019)).  $\text{CO}_2$  systems are most efficient in cold climates. Transcritical refrigeration systems are initially applied in cold climates like Northern Europe, due to efficient heat recovery.

The 1st generation refers to the R744 booster supermarket refrigeration plant, which utilizes a flash gas by-pass valve, see Figure 2.11. In all the booster configurations the refrigerant is cooled on the high pressure side and expanded down to both the low and the medium temperatures (pressures). The refrigerant is evaporated at both the LT and MT lev-



els. There are two stages of compressors, where the LT compressor operates subcritically and the MT compressor operates either subcritically or transcritical. This is dependent on the ambient conditions (Ge and Tassou (2011)). A de-superheater is often placed on the high pressure side for heat recovery for space heating and domestic heat water purposes as well as after the LT compressor, as seen in Figure 2.11.

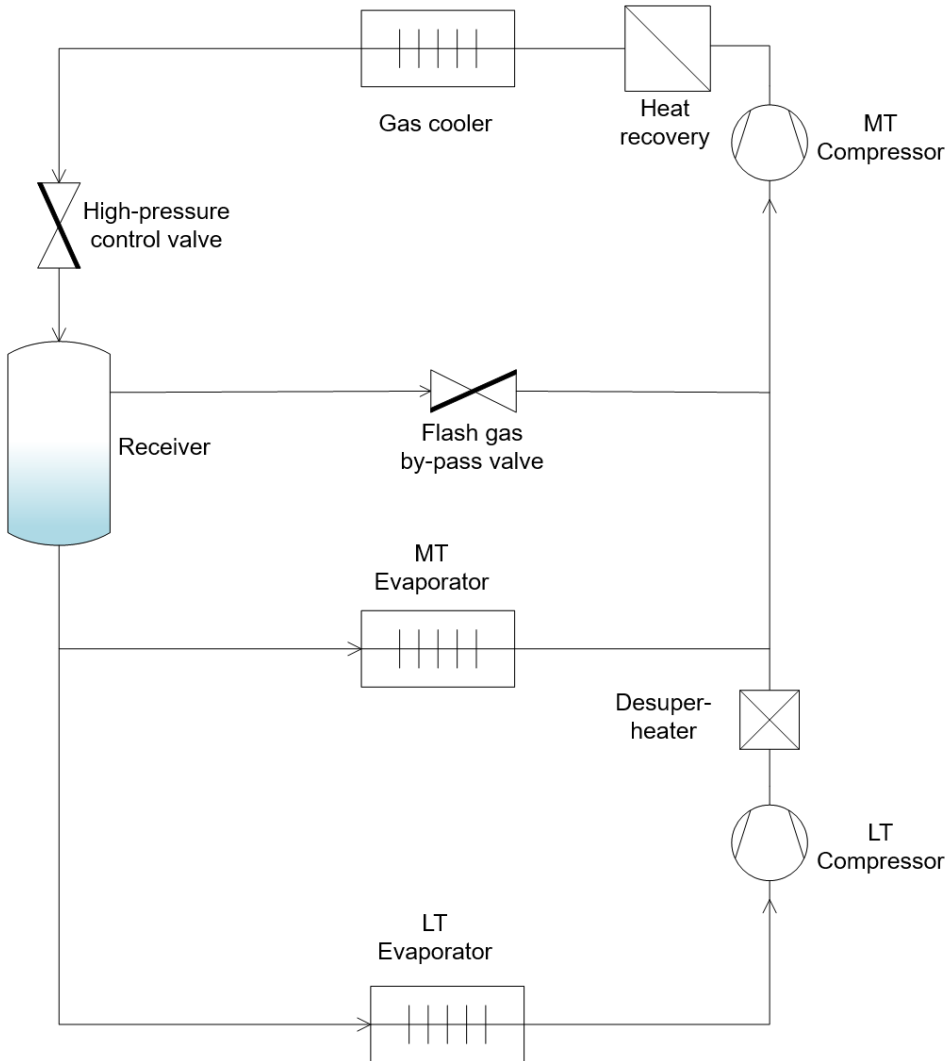


**Figure 2.11:** First generation of "CO<sub>2</sub> only" refrigeration system

Sawalha et al. (2017) compared three HFC refrigeration supermarkets in Sweden with R744 supermarket. The study from Sweden proved that the new CO<sub>2</sub> transcritical refrigeration systems are more energy efficient solutions for supermarkets than typical HFC systems at lower outdoor temperatures than 24°C. The booster system has been applied in

most of the installations in Sweden.

The second generation illustrated in Figure 2.12, made it possible to have a HFC-free solution in warm climates. It consists of a parallel compression unit including an air condition unit (AC). The MT compressor can be unloaded, when a parallel unit is used. This leads to a higher suction pressure, which in turn leads to higher energy savings. Parallel compression has the advantage that it has reduction in swept volumes of compressors. A disadvantage of this system is however, that in warm regions it cannot be combined energetically with AC units. Moreover, it also has higher investment cost than conventional booster systems.

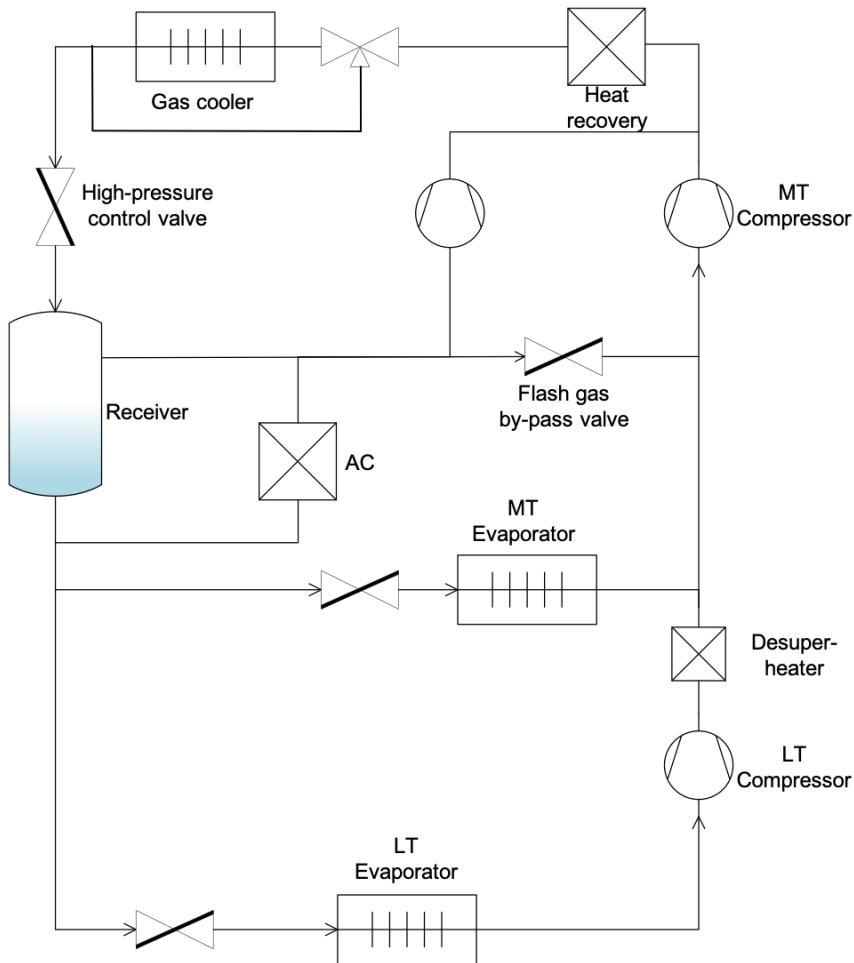


**Figure 2.12:** Second generation of "CO<sub>2</sub> only" refrigeration system with parallel compression.

Purohit et al. (2017) compared a booster with parallel compression to a R404A direct expansion refrigeration system, it revealed that the indirect systems outperform "CO<sub>2</sub> only"

configuration by extreme climate conditions. Nevertheless, the parallel compression can be energetically more advantageous if mechanical subcooling is applied in warm climates.

The third generation of "CO<sub>2</sub> only" supermarket is the introduction of the multi-ejector concept, which was introduced by Hafner et al. (2012). Multi-ejectors are applied in industrial refrigeration applications featured by large cooling loads. Figure 2.13 shows the principal CO<sub>2</sub> arrangement in a supermarket parallel compression cycle in which the expansion work is recovered with the aid of an ejector arrangement. The reduction in mass flow rate to the MT compressor results in substantial energy savings in comparison with a conventional booster solution.

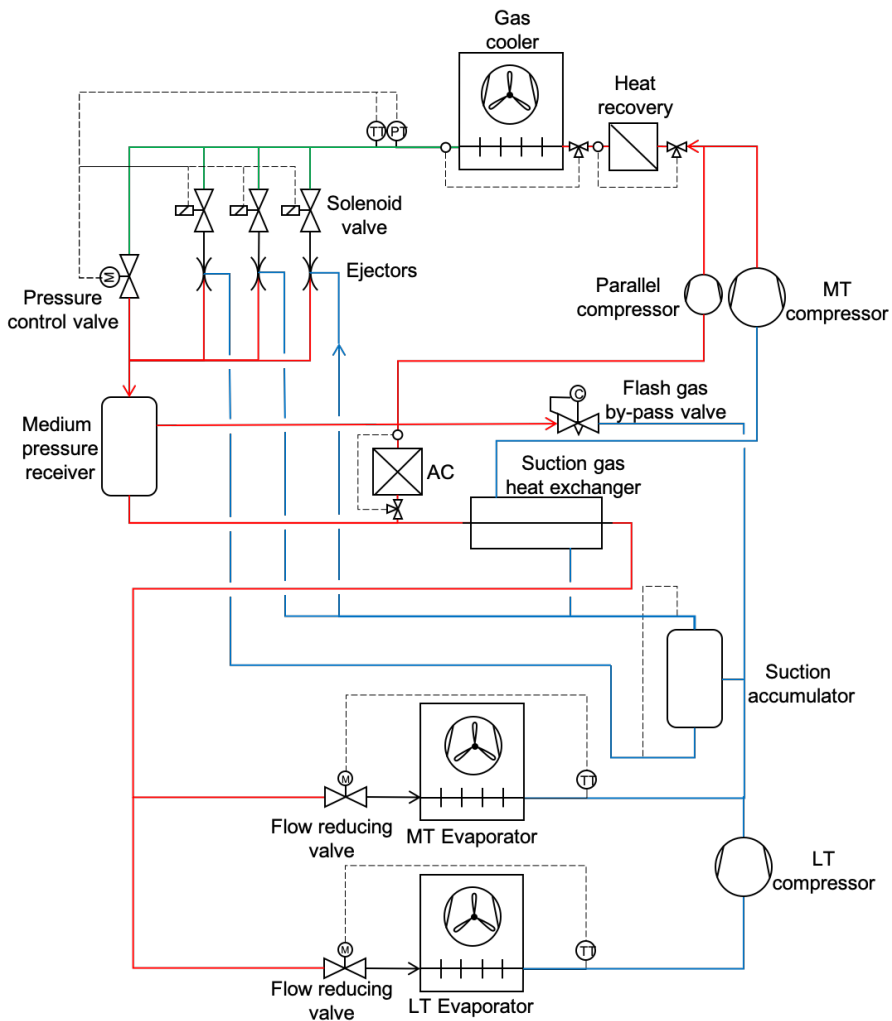


**Figure 2.13:** A booster system with multi-ejector, parallel compression and AC in a supermarket.

The three-way valve bypasses the flow on the high pressure side in Figure 2.13, when the heat exchangers (gas cooler and heat recovery units) are not in use. The "CO<sub>2</sub> only" refrigeration systems utilizes heat recovery and domestic hot water (DHW) as a advantage compared with HFC, due to the low CO<sub>2</sub> gas cooler return temperature (Sawalha (2013)). The heat recovery can include two de-superheaters, where one is used for DHW, while the following de-superheater provide space heating. In addition a third heat recovery unit for snow-melting downstream the gas cooler can also be installed. This applies to countries with cold climates and is often utilized in a conventional booster system in Figure 2.11. The snow melting has the lowest temperature of the heat recovery units and can be cooled down to 10°C or lower, dependent on the conditions. In the summer the heat recovery is only used for the DHW and the MT compressor can run in subcritical mode. In the winter, when all the heat recovery is needed, the MT compressor must run transcritically (Haukås (2016)).

The AC unit can only operate with parallel compression, because the AC unit is normally operated at the same pressure level as the receiver. On the AC-unit there is a valve with superheat control, which takes care of the compressor. The same flow reducing valves with superheat control are installed on the LT and MT evaporators to take care of the compressors. In addition to the suction gas heat exchanger before the MT compressor in Figure 2.13, a suction gas heat exchanger can be installed before the parallel compressor in a real system. This unit cools down the gas after the gas cooler, which guarantees superheat towards the parallel compressor.

The ejector supported parallel compression enables also flooded evaporators all year, which requires low pressure accumulator. Flooded evaporators allows a liquid phase at the evaporator outlet. It does not impose a danger for the compressor. The benefits are a possible elevation of the evaporation temperature (pressure) which improve the efficiency in the system in addition to reduced requirement for defrosting.

The ambient conditions play an important role on how the ejector operates. The multi-ejector has the same functions as a conventional high-pressure valve, which controls the system at COP optimum under cold ambient conditions. However, in warm ambient conditions some of the gas from the evaporators are lifted to the receiver. The gas compresses directly from the receiver to the parallel compressor. A part of the MT load is moved to the parallel compressor. As the load is moving, the load on the MT compressor reduces. The energy consumption decreases, due to the higher suction pressure at the parallel compressor.

According to Gullo et al. (2017a) the multi-ejector concept reduces the energy consumption at least 19.4% compared with a R404A system. Additionally, the integrated CO<sub>2</sub> solution at least 15.6% more energy than separated HFC system. Bodys et al. (2016) showed that a well-designed set of fixed ejectors, which combined to form a multi-ejector pack, provided high and stable performance over the entire operating range in supermarket applications.

Haida et al. (2016) showed that the R744 multi-ejector refrigerant system performs better in the COP by 7% compared to an R744 system with parallel compression. In addition, especially under high outdoor temperature periods, the efficiency of the system can increase up to 30% over a conventional booster system (Hafner et al. (2014)). Experimental data were collected from a refrigeration facility located in Spiazzo in Italy. The external temperatures ranged from 22°C to 35°C between first of May until end of October 2015. The energy consumption was reduced from 15% to 30% with the use of parallel compression, where the outdoor temperature and the AC demand had a strong impact (Hafner and Banasiak (2016)). Gullo et al. (2017b) showed that a multi-ejector based system without an AC-unit had energy saving from 8.6% to 22.3% in Athens compared to a R744 refrigeration system with parallel compression. This applied to both with as well as without overfed evaporators. According to Gullo et al. (2018), the multi-ejector concept excluding the AC demand leads to energy savings from 18.6% to 28.6% in locations with yearly temperatures between 14.1°C and 18.9°C.

### 2.4.2 R744 Transcritical supermarkets locations

Transcritical CO<sub>2</sub> supermarkets are located in different climates all over the world. According to Shecco (2020), there are more than 35 500 transcritical CO<sub>2</sub> installations globally today, illustrated in Figure 2.14. The direct consequence of the replacement of R404a and other HFC based systems are severe reductions in CO<sub>2</sub> equivalents, reductions in energy consumption and reductions in energy costs for the supermarket owner. Gullo et al. (2018) showed that the "CO<sub>2</sub> equator" is crossed and does not exist anymore.

### CO<sub>2</sub> transcritical installations in the world

sheccoBase



**Figure 2.14:** Transcritical CO<sub>2</sub> supermarkets globally in 2020. Adopted from Shecco (2020).

The “CO<sub>2</sub> only” installations generate significant energy savings, when adopted to local conditions, which implies climate and load profile. For conventional booster system, in Figure 2.11 is good enough for northern countries like Norway. For warmer climates, there are need for parallel compression or even a booster supported by an multi-ejector. According to Banasiak and Pardiñas (2019), the very essential point from the user’s or the supermarket owner’s perspective when investing in a “CO<sub>2</sub> only” refrigeration system is that there are no legal uncertainties or restrictions concerning CO<sub>2</sub> globally, which means that an imminent phase-out of CO<sub>2</sub> will never happen. The heat recovery is almost free of charge. If the heat is not utilized in the supermarket, it can be sold to a nearby company.

The challenges and barriers of installing “CO<sub>2</sub> only” systems are mainly non-technical, especially outside Europe. This can be a shortage of trained installers, service technicians, social and or political factors (Karampour et al. (2016), Banasiak and Pardiñas (2019)). According to Banasiak and Pardiñas (2019), there are a challenge with higher ambient conditions for example in India. Nevertheless, regards the level of annual temperature profiles, there are no significant technical issues related to “CO<sub>2</sub> only” systems anymore.

# Methodology

This chapter presents the ejector parameters, the test facility, the uncertainty analysis and the software Coolselector.

## 3.1 Ejector performance parameters

The performance of two-phase ejector can be described by the entrainment ratio, pressure ratio, the pressure lift and ejector efficiency. In this master thesis the performance is described for the multi-ejector, and not for a single ejector. The objective of using an ejector is to both entrain a fluid and to increase its pressure.

Pressure ratio is the quotient of pressure level of the outlet to the inlet suction pressure.

$$\Pi = \frac{p_{outlet}}{p_{suction}} [-] \quad (3.1)$$

The pressure lift is determined by the geometry of the ejector, operational conditions and system control. It is defined as the difference between the the ejector outlet pressure and the ejector inlet suction pressure. Whereby the outlet pressure of the ejector corresponds to the receiver pressure (liquid separator pressure) in a refrigeration system and the inlet suction pressure corresponds to the evaporator pressure. The definition of pressure lift is shown in Equation 3.2.

$$p_{lift} = \Delta p = p_{outlet} - p_{suction} [bar] \quad (3.2)$$

To evaluate the ejector work and ability to pump the low-pressure stream from the evaporator, it is necessary to know the mass flow rate of the motive and suction fluids. The low-pressure fluid can be entrained by the ejector until the pressure in the mixing chamber is lower than the pressure of the suction fluid. The mass entrainment ratio, Equation

3.3, is the quotient of the mass flow rate of the entrained (sucked) fluid and the mass flow rate of the motive fluid. Rising evaporator pressure helps increasing the entrainment ratio (Chunnanond and Aphornratana (2004)).

$$\Phi = \frac{\dot{m}_{suction}}{\dot{m}_{motive}} [-] \quad (3.3)$$

Elbel and Hrnjak (2008) define ejector efficiency on the basis of standard measured pressure, temperature, and mass flow rate. The ejector efficiency compares the amount of expansion work rate recovered by the ejector with the maximum possible expansion work rate recovery potential.

$$\eta_{ejector} = \frac{\dot{W}_{rec}}{\dot{W}_{max,rec}} [-] \quad (3.4)$$

where

$$\dot{W}_{rec,max} = \dot{m}_{MN}(h_A - h_B) \quad [kW] \quad (3.5)$$

and

$$\dot{W}_{rec} = \dot{m}_{MN}(h_C - h_D) \quad [kW] \quad (3.6)$$

can be expressed as

$$\eta_{ejector} = \frac{\dot{m}_{SN}(h_C - h_D)}{\dot{m}_{MN}(h_A - h_B)} = \Phi \frac{(h_C - h_D)}{(h_A - h_B)} [-] \quad (3.7)$$

In the equation above the  $\dot{m}_{SN}$  is the suction mass flow rate and the  $\dot{m}_{MN}$  is the mass flow rate of the ejector motive nozzle. The enthalpies at point A, B, C and D are respectively identified by  $h_A$ ,  $h_B$ ,  $h_C$ ,  $h_D$  in Figure 3.1.

Furthermore in Figure 3.1, point A presents the specific enthalpy at the motive inlet flow of the ejector. The specific enthalpy for point B found on the isentropic line of the motive inlet crossing the outlet pressure line in the two-phase area of the pressure and specific enthalpy diagram. The specific enthalpy of point D is the specific enthalpy of the inlet suction flow. Whereas point C is found on the suction flow isentropic line, which crosses the constant outlet pressure line. The ejector efficiency increases when entrainment ratio increases or the pressure lift decreases.



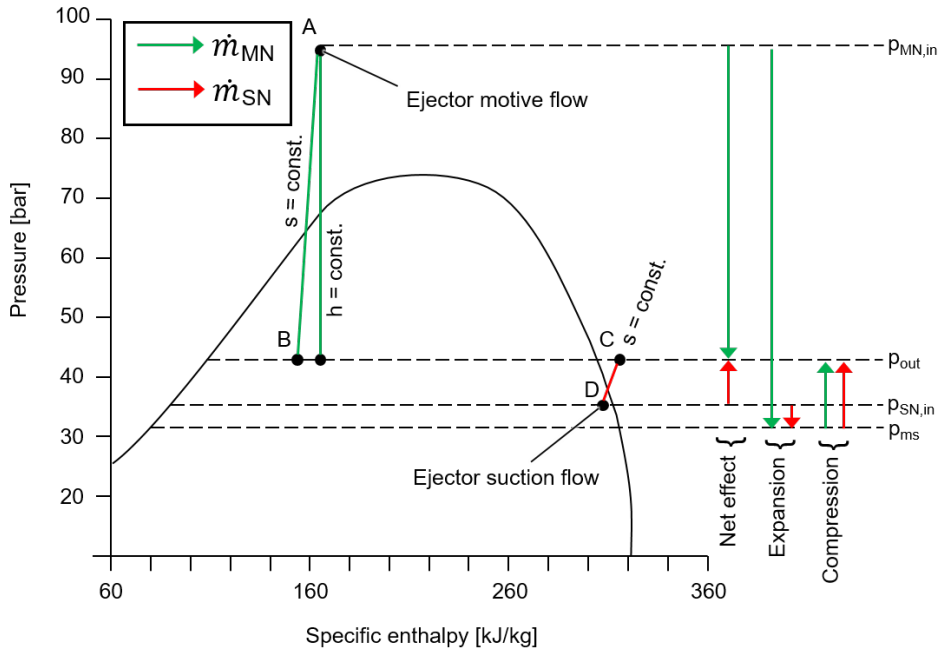


**Figure 3.1:** Pressure and specific enthalpy diagram to recognize the enthalpies  $h_A$ ,  $h_B$ ,  $h_C$ ,  $h_D$  that are included in the equation of the ejector efficiency of a two-phase ejector.

The vapour mass fraction (or quality) depends on the specific enthalpy and the pressure at the inlet of the evaporator. The vapour mass fraction varies between 0 and 1 for the inlet suction flow, which means saturated liquid or saturated vapour, respectively. The vapour mass fraction can be calculated as:

$$q = \frac{\dot{m}_{\text{suction inlet nozzle, vapour}} + \dot{m}_{\text{suction inlet nozzle, liquid}}}{\dot{m}_{\text{motive inlet}}} \quad [-] \quad (3.8)$$

## 3.2 Test facility

The R744 multi-ejector refrigeration test rig with parallel compression is located at Varmeteknisk at NTNU Trondheim. The rig was manufactured by Enex Company in collaboration with Danfoss Company and SINTEF. The prototype of the advanced multi-ejector from Danfoss was installed in 2019. The test facility is divided into three individual modules: R744 unit with oil management circuit, glycol module and the electrical cabinet. The R744 rig is shown in Figure 3.2, where pressure gauges and the compressors are in the front. The advanced multi-ejector is on the left side of the rig censored behind a pink rectangle.

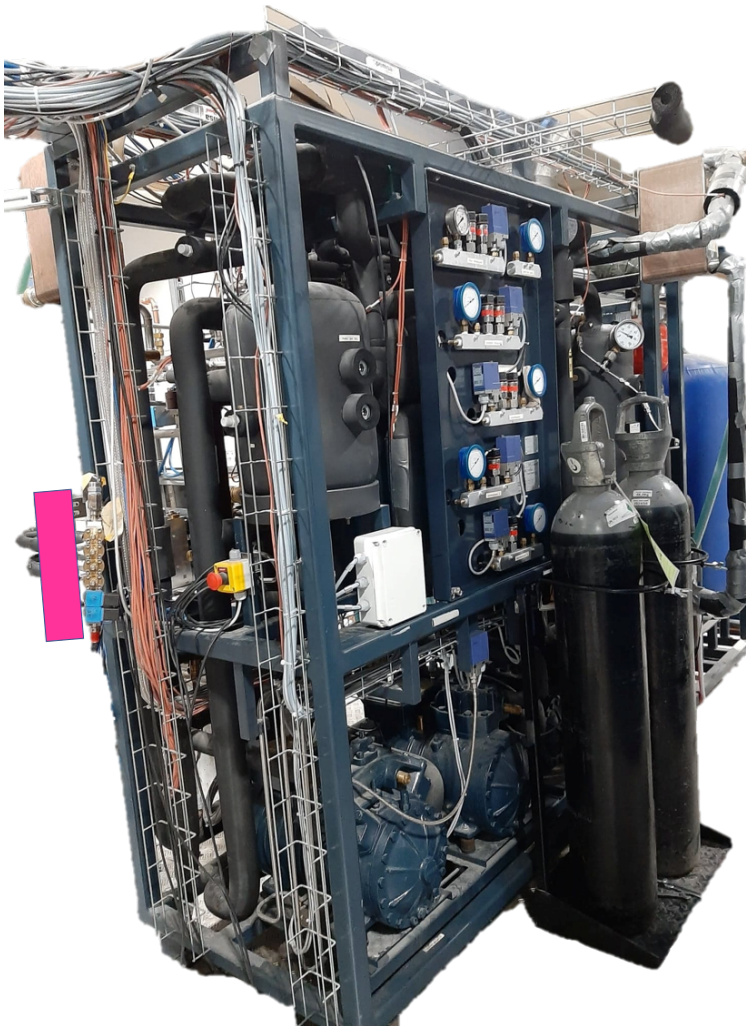


**Figure 3.2:** Experimental test facility with pressure gauges and compressors in front. The advanced multi-ejector is censored behind a pink shaped rectangle on the left side of the rig.

The pipeline and instrumental diagram of the R744 test rig is shown in Figure 3.3. The advanced multi-ejector is censored behind the pink rectangle.

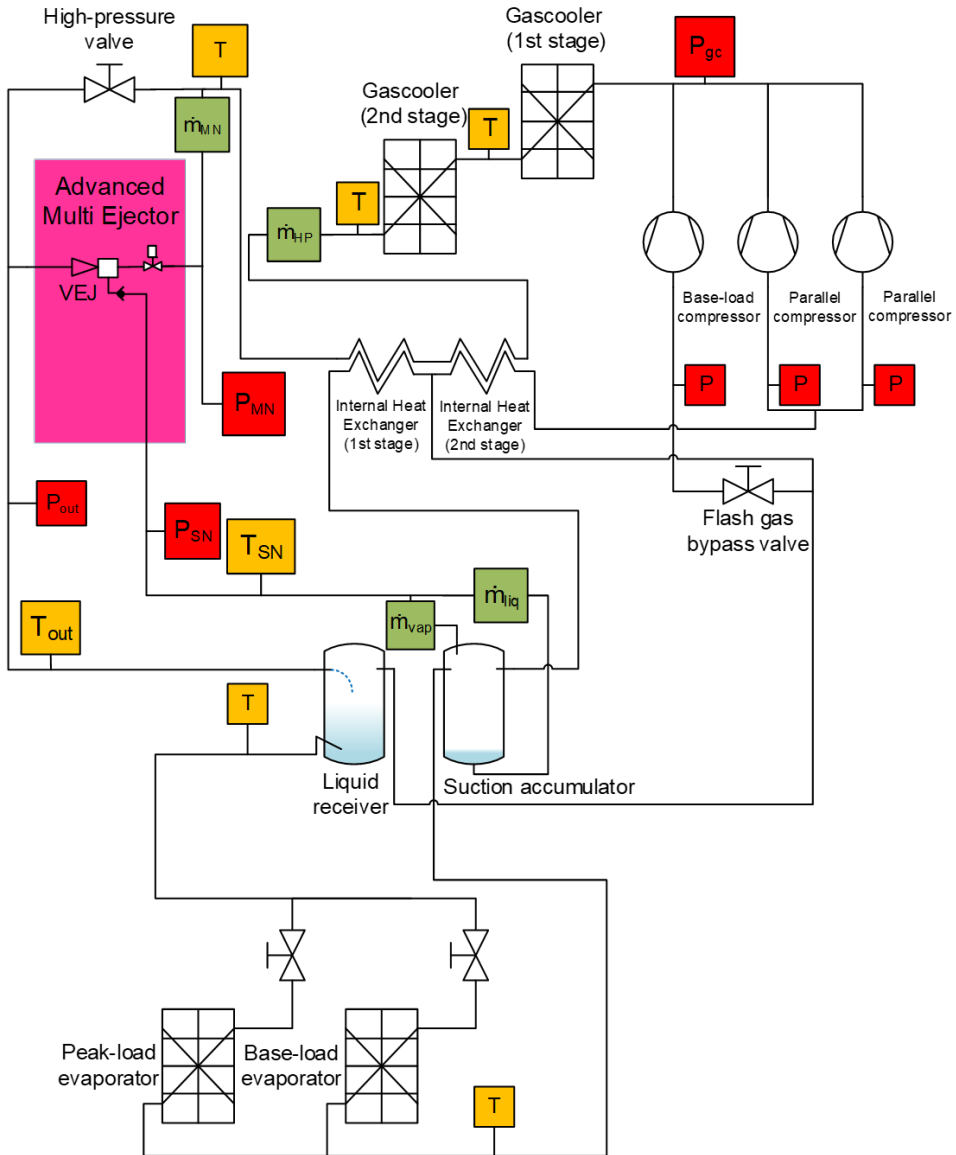


**Figure 3.3:** Illustrates the pipeline and instrumental diagram of the CO<sub>2</sub> test rig, where all main components are included. The water loop and glycol loop are excluded.

The temperature sensors (T) are coloured yellow, the mass flow sensors are coloured green and the pressure sensors are red in Figure 3.3.

The advanced multi-ejector is illustrated with one vapour ejector cartridge to show the principle. The number of cartridges in this thesis is secret, due to the patent situation.

The high pressure motive stream mixes with the vapour from the suction side. The working fluid CO<sub>2</sub> flows from the outlet of the multi-ejector at medium pressure level into the liquid receiver (known as receiver in this thesis). The liquid exits the liquid receiver at the bottom and the vapour escapes at the top. The pressure level in the liquid receiver can be regulated, because CO<sub>2</sub> has a constant density, which means the liquid level depends on the pressure level. The liquid receiver can be controlled by the flash gas valve.

The evaporator receives saturated liquid from the liquid receiver. The number of evaporators activated depends on the required capacity.

The working fluid continues to flow into the suction accumulator. If the testing requires liquid suction conditions, the level of liquid in the suction accumulator should be between 40% and 60%, to avoid damage on the compressor. This is regulated by the expansion valve. The peak-load evaporator should have no superheat, to get more liquid into the suction accumulator. However, in this thesis the vapour mass fraction is 1.

From the suction accumulator saturated or superheated vapour enters the compressors, in addition to the suction side of the vapour ejector. The suction side of the liquid ejector can be supplied by the liquid phase of the CO<sub>2</sub>. This makes it possible to utilize the evaporator in flooded mode.

The vapour from the liquid receiver is compressed by the compressor rack, which consist of a medium temperature compressor (base-load compressor) and two parallel compressors. When the parallel compressors are not in operation, the vapour from the liquid receiver is throttled by the flash gas bypass valve connected to the medium temperature compressor (base-load compressor). Depending on the operating mode, the pressure level in the liquid receiver is determined by the degree of opening of the flash gas bypass valve, the suction pressure of the base-load compressor or the ejector capacity. There are two manual valves on the suction side, respectively for vapour and liquid.

The vapour phase from both the accumulator and the receiver flow through the internal heat exchangers, and thereby absorb the heat from the high-pressure CO<sub>2</sub> downstream of the gas cooler section.

After the compression, the high pressure flow passes through the gas cooler stages. It flows into the multi-ejector and the high-pressure valve. The gas cooler outlet temperature is equal to the inlet motive temperature of the multi-ejector. The motive mixes with the suction and the process is fulfilled.

The test facility has a glycol loop that is connected to the first gas cooler and the evaporators. The purpose of the glycol loop is to absorb heat from the first stage gas cooler

and transfer the heat to the evaporators. The evaporator temperature (and the pressure) is proportional to the glycol temperature in the heat exchanger. The evaporator pressure is equal to the multi-ejector suction pressure.

A water loop is connected to the second stage gas cooler. The outlet temperature of the gas cooler is regulated by the mass flow rate of the cooling water since the water loop absorbs heat from the second stage gas cooler. The ejector motive temperature increases proportionally with the water temperature in the gas cooler.

A closer inspection of the advanced multi-ejector is found in Figure 3.4. The motive and the suction stream of the advanced multi-ejector flow into the each of the inlets of the left side and the ejector outlet is on the right side of the picture.

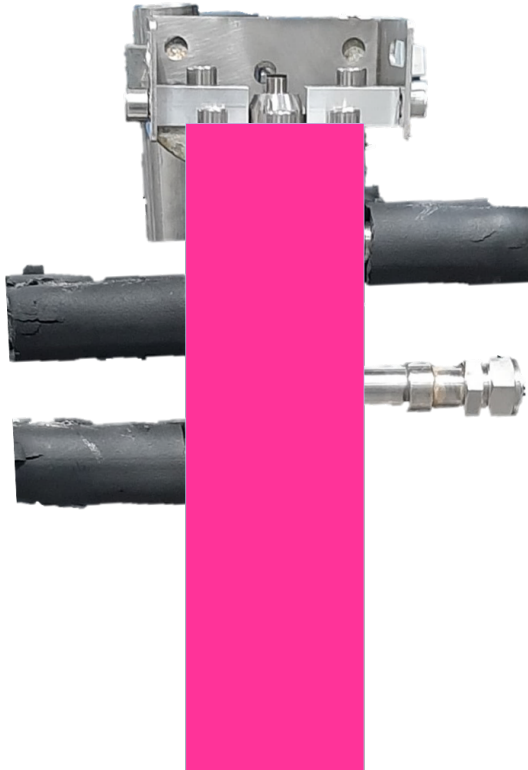


**Figure 3.4:** A closer look at the censored advanced multi-ejector developed by Danfoss.

### 3.2.1 Component description and MiniLog

The advanced multi-ejector in Figure 3.4 is not described, due to the prototype's restrictions. The construction and design inside the prototype is strictly classified. The main components in the rig are in Table 3.1. Since the main objective of this master thesis focuses only on the multi-ejector, a comprehensive description of the components in Table 3.1 and sensors in Table 3.2 will be excluded. However, a more detailed description of the components in the test facility can be found in the thesis from Haida (2015).

**Table 3.1:** Set of main components in the R744 multi-ejector test rig.

System Component	Model	Type
Base-load compressor	Dorin CD 1400H	Semi-hermetic reciprocating
Parallel compressor #1	Dorin CD 1000H	Semi-hermetic reciprocating
Parallel compressor #2	Dorin CD 380H	Semi-hermetic reciprocating
First-stage gas cooler	SWEP B18Hx100	Brazed plates heat exchanger
Second-stage gas cooler	KAORI K095C-30C-NP8M	Brazed plates heat exchanger
Base-load evaporator	SWEP B16DWHx100	Brazed plates heat exchanger
Liquid receiver tank	Frigomec 39-litre	Pressure vessel
Liquid separator tank		
Oil accumulator tank	Frigomec 21-litre	Pressure vessel
Cold glycol tank	IMA 200-litre	Thermal storage tank
High-pressure valve	Danfoss CCMT8	Electronic expansion valve
Flash valve		
Base-load evaporator - metering valve	Danfoss CCM20	Electronic expansion valve

Set of sensors installed to monitor the test facility is presented in Table 3.2. The accuracies of the temperature, pressure and mass flow rate sensors are taken from product data sheets. The pressure sensors are from Danfoss (2020b). The temperature sensors are from the company Omega. They are PT1000 Class A and the accuracy is found in the standard for thermometers, IEC 60751:2008. The mass flow rate sensor type RHM 06 is from Rheonik (2019a) and the type RHM 08 is from Rheonik (2019b). The accuracies and the uncertainties are utilized in the uncertainty analysis found in Section 3.3.

**Table 3.2:** Sensor specifications at the test facility. FS means full scale (range).

Variable	Transducer	Accuracy	Range
Pressure	Piezoelectric transmitter MBS8250 064G1136	$\pm 0.5\%$ FS (FS= 160 bar)	-1 –159 bar
Temperature	Resistance thermometer PT1000 (PR21A31000-A-M6-0150-M12)	$\pm(0.15 + 0.002 t )$ (Class A, t in $^{\circ}C$ )	$-30^{\circ}C - +300^{\circ}C$
Uncertainty			
Mass flow rate	Coriolis type RHM 06	$\pm 0.12\%$ <i>m</i> (Goldline calibration)	0.5 – 20 kg/min
Mass flow rate	Coriolis type RHM 08	$\pm 0.12\%$ <i>m</i> (Goldline calibration)	1.0 – 50 kg/min

The main operating and controlling program of the test facility is MiniLog developed by Danfoss. The output signals from the sensors are transmitted to MiniLog, which is installed on the operator computer. MiniLog has a graphical 2- dimensional representation of the selected parameters. If the graph is adjusted correctly, it is easy to identify if the system is running steady. The time step was set to minimum 7 minutes to ensure stability of the pressures, temperature and mass flow rates. After a successful recorded measurement, the data was exported from MiniLog to Microsoft Excel as spreadsheets. The entrainment ratios, pressure lifts, ejector efficiencies in addition to the uncertainties were calculated for every single recording in Microsoft Excel. The fluid properties for R744 were calculated using CoolProp version 6.4.1 installed in Microsoft Excel.

### 3.2.2 Test conditions

The test conditions provided by Danfoss are listed in Table 3.3. The measurements in the laboratory are based on these operational modes. Further test conditions were specified by Danfoss, which ranged up to 120 bar for the inlet motive nozzle pressure. However, due to the test facilities pressure limitation at 100 bar for safety reasons, the highest measurement was carried out at 89 bar. The results of the measurements can be found in Section 4.1.

**Table 3.3:** Multi-ejector test conditions from Danfoss.

$p_{MN}$ [bar]	$t_{MN}$ [°C]	$p_{SN}$ [bar]	$t_{SN}$ [°C]	$p_{out}$ [bar]	$\Delta p$ [bar]
58.65	19	26.5	-4	28.66	2.16
58.65	19	26.5	-4	29.03	2.53
58.65	19	26.5	-4	29.40	2.90
65.84	26	26.5	-4	29.06	2.56
65.84	26	26.5	-4	29.62	3.12
65.84	26	26.5	-4	30.15	3.65
83	34	26.5	-4	31.85	5.35
83	34	26.5	-4	32.95	6.45
83	34	26.5	-4	33.99	7.49
89	34	26.5	-4	33.99	7.49



### 3.3 Uncertainty analysis

The goal of a measurement is to determine certain characteristic features on an object or a performance. The reliability of the acquisition of the measurements gives a statement over the quality of the results (Testo industrial services GmbH (2020)).

The error of the measurement is defined by the difference between the true value and the measured value. The only way to determine both the true and the measured value is through calibration. On the other hand, the accuracy of the measured value can be expressed by the concept of uncertainty, which refers to a possible value that an error can have with a defined probability (Moffat (1988)).

Generally, the uncertainties of the result are divided into two different categories, Type A and Type B, depending on the method used to estimate their numerical values. Type A is evaluated by statistical methods, whereas Type B is evaluated by other means. A common way to describe the terms are respectively "random" and "systematic" (Taylor and Kuyatt (1994)).

The evaluation and expression of the uncertainties were carried out based on the NIST guideline (Taylor and Kuyatt (1994)), the GUM guideline in JCGM (2008) and the description of the uncertainties in experimental results from Moffat (1988).

#### 3.3.1 Type A and Type B evaluation of standard uncertainty

The sample mean of input quantity  $X_i$  for  $n$  independent recorded measurements is expressed as:

$$x_i = \bar{X} = \frac{1}{n} \sum_{k=1}^n X_{i,k} \quad (3.9)$$

The standard deviation  $s$  is defined as:

$$s = \sqrt{\frac{1}{(n-1)} \sum_{k=1}^n (X_{i,k} - \bar{X}_i)^2} \quad (3.10)$$

The uncertainty of Type A, denoted  $u_A(x)$ , is defined as the standard deviation divided by the square root of  $n$  samples. In other words the standard uncertainty is the standard deviation of the mean sample.

$$u_A(x) = \frac{s(x)}{\sqrt{n}} \quad (3.11)$$

Equation 3.11 applies as long as each of the measurements is independent. If there is repeated observations of each measurement, that would mean a Gaussian distribution. Finally, the uncertainty in each measurement is initially expressed at the same odds. The

purpose of the uncertainty analysis is to determine the uncertainty of the result at known odds.

The rectangular probability distribution is used for the Type B evaluation. This is due to the fact that it is possible to estimate the accuracy, which is the upper and the lower limit range for  $\bar{X}$  indicated in Figure 3.5. The accuracy is provided by the manufacturer. It can only be assumed that the mean value  $\bar{X}$  is the midpoint of the interval:

$$x_i = \frac{a_+ + a_-}{2} = \frac{(\bar{X} + a_{\text{accuracy}}) + (\bar{X} - a_{\text{accuracy}})}{2} \quad (3.12)$$

The associated variance  $u_{x_i}^2$  is then

$$u_{x_i}^2 = \frac{(a_+ - a_-)^2}{12} \quad (3.13)$$

where the difference of the bounds,  $a_+ - a_-$ , is denoted by  $2a$ , then Equation 3.13 becomes the uncertainty of Type B:

$$u_B = u_{x_i} = \frac{\frac{a_+ + a_-}{2}}{\sqrt{3}} = \frac{a}{\sqrt{3}} \quad (3.14)$$

Figure 3.5 illustrates the rectangular probability distribution of a parameter  $x$ , which can be temperature or pressure etcetera. The accuracy range of the parameter is  $a$ . The accuracy area in green is indicated between the lower limit  $a_-$  and the higher limit  $a_+$  on the x-axis. The real value including the uncertainty lies somewhere between the lower limit  $\bar{X} - \frac{a}{\sqrt{3}}$  and the higher limit  $\bar{X} + \frac{a}{\sqrt{3}}$ , which is in the blue area of the figure. The probability density of  $x$  is  $\frac{1}{2}a$ , and illustrates how likely different results are in relation to each other (JCGM (2008)).

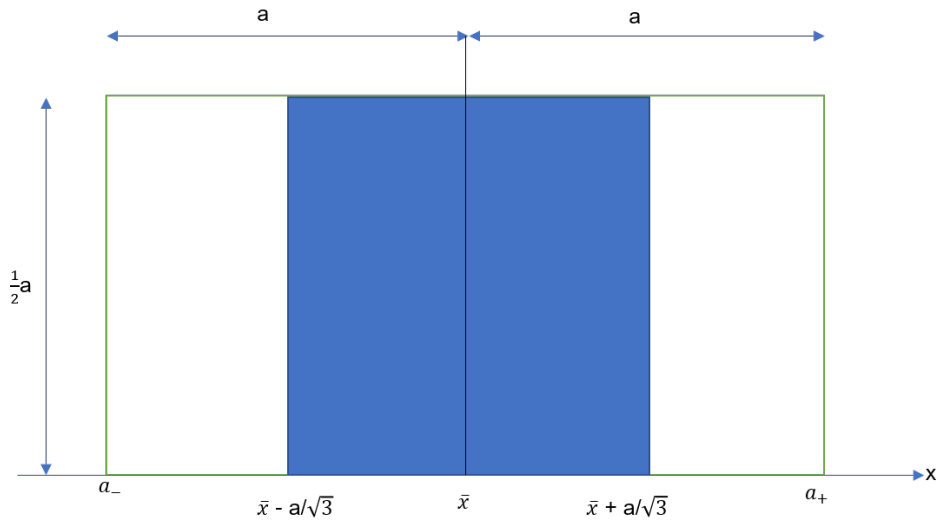


**Figure 3.5:** A illustration of the rectangle distribution in Type B. The accuracy from data sheets is symbolised as  $a$ .

The uncertainty of a result should always be presented with its boundaries of probability, since each measured variable contributes to the uncertainty of the final result. The combined uncertainty of a function, known as the root-sum-square method, depends on several independent variables.

$$u_{c,j} = \sqrt{\sum_{n=1}^{i=1} \left[ \frac{\partial f}{\partial x_i} u_j(x_i) \right]^2} \quad (3.15)$$

where  $u_{c,j}$  can be the uncertainty of Type A or Type B. The partial derivation of a function is formulated as:

$$\frac{\partial f}{\partial x} = \frac{f(x + dx, y) - f(x, y)}{dx} \quad (3.16)$$

The forgoing approach is shown in Section 3.3.2, where the calculation steps for the ejector efficiency are described.

The overall uncertainty is calculated as the root sum square of the fixed errors (Type A) and the random errors (Type B).

$$U = \sqrt{(u_A)^2 + (u_B)^2} \quad (3.17)$$

### 3.3.2 Uncertainty of the ejector efficiency

The calculation of the root-sum-square method shown in Equation 3.15 will be deducted as an example for calculating the uncertainty of the ejector efficiency.

The ejector efficiency  $\eta_{EJ}$  described previously in Section 3.1 is calculated by:

$$\eta_{ejector} = \frac{\dot{m}_{suction}(h_C - h_D)}{\dot{m}_{motive}(h_A - h_B)} \quad (3.18)$$

where the  $\dot{m}$  is the mass flow rate and  $h$  is the specific enthalpy.

The ejector efficiency, in Equation 3.18, consist of the six independent parameters:

$$\eta = f(\dot{m}_{MN}, \dot{m}_{SN}, h_A, h_B, h_C, h_D) \quad (3.19)$$

Thus, the uncertainty for the ejector efficiency is:

$$U_\eta = \sqrt{\left[\frac{\partial \eta}{\partial \dot{m}_{MN}} u_{\dot{m}_{MN}}\right]^2 + \left[\frac{\partial \eta}{\partial \dot{m}_{SN}} u_{\dot{m}_{SN}}\right]^2 + \left[\frac{\partial \eta}{\partial h_A} u_{h_A}\right]^2 + \left[\frac{\partial \eta}{\partial h_B} u_{h_B}\right]^2 + \left[\frac{\partial \eta}{\partial h_C} u_{h_C}\right]^2 + \left[\frac{\partial \eta}{\partial h_D} u_{h_D}\right]^2} \quad (3.20)$$

where the partial derivative terms of the independent parameters in Equation 3.19 can be calculated as follows:

$$\frac{\partial \eta}{\partial \dot{m}_{MN}} = -\frac{\dot{m}_{SN}}{\dot{m}_{MN}^2} \frac{(h_C - h_D)}{(h_A - h_B)} \quad (3.21)$$

$$\frac{\partial \eta}{\partial \dot{m}_{SN}} = \frac{1}{\dot{m}_{MN}} \frac{(h_C - h_D)}{(h_A - h_B)} \quad (3.22)$$

$$\frac{\partial \eta}{\partial h_A} = -\frac{\dot{m}_{SN}}{\dot{m}_{MN}} \frac{(h_C - h_D)}{(h_A - h_B)^2} \quad (3.23)$$

$$\frac{\partial \eta}{\partial h_B} = \frac{\dot{m}_{SN}}{\dot{m}_{MN}} \frac{(h_C - h_D)}{(h_A - h_B)^2} \quad (3.24)$$

$$\frac{\partial \eta}{\partial h_C} = \frac{\dot{m}_{SN}}{\dot{m}_{MN}} \frac{1}{(h_A - h_B)} \quad (3.25)$$

$$\frac{\partial \eta}{\partial h_D} = -\frac{\dot{m}_{SN}}{\dot{m}_{MN}} \frac{1}{(h_A - h_B)} \quad (3.26)$$

Now, the uncertainties for the mass flows and the enthalpies must be calculated. The uncertainty of specific enthalpy has to be destined for the positions  $i = A, B, C$  and  $D$ , where the specific enthalpy in a certain location inside the system is dependent on the local temperature and pressure.

The uncertainty of the specific enthalpy is:

$$u_{h_i} = \sqrt{\left(\frac{\partial h_i}{\partial t_i} u_t\right)^2 + \left(\frac{\partial h_i}{\partial p_i} u_p\right)^2} \quad (3.27)$$

where the partial derivatives can be calculated by:

$$\frac{\partial h_i}{\partial t_i} = c_{p,ref}(t_i, p_i) \quad (3.28)$$

where the specific heat capacity  $c_{p,ref}$  is calculated in *Microsoft Excel* as a direct function using *CoolProp*.

$$\frac{\partial h_i}{\partial p_i} = \frac{h(t_i, p_i + \Delta p) - h(t_i, p_i)}{\Delta p} \quad (3.29)$$

where  $\Delta p$  is a small pressure difference which is implemented to calculate the partial derivation gradient.

The uncertainty of the six parameters in the ejector efficiency must independently be calculated for Type A uncertainty and thereafter for Type B uncertainty. Type A is simply the standard deviation of the mean sample.

For Type B calculations the accuracies or the uncertainties are found in the respective data sheets of the manufacturer. For this thesis, the Type B uncertainties are as follows:

Mass flow rate:

$$u_{\dot{m}} = 0.12\% * \bar{\dot{m}} \quad (3.30)$$

Temperature:

$$u_t = \frac{0.15 + 0.002 * \bar{t}}{\sqrt{3}} \quad (3.31)$$

Pressure:

$$u_p = \frac{0.5\% * 160}{\sqrt{3}} \quad (3.32)$$

The sensor information is found in Table 3.2.

The ejector efficiency for Type A is calculated by Equation 3.20 with use of only Type A uncertainties from the mass flow rates, the pressures and the temperatures. The ejector efficiency for type B is calculated by Equation 3.20 with use of only type B uncertainties. After the ejector efficiency for Type A and Type B is calculated, the two uncertainties can be combined in an overall uncertainty by the above mentioned root-sum-square method in Equation 3.17.

The pressure lifts and the entrainment ratios of the laboratory results were calculated with the same method as the ejector efficiency.

### 3.3.3 Uncertainty of the superheat

Superheat is defined as the difference between the ejector suction nozzle temperature and the saturated ejector suction nozzle temperature:

$$SH = T_{SN} - T_{SN,sat} \quad [K] \quad (3.33)$$

In case of superheat, the uncertainties from the pressure sensor and the temperature sensor must be evaluated in the same calculation. The suction temperature is measured by a temperature sensor, while the saturated suction temperature is a function of the suction pressure.

First, the uncertainties of Type A and Type B is evaluated for the ejector suction temperature. The Type A uncertainty is calculated by the standard deviation of the mean in Equation 3.11. The uncertainty for Type B is calculated in Equation 3.31, which is based on the uncertainty data from the manufacturer.

Second, the uncertainties for Type A and Type B is evaluated for the saturated ejector suction temperature. The Type A uncertainty for the saturated ejector suction temperature is calculated by inserting the Type A uncertainty for the suction pressure,  $u_{p_{SN}}$  given in Equation 3.32, into the rectangular distribution. The Type B uncertainty of the saturated ejector suction temperature is calculated by inserting the Type A uncertainty for the suction pressure,  $u_{p_{SN}}$  given in Equation 3.32 into the rectangular distribution. The rectangular distribution is calculated as follows, where j is Type A and Type B uncertainty.

$$u_{T_{SN,sat,j}} = \frac{\frac{T_{SN,sat,max} - T_{SN,sat,min}}{2}}{\sqrt{3}} \quad (3.34)$$

where the upper temperature limit is

$$T_{sat,max} = T(p_{SN} + u_{p_{SN,j}}) \quad (3.35)$$

and the lower temperature limit is

$$T_{sat,min} = T(p_{SN} - u_{p_{SN,j}}) \quad (3.36)$$

The above calculations were calculated by CoolProp in Microsoft Excel. Finally, the uncertainties for the superheat are calculated by

$$u_{SH,j} = \sqrt{(u_{T_{SN,j}})^2 - (u_{T_{SN,sat,j}})^2} \quad (3.37)$$

where j is Type A or Type B uncertainty.

Thus, the overall uncertainty for the superheat with the use of the root-sum-square method in Equation 3.17, is

$$U_{SH} = \sqrt{(u_{SH,TypeA})^2 - (u_{SH,TypeB})^2} \quad (3.38)$$

### 3.4 Coolselector<sup>®</sup>2 calculation and selection software from Danfoss

Coolselector<sup>®</sup>2 version 3.8.1, henceforth called Coolselector, is a calculation and selection software developed by Danfoss. The software is free of charge and can be downloaded easily from their website. The software was developed to assist the user in selecting Danfoss refrigeration components. The user has to select performance, operating temperatures and refrigerant that are relevant. The program immediately suggests the optimal Danfoss products to the user. Each recommendation is based on a calculation of the actual performance of the component in the desired cooling system. In this thesis the multi-ejector option under valves and line components are used in Coolselector.

The main reason for using Coolselector in this thesis, is to compare the advanced multi-ejector with R744 transcritical multi-ejectors from Danfoss under the same operating conditions. In order to do that, recommended multi-ejectors in Coolselector with the same conditions are compared in Microsoft Excel with the advanced multi-ejector. The final result of the comparison is found in Section 4.2.

In Coolselector, see Figure 3.6, two options of multi-ejector systems were used in this thesis; the transcritical low pressure lift (LP) ejector system and the transcritical high pressure lift (HP) ejector system. The generation of equations behind the ejector calculations in Coolselector is based on the ejector results of the work of Banasiak et al. (2015a), which was presented in the literature review in Section 2.3.

The multi-ejector low pressure lift (LP) multi-ejector is optimal for CO<sub>2</sub> booster systems. The optimal size is between 40 and 150 kW. It is well suited for warm climates. At example 23 degrees it has 3 bar pressure lift and 63% entrainment ratio. At higher ambient temperatures as 36 degrees, the pressure lift is 7 bar and entrainment ratio is 50%. The energy consumption can be reduced up to 15% compared to a conventional booster system. The LP multi-ejector provides higher savings in locations with higher than lower ambient temperatures.

A multi-ejector high pressure (HP) is optimal for parallel compression systems. By example 23°C the pressure lift is 6 bar and the entrainment ratio 25%. At 36°C the pressure lift is 11 bar and has the same entrainment ratio as the latter. Compared to LP multi-ejector at the same temperature, the pressure lifts are higher and the entrainment ratios lower. The cooling capacity is between 100 and 300 kW (Danfoss (2018a)).

The first calculations in Coolselector were made for the transcritical LP multi-ejector and then for the transcritical HP multi-ejector, which will be described in the same order in the next two subsections.



### 3.4.1 LP multi-ejector

The results from the laboratory are inserted one after another into the transcritical LP multi-ejector system. The scheme, see Figure 3.6 shows a low temperature (LT) evaporation and a medium temperature (MT) evaporation section.

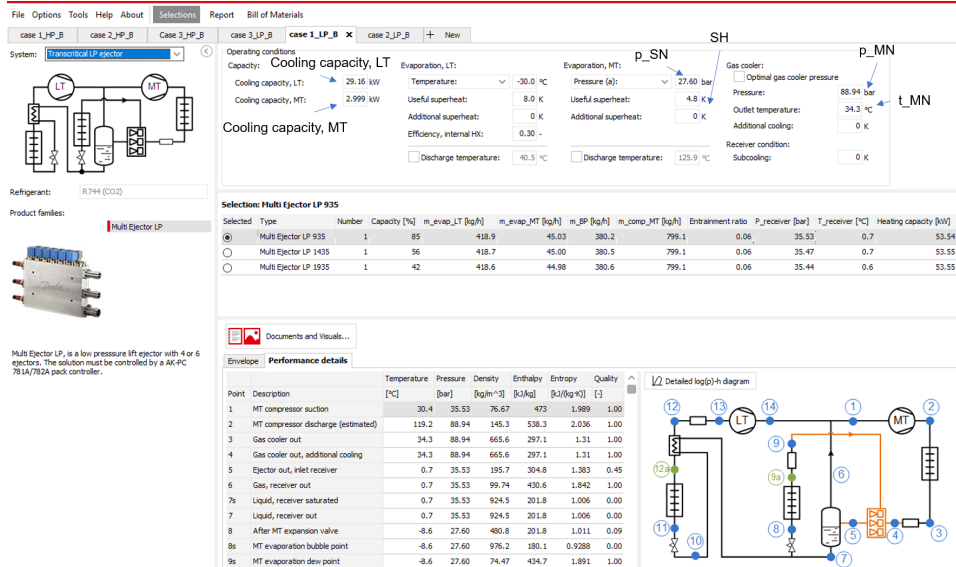


Figure 3.6: Example on a calculation of a LP multi-ejector system in Coolselector.

A single test from the results are only inserted into the MT part of the scheme as follows: The absolute pressure given in bar is equal to the suction nozzle pressure  $p_{SN}$  for a single test of the advanced multi-ejector. Next, the *useful superheat* is inserted, which is calculated in Equation 3.33. Then the values for the gas cooler are inserted. The motive inlet nozzle pressure is inserted for the *gas cooler pressure*. The *gas cooler outlet temperature* is the inlet motive nozzle temperature of the multi-ejector. The *additional cooling* is set to zero as well as *subcooling*.

The comparison calculations are based on three different cases, which is shown in Table 3.4.

**Table 3.4:** Three cases for comparison in Coolselector.

	Case 1	Case 2	Case 3
Find	$\dot{m}_{suction}$	$p_{receiver}$	$\dot{m}_{motive}$
Constant value	$p_{receiver}$	$\dot{m}_{suction}$	$p_{receiver}$
Constant value	$\dot{m}_{motive}$	$\dot{m}_{motive}$	$\dot{m}_{suction}$

The suction mass flow rate, receiver pressure (outlet ejector pressure) and motive nozzle mass flow rate are the different parameters used in all the three cases. For each case, there are one variable and two constants, which follow the same order as mentioned above. The cases are used both for the LP and the HP option.

Case 1 has the suction nozzle mass flow rate as a variable of interest, while the two other two parameters are constants. For the LP option, see Figure 3.6, the suction nozzle mass flow rate is the same as the MT evaporator mass flow rate ( $m_{evap\_MT}$  [kg/h]). The receiver pressure is  $P_{receiver}$  [bar] and the motive nozzle mass flow rate is the medium temperature compressor mass flow rate ( $m_{comp\_MT}$  [kg/h]).

The motive nozzle mass flow rate is regulated proportionally by change of the lower temperature cooling capacity (*Cooling capacity, LT*). The receiver pressure is controlled by the medium temperature cooling capacity and those are inversely proportional to each other. When the cooling capacities are perfect adjusted in such a way that the motive nozzle mass flow rate and the receiver pressure are the same as a laboratory measurement, then it results in a new suction mass flow rate. In addition a new entrainment ratio is calculated automatically. The new pressure lift is found by the subtraction between the receiver pressure and the suction nozzle pressure. Case 1 is solved and is thereafter compared with the advanced multi-ejector.

Next, Case 2 is to find the receiver pressure. The same is done as in Case 1, but this time the suction nozzle mass flow rate,  $m_{evap\_MT}$  [kg/h], is being proportionally regulated by the medium temperature cooling capacity.

Finally, Case 3 is to find the motive nozzle mass flow rate. The two constant parameters is found by changing the capacity as previous described.

In each case Coolselector shows the best comparable LP multi-ejector. The three cases are performed for each test. The system sketch for the LP multi-ejector system and the corresponding ph-diagram is shown in Figure 3.7 and Figure 3.8. The ejector process is shown by the thermodynamic states 4, 5 and 9 presented in orange colour in Figure 3.8. The LP system is a 3. generation of booster system, which was presented in the literature review in Section 2.4.1. The difference from a HP system, is that there are no AC and parallel compressor.

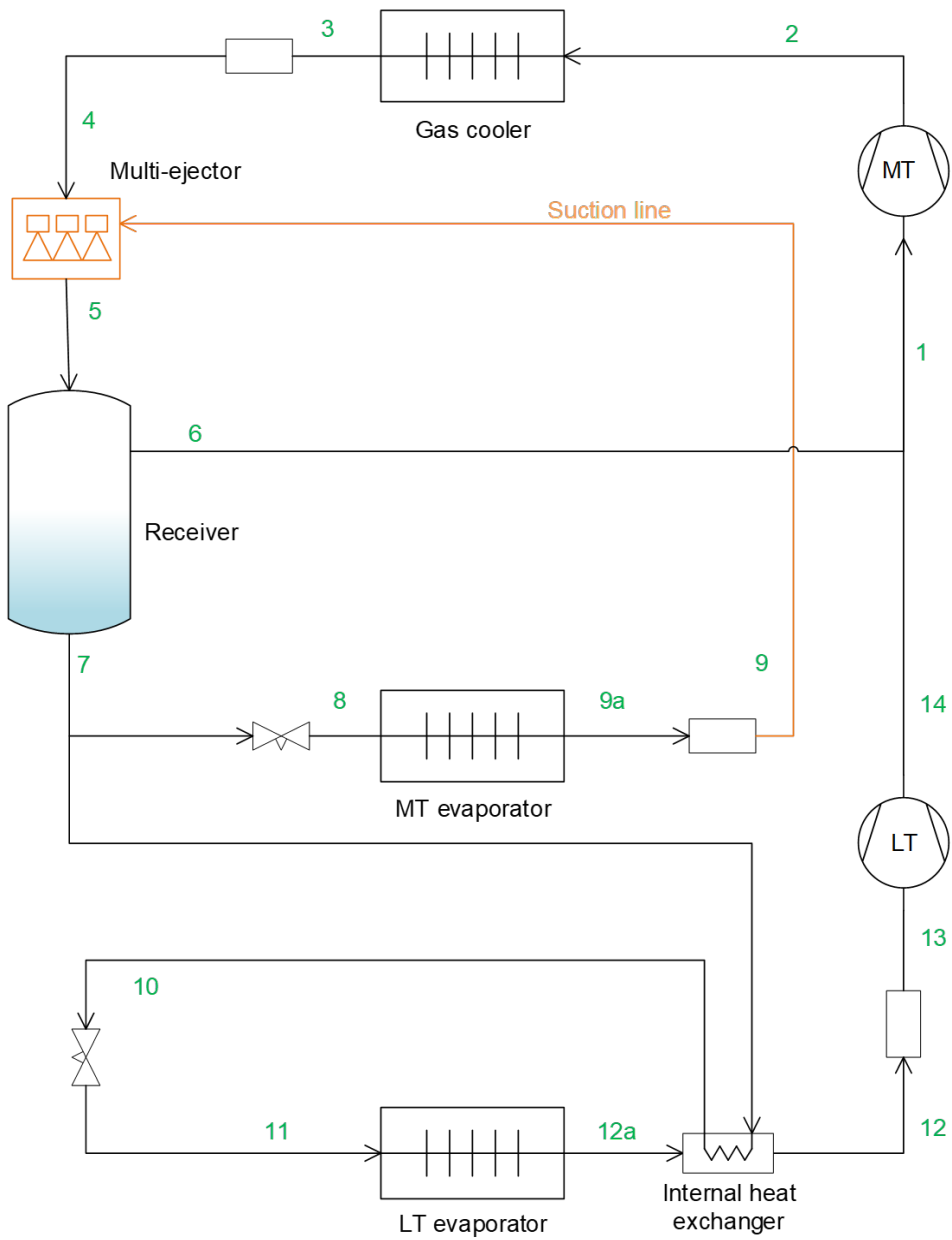


**Figure 3.7:** System sketch for the LP multi-ejector system in Coolselector

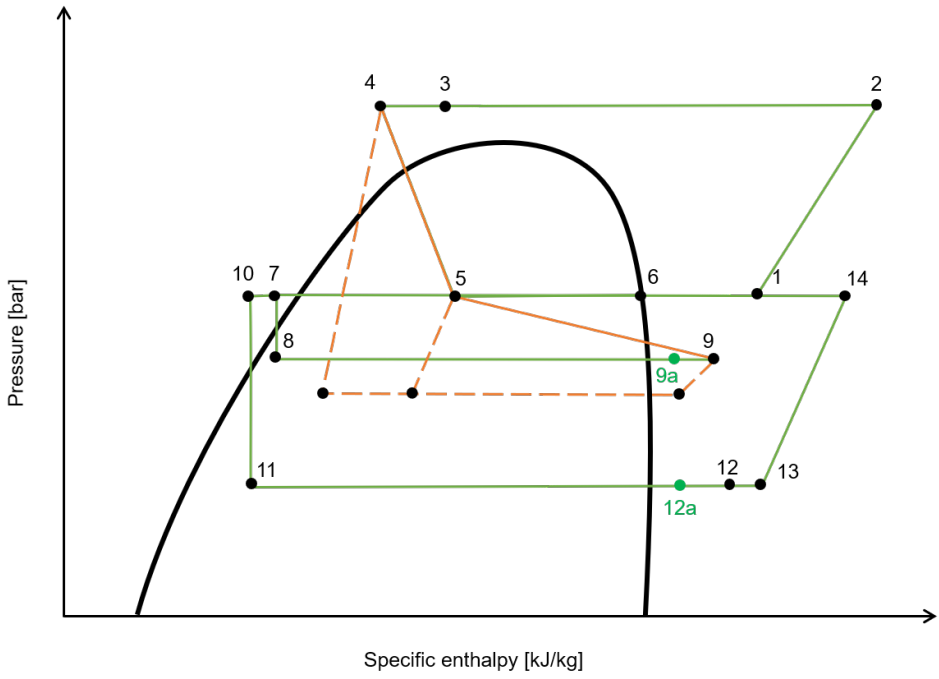


**Figure 3.8:** Pressure-specific enthalpy (ph) diagram for the LP multi-ejector system in Coolselector

### 3.4.2 HP multi-ejector

Coolselector for the transcritical HP multi-ejector is shown in Figure 3.9.

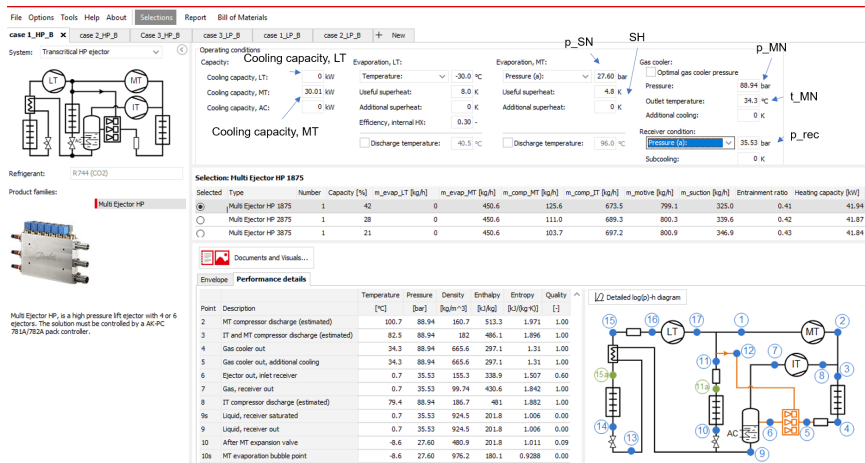


**Figure 3.9:** Example on a calculation of a HP multi-ejector system in Coolselector

The operating conditions are the the same as the LP system apart from the *receiver condition*, which is inserted. This is because of the insert of the parallel compressor, which is shown between the thermodynamic states 7 and 8 in Figure 3.10. The HP-system is the same as the presentation of the 3.generation of booster system introduced in Section 2.4.1. The illustration is simpler than in the literature review, but here are also the belonging ph-diagram presented. The multi-ejector starts to pump when the gas cooler is warm. The gas from the MT compressor is pumped through the ejector and is lifted to the receiver, where it is separated with the gas from the expansion. The liquid flows to the evaporator and the gas is moved to the parallel compressors where it is compressed. The ejector process is illustrated orange in the ph-diagram in Figure 3.11, where the dotted lines show the real process between 5, 6 and 12. The dotted line up to 6 shows what is taken out of the flow, which originally should have gone to the MT compressor, if the ejector where not in the process.

For the HP system the motive- and the suction nozzle flow rate is respectively  $m_{motive}$  [kg/h] and  $m_{suction}$  [kg/h] in Coolselector illustrated by Figure 3.9.

The LT cooling temperature is set to zero in all three cases, since the receiver pressure does not have to be regulated. The only regulation needed, is the regulation of the MT cooling capacity.

The same cases applies for the HP system as for the LP system, see Table 3.4. In Case 1 the suction nozzle mass flow rate is to be found and since the receiver pressure is already set in the operating conditions, the only parameter to control is the motive nozzle mass flow rate. In Case 2 the receiver pressure changes automatically, when the motive- and

the suction nozzle mass flow rates are found by changing the capacity. At last, in Case 3 where the motive nozzle mass rate is found, the receiver pressure is already given and therefore only the suction nozzle flow rate has to be regulated.

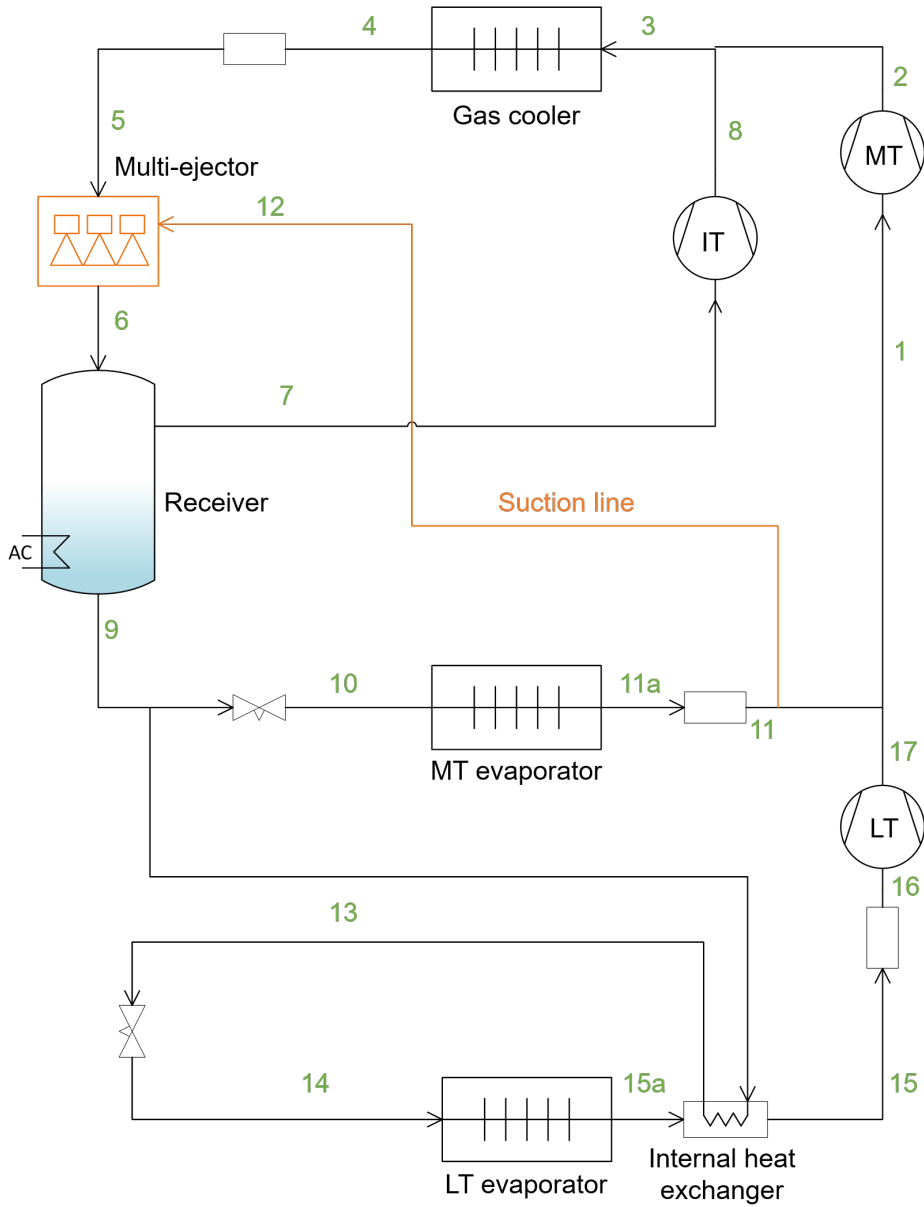


**Figure 3.10:** System sketch for the HP multi-ejector in Coolselector

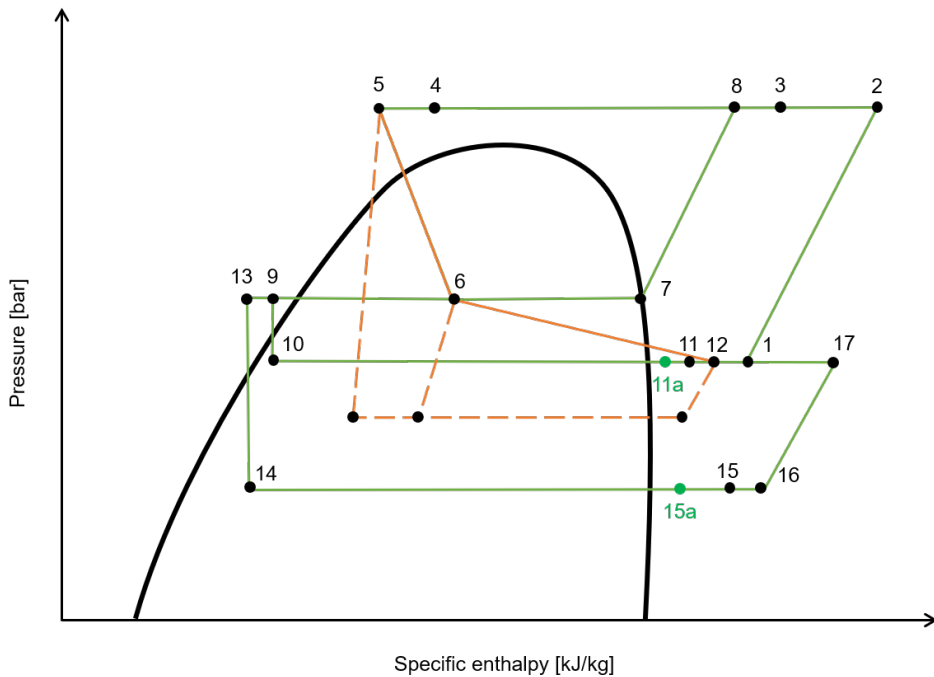


**Figure 3.11:** Pressure-specific enthalpy diagram for the HP multi-ejector system in Coolselector

### 3.4.3 Ejector efficiency calculation from Coolselector

To calculate the ejector efficiencies of the multi-ejectors for both LP and HP systems, equation 3.7 was used.

Under *performance details* in the Coolselector scheme the following parameters are found and needed for the ejector efficiency calculation: temperature [ $^{\circ}\text{C}$ ], pressure [bar], specific enthalpy [kJ/kg] and entropy [kJ/kgK].

The LP multi-ejector efficiency is found by point 3 (gas cooler out), 5 (ejector out, inlet receiver) and 9 (ejector suction) in the LP configuration system, see Figure 3.7. The HP configuration, see Figure 3.10, point 4 (gas cooler out), point 6 (ejector out, inlet receiver) and point 12 (ejector suction inlet) are needed for the ejector efficiency calculation. The calculations were performed using Microsoft Excel.





# Results

This chapter presents the experimental results of the advanced multi-ejector at various operational modes at the test facility. An uncertainty analysis is carried out, in addition to a number of results that have been compared to other multi-ejectors on the commercial market today with the use of Coolselector. The methodology behind the results is previously presented in Chapter 3.

## 4.1 Laboratory tests with the advanced multi-ejector

The main objective of this thesis entails how the advanced multi-ejector responds in terms of entrainment ratio, pressure lift and ejector efficiency under different operational modes. As already mentioned in Section 3.2.2, the test conditions from Danfoss in Table 3.3 are the basis for the laboratory measurements.

An overall view of the 35 results performed in the laboratory with the use of the R744 transcritical advanced multi-ejector is found in Table 4.1. The Table is sorted into 10 groups divided by horizontal lines, which present the 10 test conditions given by Danfoss. The individual tests in a group have the lowest deviation compared with the test conditions. The tests are arranged and sorted after increasing motive pressure, increasing motive temperature and increasing pressure lift.

Furthermore, the mean values of the results are found in Table 4.1 with the overall uncertainty as  $\pm$  indicators. The overall uncertainty is previous described in Equation 3.17. Table C1 in Appendix includes both the uncertainty from the standard deviation (Type A) and the uncertainty from the sensors (Type B). The parameters in Table 4.1 with the same overall uncertainty for all tests are found in the headline. The suction nozzle pressure ( $p_{SN}$ ), the ejector outlet pressure ( $p_{out}$ , also known as receiver pressure) have a constant uncertainty of  $\pm 0.46$  bar. The pressure lift ( $\Delta p$ ) has a constant overall uncertainty of  $\pm 0.65$  bar.

The motive pressures,  $p_{MN}$ , ranges from 59.26 bar to 90.30 bar with an overall uncertainty of  $\pm 0.46$  bar. The motive temperature ( $t_{MN}$ ) varies from 18.40°C to 35.21°C and the overall uncertainty is between  $\pm 0.11$ °C and  $\pm 0.14$ °C. The suction nozzle pressure varies from 25.15 bar to 28.25 bar. In order to keep the visibility of Table 4.1, the suction nozzle temperatures are found in Table C1. However, the suction temperature ranges from -8.7°C to 10.75°C with an overall uncertainty ranging between  $\pm 0.09$ °C and  $\pm 0.11$ °C. The uncertainties are further discussed in Section 5.2.

Table 4.1: Overview over the measurements with overall uncertainty for the advanced multi-ejector.

$T_{est}$	$p_{MN}$	$t_{MN}$	$p_{SN}$	$p_{out}$	$\dot{m}_{MN}$	$\dot{m}_{SN}$	$\eta_{EJ}$	$\Delta p$	$ER$	$SH$
	[bar]	[deg C]	[bar]	[bar]	[kg/h]	[kg/h]	[%]	[bar]	[-]	[K]
1	60.87	19.54±0.11	26.11	28.28	785±47.4	244±14.75	14±2	2.17	0.31±0.03	5.14±0.37
2	62.94	20.71±0.11	25.82	28.03	777±48.67	263±16.48	14±2	2.21	0.34±0.03	6.61±0.37
3	63.86	21.03±0.11	25.64	27.81	784±39.38	265±13.32	14±2	2.17	0.34±0.02	10.27±0.37
4	59.26	18.40±0.11	25.48	28.03	802±41.41	200±10.32	16±2	2.55	0.25±0.02	22.10±0.38
5	59.79	18.96±0.11	25.38	28.05	787±41.69	199±10.52	16±2	2.67	0.25±0.02	16.99±0.38
6	60.93	19.76±0.11	25.74	28.66	771±46.52	194±11.72	16±2	2.92	0.25±0.02	10.97±0.37
7	62.26	20.85±0.11	25.92	28.82	741±44.74	210±12.69	17±3	2.90	0.28±0.02	10.92±0.37
8	69.24	26.17±0.12	27.28	29.92	621±32.07	329±16.96	19±3	2.64	0.53±0.04	1.95±0.36
9	70.81	25.96±0.12	28.25	30.88	695±32.94	343±16.24	18±3	2.62	0.49±0.03	1.96±0.35
10	68.38	25.51±0.12	25.21	28.51	625±29.64	256±12.11	22±3	3.30	0.41±0.03	17.36±0.38
11	68.80	25.50±0.12	25.71	29.39	642±30.40	234±11.07	22±3	3.68	0.36±0.02	17.57±0.37
12	69.44	26.03±0.12	25.68	29.45	627±29.70	233±11.05	23±3	3.77	0.37±0.02	16.31±0.37
13	69.96	26.25±0.12	25.54	28.95	630±38.02	258±15.57	23±4	3.41	0.41±0.03	21.44±0.38
14	70.12	26.50±0.12	25.16	29.15	619±31.08	218±10.94	23±3	3.98	0.35±0.03	20.3±0.38
15	70.70	26.68±0.12	25.93	29.74	628±30.69	239±11.69	23.02±3	3.82	0.38±0.03	18.98±0.37
16	71.10	26.49±0.12	25.14	28.64	657±39.65	262±15.79	22±3	3.49	0.40±0.03	17.36±0.38
17	81.06	33.48±0.13	26.75	31.61	630±28.93	269±12.54	20±4	4.86	0.43±0.03	4.36±0.37
18	81.14	33.84±0.13	26.74	31.67	622±29.45	268±12.68	20±3	4.93	0.43±0.03	4.32±0.36
19	81.18	34.23±0.13	26.22	31.11	611±30.67	274±13.74	20±4	4.88	0.45±0.03	4.69±0.37
20	81.74	34.34±0.13	26.74	31.90	619±29.30	255±12.09	19±3	5.16	0.41±0.03	4.04±0.36
21	80.83	34.09±0.13	27.28	33.89	606±37.30	94±5.76	10±2	6.61	0.15±0.01	4.03±0.36
22	81.17	34.02±0.13	26.32	32.66	612±29.00	130±6.15	14±3	6.34	0.21±0.01	17.88±0.37
23	81.41	34.66±0.13	26.20	32.54	596±28.24	137±6.47	14±3	6.34	0.23±0.02	18.28±0.37
24	81.75	34.39±0.13	27.04	33.68	612±37.65	101±6.24	11±2	6.64	0.17±0.01	15.01±0.36
25	82.14	34.44±0.13	27.17	33.99	622±29.46	86±4.08	9±2	6.82	0.14±0.01	4.81±0.36
26	82.21	34.39±0.13	26.67	32.75	623±31.27	168±8.43	17±3	6.08	0.27±0.02	19.23±0.37
27	82.63	34.90±0.13	27.21	33.92	618±23.16	107±4.03	11±2	6.71	0.17±0.01	3.73±0.36
28	82.80	34.44±0.13	26.39	32.39	637±31.97	185±9.31	17±3	6.00	0.29±0.02	4.42±0.37
29	83.11	34.62±0.13	26.18	32.96	632±30.87	108±5.29	12±2	6.77	0.17±0.01	18.00±0.37
30	83.32	35.06±0.13	26.28	32.99	623±30.48	118±5.72	13±2	6.72	0.19±0.01	17.87±0.37
31	82.69	34.44±0.13	27.83	34.90	634±28.10	58±2.59	7±1	7.07	0.09±0.01	8.56±0.35
32	88.04	34.67±0.13	27.10	35.15	758±23.83	45±1.63	5±1	8.05	0.06±0.00	4.95±0.36
33	88.94	34.29±0.13	27.60	35.53	799±40.14	73±3.82	8±1	7.93	0.09±0.01	4.76±0.35
34	90.04	35.21±0.14	27.14	35.29	788±37.33	64±3.15	7±1	8.15	0.08±0.01	11.61±0.36
35	90.30	34.96±0.13	27.04	35.20	807±40.55	68±3.53	7±1	8.16	0.08±0.01	7.35±0.36

The overall efficiency of the advanced multi-ejector as a function of pressure lift is described in Figure 4.1. The 10 groups presented in Table 4.1 are presented in different colours, following the same order. Therefore, the groups are sorted from the lowest pressure lift of 2.17 bar to the highest pressure lift of 8.16 bar with an increased motive nozzle pressure. The corresponding motive nozzle pressures and the ejector outlet pressures are presented next to the coloured dots beneath the graph.

At the lowest measured pressure lift at 2.17 bar the multi-ejector efficiency is 14%. The ejector efficiency increases until it reaches its maximum value at 3.8 bar. The highest measured efficiency is 23.02% (green dot, Test 15). The motive nozzle pressure is 70.7 bar and the motive temperature is 26.68°C. The highest efficiencies are found in the light blue (test 10) and green group (test 11 to 16). Hence, the efficiencies are at maximum where the motive nozzle pressure range from 68.4 bar until 71.1 bar with motive temperatures from 25.50°C until 25.93°C and the ejector outlet pressures are from 28.5 bar until 29.7 bar.

After the highest efficiencies, from the pressure lift of 4 bar and higher, the ejector efficiency decreases simultaneously as the motive nozzle pressure and the pressure lift increase. The lowest ejector efficiency is 5.0% with a pressure lift of 8.05 bar (Test 32). The corresponding motive nozzle pressure is 88.09 bar. The lowest efficiencies are all found in the Tests 31 to 35 (brown and purple coloured dots) with motive nozzle pressures between 82.69 bar and 90.3 bar.

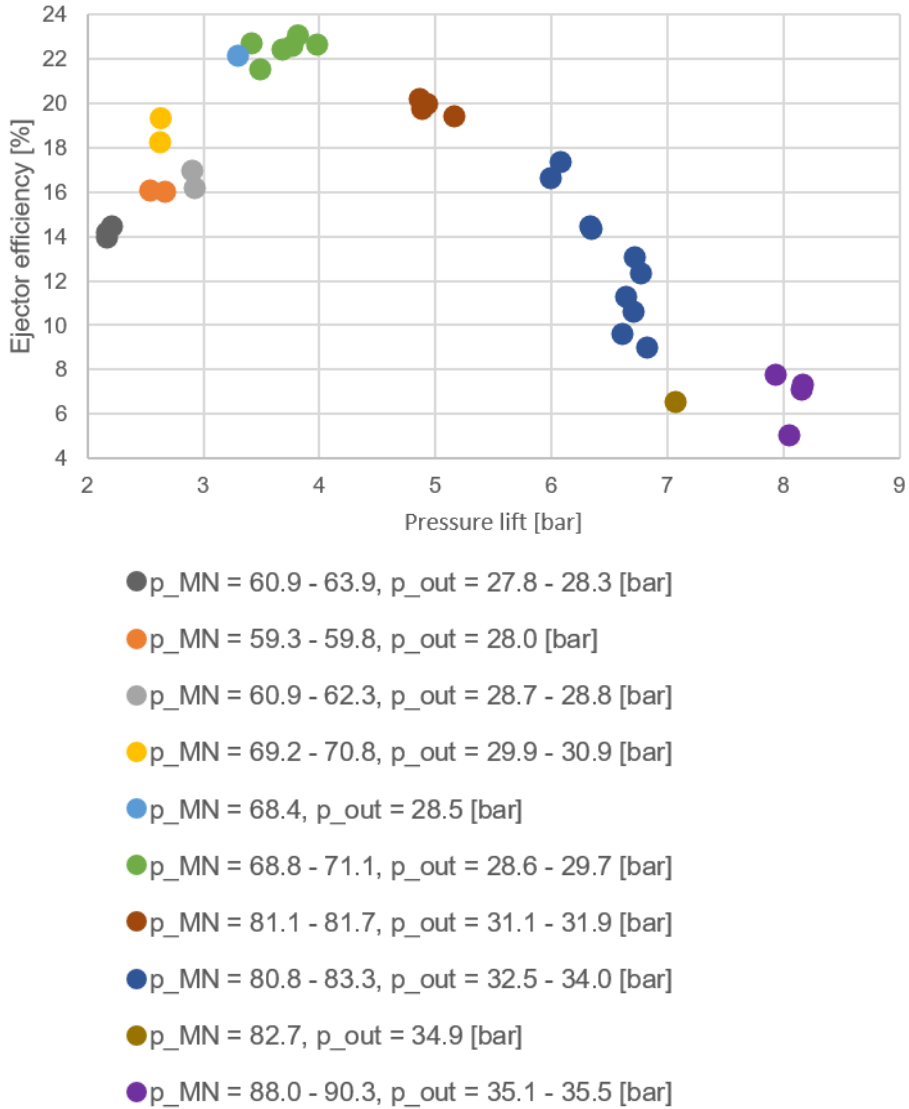


**Figure 4.1:** Ejector efficiency and pressure lift for all the measurements in Table 4.1. The coloured dots represent the divided sections/groups outlined in the table successively in the same order. For instance, dark grey is Test 1-3 in the table.

The ejector efficiency as a function of suction nozzle mass flow rate is illustrated in Figure 4.2 and has the same groups of colours with information as Figure 4.1.

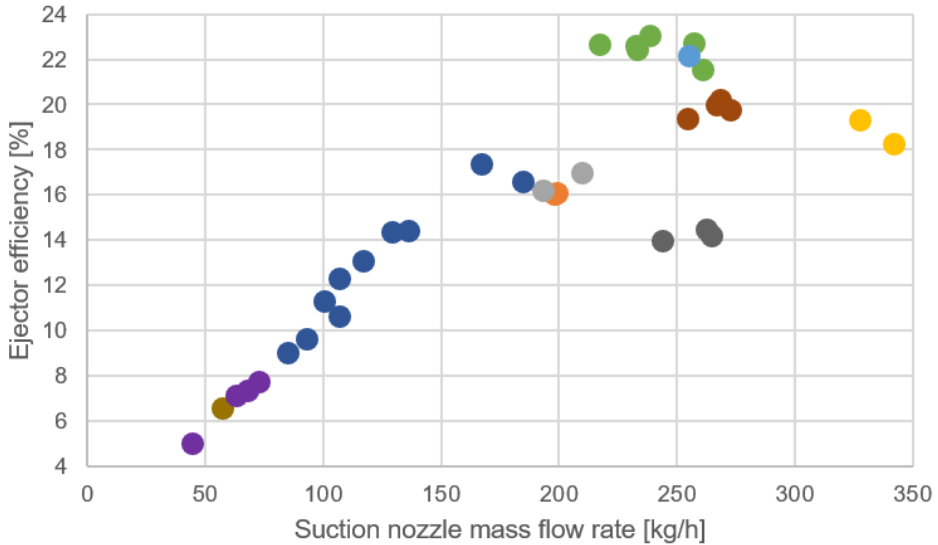


**Figure 4.2:** The ejector efficiency for the advanced multi-ejector as a function of suction nozzle mass flow rate.

As seen in Figure 4.2, the ejector efficiencies, especially beneath 14%, are very dependent on the suction mass flow rate. As an example, the blue dots (Test 21-30) has an 48% decrease in ejector efficiency from 17% to 9%, with a pressure lift increase by only 14% from 6.00 bar to 6.82 bar, as illustrated in Figure 4.1. The decrease in ejector efficiency from 17% to 9% in Figure 4.1 is due to the 54% decrease of suction nozzle mass flow rate from 185 kg/h to 85 kg/h shown in Figure 4.2.

The blue dots (Test 21-30) are further investigated in Figure 4.3, where the motive nozzle pressures are still between 80.8 and 83.3 bar and the ejector outlet pressures are from 32.5 to 34 bar. The ejector efficiency (blue colour) is a function of pressure lift, in addition to a dependency of suction superheat (orange colour).

To distinguish the tests with a low superheat, between 3 and 4 K, from the tests with a high superheat, between 15 K and 20 K, the lower superheat values are displayed as orange triangles while the higher superheat values are illustrated as orange dots. The blue triangles show the efficiencies for the corresponding orange triangles at the same pressure lift.

It is apparent that low superheat (orange triangle) has no significant improved change in efficiency as high superheat (orange dot) around the same pressure lift. This can be observed at the low superheat (triangle) and the high superheat (dot) measurement at the

pressure lift of approximately 6 bar. Here, the superheat decreases by 77% from 19.23 K to 4.42 K, while the ejector efficiency only decreases by 4% from 17.37% to 16.60%.

The same pattern follows for the second pair of low superheat (triangles) at the pressure lift of 6.61 bar and the pair of high superheat (dots) next to the right side at the pressure lift of 6.64 bar. The low superheat (orange triangle) of 4.03 K is 73% lower than the high superheat (orange dot) at 15.01 K. Nevertheless, the ejector efficiency (blue triangle) at 9.61% with the lower superheat is 15% lower than the ejector efficiency (blue dot) at 11.30%. The same pattern follows for triangle pairs 3 and 4 from the left in the figure.

Although the superheat does not have a relatively negative impact on the ejector efficiency itself, it can however have a relatively negative impact on the refrigeration system due to increased compressor losses caused by increased superheat. In addition, it is because a higher superheat at the evaporator implies that the saturation temperature (pressure) need to be reduced to achieve the same conditions in the secondary fluid (air, water, glycol, etcetera). This has a very important impact on power consumption and the system performance. Taking that into consideration, it can be favourable for the refrigeration system to have a lower superheat.

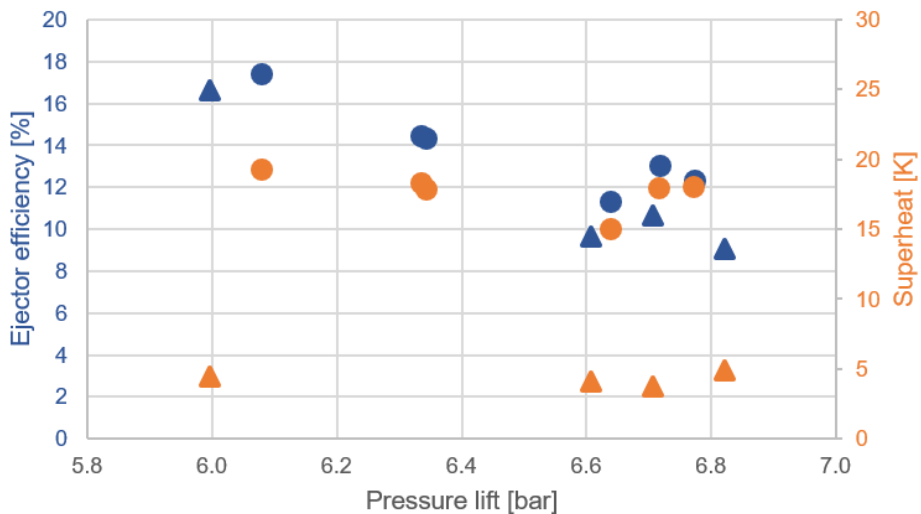


**Figure 4.3:** Ejector efficiency and superheat as a function of pressure lift (Test 21-30 in Table 4.1) Triangles show the tests with a low superheat.

Figure 4.4 presents the entrainment ratio as a function of pressure lift for all the tests found in Table 4.1. The colours are labeled with motive nozzle pressure and ejector outlet pressure and is arranged down below the graph in the same order as the groups given in Table 4.1.

The highest entrainment ratio is 0.53 found at the pressure lift of 2.65 bar and it has a motive nozzle pressure of 69.24 bar (Test 8, yellow group). The lowest entrainment ratio with 0.06 has a motive nozzle pressure of 88.04 bar and has a pressure lift of 8.05 bar (Test 32, purple group).

The lowest pressure lift at 2.2 bar shows an entrainment ratio of 0.31, then the entrainment ratio increases with a higher pressure lift until the turning point where the entrainment ratio decreases at motive pressure at 81 bar (dark red group) at the pressure lift of 5 bar.

The suction mass flow rate varies between 193 kg/h (3.22 kg/min) and 343 kg/min (5.7 kg/min) from the pressure lift from 2 bar until 5 bar. The decrease in entrainment ratio for the pressure lift above 6 bar, is due to the decrease in suction mass flow rate between 185 kg/h (3.08 kg/min) and 45 kg/h (0.75 kg/min). The entrainment ratio and ejector efficiency for the blue points between the motive pressure of 80.8 and 83.3 bar are rapidly decreasing due to the decrease of suction mass flow rate, which is seen in Figure 4.2. The suction mass flow rate is the basis for the entrainment ratio and ejector efficiency.

The yellow dots at motive pressure around 70 bar and the orange dots at motive pressure around 59 bar, have both a pressure lift of approximately 2.5 bar. However, they have a difference in entrainment ratio of 0.28, with the values 0.53 and 0.25, respectively. The yellow group has a superheat of 1.9 K, whereas the the orange has a superheat between 17 and 22 K. The yellow points have the highest entrainment ratio, due to the highest suction mass flow measured of 328 kg/h (5.4 kg/min) and 342 kg/h (5.7 kg/min), respectively. This is clearly noticeable in Figure 4.2.



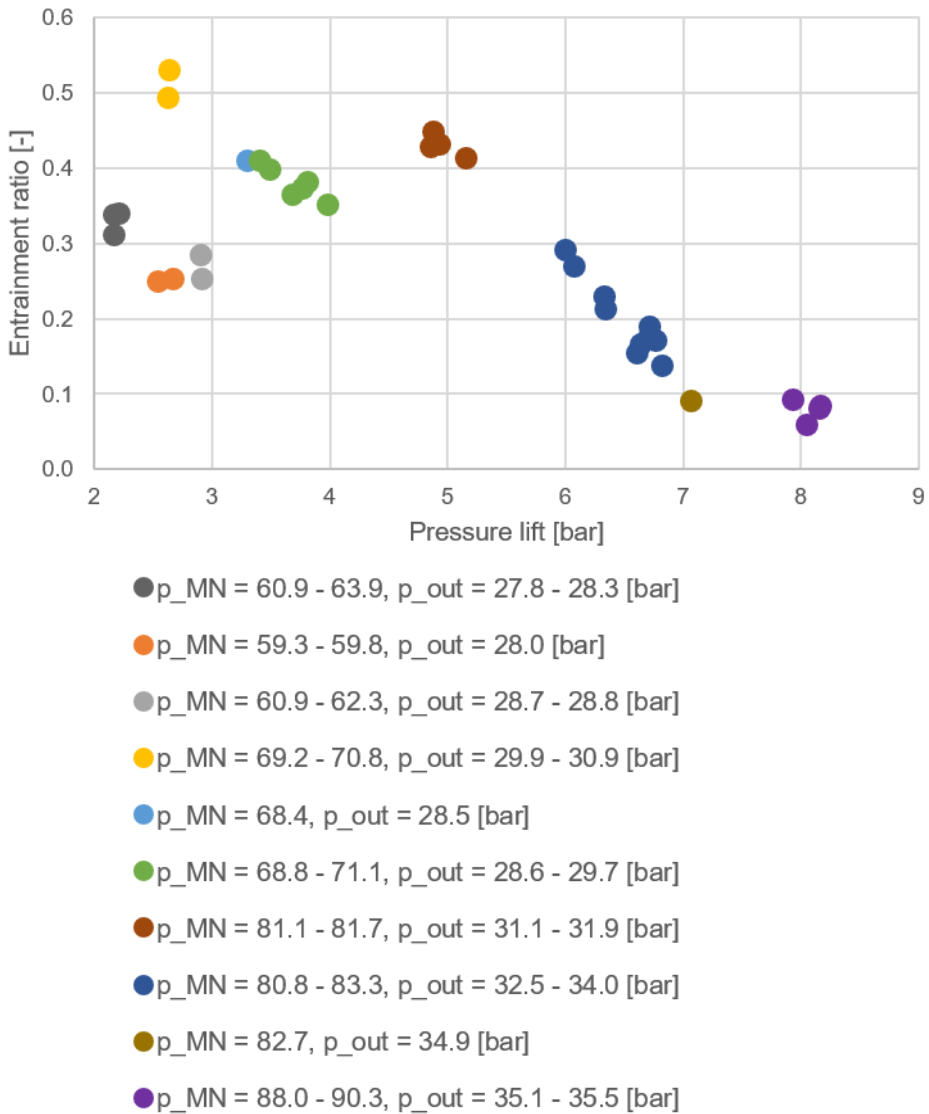


**Figure 4.4:** Entrainment ratio and pressure lift for all the measurements in Table 4.1. The coloured dots represent the divided sections/groups outlined in the table successively in the same order. For instance, dark grey is Test 1-3 in the table.

When comparing both the entrainment ratio and the ejector efficiency as functions of pressure lift, the highest ejector efficiency (green dot) in Figure 4.1 does not have the highest entrainment ratio (yellow dot) in Figure 4.4. The definition of the ejector efficiency, given in Equation 3.7, shows that it is proportional to entrainment ratio and enthalpy difference. This means that the enthalpy difference has more impact than the entrainment ratio in this situation. However, both the highest entrainment ratio and the highest ejector efficiency are found at motive nozzle pressure of respectively 69.24 bar and 70.7 bar, with pressure lifts of 2.65 bar and 3.8 bar.

Figure 4.5 shows the CO<sub>2</sub> conditions outside the gas cooler section, where the pressure of the inlet motive nozzle is a function of the specific enthalpy. The motive nozzle pressure shown in the specific enthalpy diagram presents the exit gas cooler section. This is the same position as the upper left corner of the ph-diagram in Figure 3.1. Each point in the Figure illustrates the high pressure, before the expansion process. The dots with a motive nozzle pressure above the R744 critical pressure point of 73.8 bar are all in the transcritical region, while the remaining are in the subcritical region.

The lowest specific enthalpy (orange dot) is measured at approximately 59 bar motive inlet nozzle pressure with a motive inlet temperature of around 18°C. The highest specific enthalpy is measured at approximately 81 bar and 34 °C (blue dots).

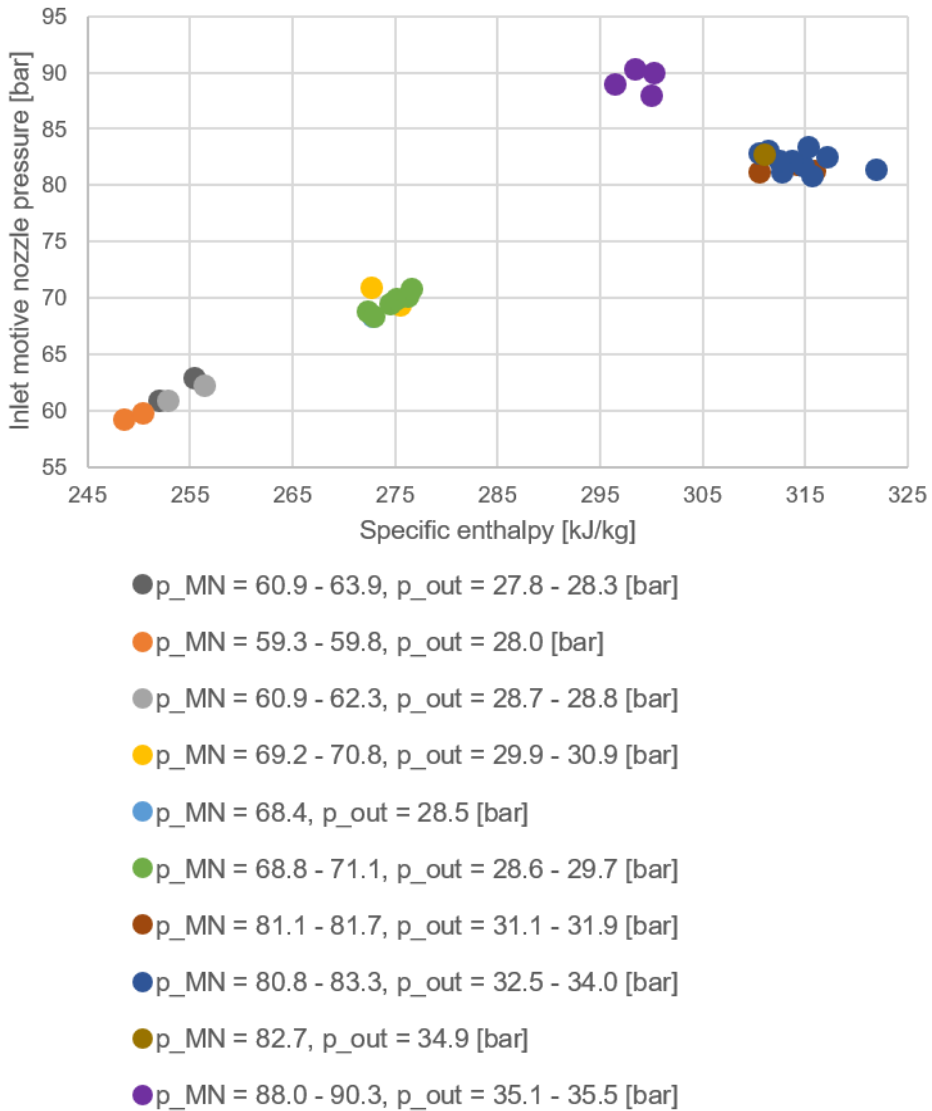


**Figure 4.5:** Inlet motive nozzle pressure as a function of enthalpy for all the the measurements in Table 4.1. The coloured dots represent the groups in the table, respectively. This is inlet motive point in ejector efficiency Figure 3.1.

Figure 4.6 illustrates the suction nozzle pressure as a function of specific enthalpy. The inlet suction nozzle pressure varies between approximately 25 and 29 bar. The measured dots are placed at the suction side, which is down to the right on a R744 pressure enthalpy diagram, as also indicated in Figure 3.1. The yellow dot (Test 9) with a suction pressure of 28.25 bar has the lowest enthalpy value on the suction side. The yellow dot corresponds to the yellow dot on the motive side with a motive pressure of 70.81 bar in Figure 4.5. The orange dot (Test 4) with a suction pressure of 25.48 bar has the highest enthalpy on the suction side, which corresponds to a motive pressure of 59.26 bar in Figure 4.5.

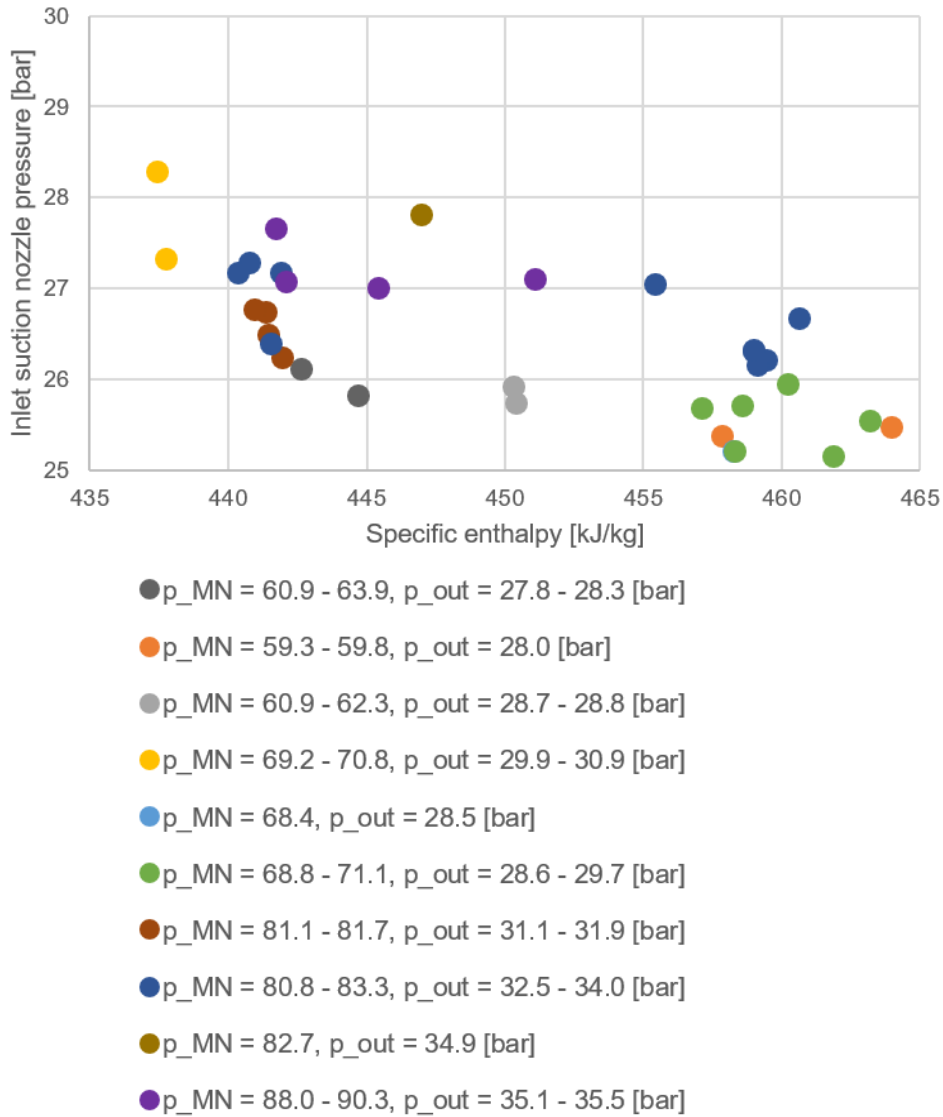


**Figure 4.6:** Inlet suction nozzle pressure as a function of enthalpy for all the the tests in Table 4.1. The coloured points represent the same order as grouped in the overview Table 4.1. This presents the inlet suction nozzle point in the ph-diagram Figure 3.1.

In summary of the results of the laboratory measurements, the highest efficiency was 23% and the highest entrainment ratio was 0.53. The design point of the advanced multi-ejector seems to be around 68 to 72 bar with a pressure lift between 3 and 4 bar, since this is where the highest efficiencies are located.

## 4.2 Comparing laboratory tests with Coolselector® 2

The calculation program Coolselector described in Section 3.4 was used to find comparable transcritical R744 low pressure lift (LP) and high pressure lift (HP) multi-ejectors from Danfoss under the same refrigeration conditions as the advanced multi-ejector in the test facility. The results from the laboratory tests, see Table 4.1 were inserted into Coolselector. Only 4 out of 35 tests were successfully adopted in Coolselector, in which the parameters matched with a multi-ejector from the commercial market. That particular matter is later discussed in Section 5.3.

The suitable tests are the Test 32 ( $p_{MN}= 88.04$  bar), Test 33 ( $p_{MN}= 88.94$  bar), Test 34 ( $p_{MN}= 90.04$  bar) and Test 35 ( $p_{MN}= 90.30$  bar) from the laboratory results in Table 4.1. The tests in question are relisted in Table 4.2. For simplification the tests 32, 33, 34 and 35 are renamed as Test A, B, C and D, respectively.

**Table 4.2:** Results from the advanced multi-ejector that are inserted into Coolselector. The motive- and the suction nozzle mass flow rate and the receiver pressure is compared with the multi-ejectors suggested in Coolselector.

Test	$p_{MN}$ [bar]	$\dot{m}_{MN}$ [kg/h]	$\dot{m}_{SN,liq.}$ [kg/h]	$p_{SN}$ [bar]	$SH$ [°C]	$t_{MN}$ [°C]	$p_{rec}$ [bar]
A	88.04	758.40	44.78	27.10	4.95	34.67	35.15
B	88.94	799.08	72.94	27.60	4.76	34.29	35.53
C	90.04	787.86	63.13	27.14	11.61	35.21	35.29
D	90.30	807.00	67.96	27.04	7.35	34.96	35.20

**Table 4.3:** Test conditions from the advanced multi-ejector that are compared with multi-ejectors suggested from Coolselector.

Test	$p_{MN}$ [bar]	$\eta_{EJ}$ [%]	$\Delta p$ [bar]	$ER$ [-]
A	88.04	5	8.05	0.06
B	88.94	8	7.93	0.09
C	90.04	7	8.15	0.08
D	90.30	7	8.16	0.08

Three independent cases were performed for the parameters above in Table 4.2 in the LP multi-ejector system and the HP multi-ejector system. Each of these cases concentrated successively on the manipulation of the mass flow rate in the ejector suction nozzle (Case 1), the receiver pressure (Case 2) and the mass flow rate in the ejector motive nozzle (Case 3). The three cases are listed in Table 4.4.

Each Case includes three parameters where two are maintained constant and one is the variable in question. In Case 1 the aim is to find the suction nozzle mass flow rate at which the pressure in the receiver and the mass flow in the motive nozzle are kept constant in both the multi-ejector and the suggested multi-ejector. In Case 2 the pressure of the receiver is the variable to be determined and the two other parameters are constant for both multi-ejectors. Finally in Case 3 the aim switches to the mass flow rate in the motive nozzle, where the two other parameters are constant.

**Table 4.4:** Three cases for comparison in Coolselector.

	Case 1	Case 2	Case 3
Find	$\dot{m}_{suction}$	$p_{receiver}$	$\dot{m}_{motive}$
Constant value	$p_{receiver}$	$\dot{m}_{suction}$	$p_{receiver}$
Constant value	$\dot{m}_{motive}$	$\dot{m}_{motive}$	$\dot{m}_{suction}$

In the next two subsections Section 4.2.1 and Section 4.2.2 the advanced multi-ejector is compared with the LP multi-ejectors suggested in Coolselector. Section 4.2.1 presents the difference in suction nozzle mass flow rate (Case 1), receiver pressure (Case 2) and motive nozzle mass flow rate (Case 3). Section 4.2.2 presents the results of the difference in ejector efficiency, entrainment ratio and pressure lift (see Table 4.3) for the difference in suction nozzle mass flow rate (Case 1), receiver pressure (Case 2) and motive nozzle mass flow rate (Case 3). Thereafter, Section 4.2.3 and Section 4.2.4 present the same results as mentioned above, but here the comparison is between the advanced multi-ejector and HP multi-ejectors suggested in Coolselector.

### 4.2.1 Advanced multi-ejector compared to LP multi-ejector from Coolselector

In this subsection three figures show the comparison between the advanced multi-ejector and a LP multi-ejector, respectively for the change in suction mass flow rate (Case 1), change in receiver pressure (Case 2) and change in motive nozzle mass flow rate (Case 3). In each figure the Test conditions A, B, C and D are presented. However, tests with unrealistic values in Coolselector are excluded from the illustrations. In the figures, the suction nozzle mass flow rate is illustrated blue, the receiver pressure is illustrated green and the motive nozzle mass flow rate are illustrated orange. The columns presenting the laboratory tests with the advanced multi-ejector are fully coloured, while the pattern-coloured columns are from the selected multi-ejector in Coolselector.

#### Case 1

Figure 4.7 shows the motive nozzle pressure ( $p_{MN}$ ) is equal to 88.04 bar (test A) with a constant receiver pressure ( $p_{rec}$ ) of 35.15 bar. In addition the motive nozzle pressure equal to 88.94 bar (test B) with a constant receiver pressure of 35.53 bar. The difference in suction mass flow rate (Case 1) is shown for both Test A and B. For both multi-ejectors, the motive nozzle mass flow rate is constant for both Test A with 758.40 kg/h and Test B with 799.1 kg/h. The selected Danfoss multi-ejector under these test conditions is the transcritical low pressure lift multi-ejector LP 935. It is observed, that the second group of columns (Test B) has the highest difference in suction nozzle mass flow rate compared with the first group of columns (Test A).



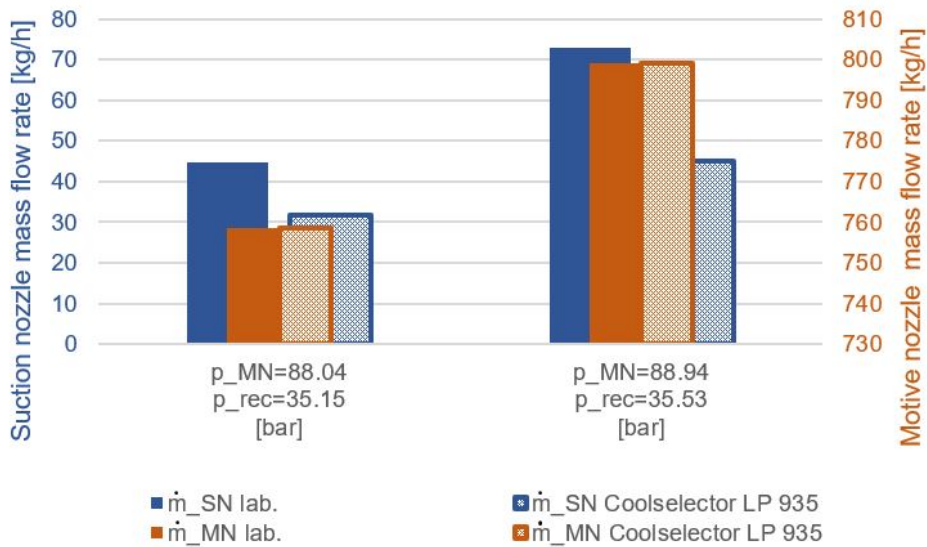


**Figure 4.7:** Suction nozzle mass flow rate for low pressure lift ejector performance comparison at equal motive nozzle mass flow rate and receiver pressure (Case 1, Test A and B).

For the first group of columns (Test A), the suction mass flow rate is 44.78 kg/h for the advanced multi-ejector, which is an increase by 41% from the LP 935 with 31.80 kg/h.

For the second group of columns (Test B), the suction mass flow is 72.94 kg/h for the advanced multi-ejector which is an increase by 62% from the LP 935 with 45.03 kg/h.

## Case 2

Figure 4.8 presents the difference in receiver pressure (Case 2) between the advanced multi-ejector and the recommended multi-ejector LP 935 in Coolselector for a constant motive pressure of 88.04 bar (Test A), 88.94 bar (Test B), 90.04 bar (Test C) and 90.30 bar (Test D). The motive nozzle mass flow rates and the suction mass flow rates are constant for each individual test.

For the first group of columns from the left (Test A), the suction nozzle mass flow rate is 44.78 kg/h and the motive nozzle mass flow rate is 758.40 kg/h for both the advanced multi-ejector and the multi-ejector LP 935. The receiver pressure for the advanced multi-ejector with 35.15 bar is an 0.33% increase from LP 935 with 35.03 bar. The pressure difference is only 0.12 bar.

For the second group of columns from the left (Test B), the receiver pressure for the advanced pressure multi-ejector is 35.53 bar which is an increase by 0.63% from 35.30 bar at the multi-ejector LP 935. This gives a pressure difference 0.23 bar. The constant motive- and suction nozzle mass flow rates are respectively 799.10 kg/h and 72.94 kg/h.

The third group of columns (Test C) from the left, the suction nozzle mass flow rate is 63.13 kg/h and the motive nozzle mass flow rate is 787.9 kg/h are constant for both the advanced multi-ejector and LP 935. The receiver pressure is 35.29 bar for the advanced multi-ejector which is an increase by 1.41% from 34.80 bar at the multi-ejector LP 935. This gives a pressure difference of 0.49 bar.

The fourth group of columns (Test D) from the left, the receiver pressure for the advanced pressure multi-ejector is 35.20 bar which is an 1.74% increase from LP 935 with 34.60 bar. The difference is 0.60 bar. The constant motive- and suction nozzle mass flow rates are respectively 807.00 kg/h and 67.96 kg/h.

In summary, the receiver pressure is higher for the advanced multi-ejector at the laboratory than LP 935 in Coolselector for all the test conditions in Case 2. The largest receiver pressure difference between the multi-ejector and LP 935 is 0.60 bar, an increase by 1.74% found in Test D, meanwhile the minimum difference in receiver pressure is 0.12 bar, an increase by 0.33% found in Test A.

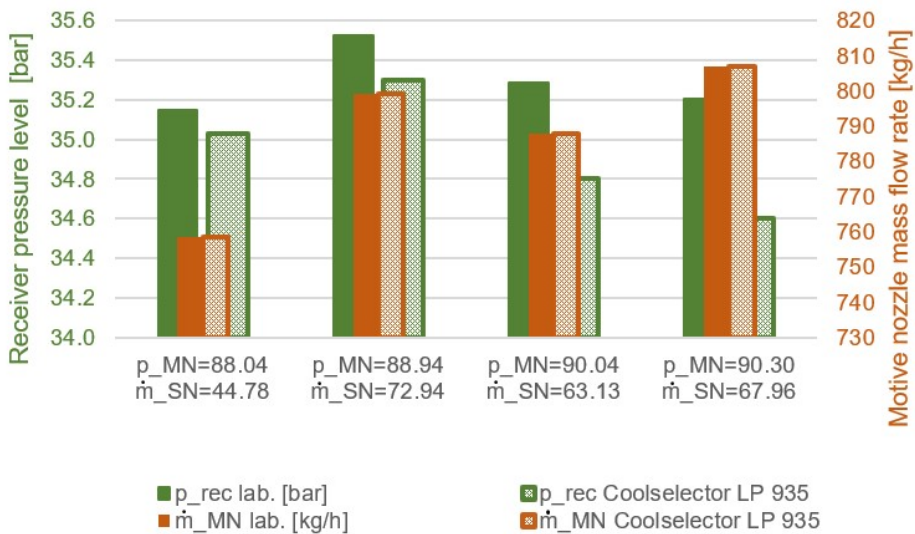


**Figure 4.8:** Receiver pressure level for low pressure lift ejector performance comparison at equal motive- and suction nozzle mass flow rate (Case 2).

### Case 3

Figure 4.9 presents the difference in motive nozzle mass flow rate (Case 3) for a constant motive nozzle pressure of 88.04 bar (Test A) and 88.94 bar (Test B). The most suited multi-ejector recommended from Coolselector is LP 1435 under the conditions at Test A. For Test B however, the most suitable multi-ejector is the LP 1935.

For the first group of columns (Test A), the suction nozzle mass flow rate at 44.78 kg/h and

the receiver pressure at 35.15 bar are constant for both multi-ejectors. The motive nozzle mass flow rate is 758.60 kg/h for the advanced multi-ejector, which is a reduction by 43% from the LP 1435 with 1333 kg/h. This is a difference in motive nozzle mass flow rate of 574.60 kg/h.

For the second group of columns (Test B), the receiver pressure is constant at 35.53 bar and the suction nozzle mass flow rate is constant at 72.94 kg/h for both multi-ejectors. The motive nozzle mass flow is 799.04 kg/h for the advanced multi-ejector, which is a reduction by 53% from the LP 1935 with 1683 kg/h. This is a difference in motive nozzle mass flow rate of 885 kg/h.

In summary, the multi-ejectors in Coolselector have a higher motive nozzle mass flow rate than the advanced multi-ejector in the laboratory. Test B shows the largest motive nozzle flow rate reduction of 53% from Coolselector which is difference of 884.92 kg/h, whereas the Test A shows a reduction of 43% from Coolselector, which is a difference of 574.60 kg/h.

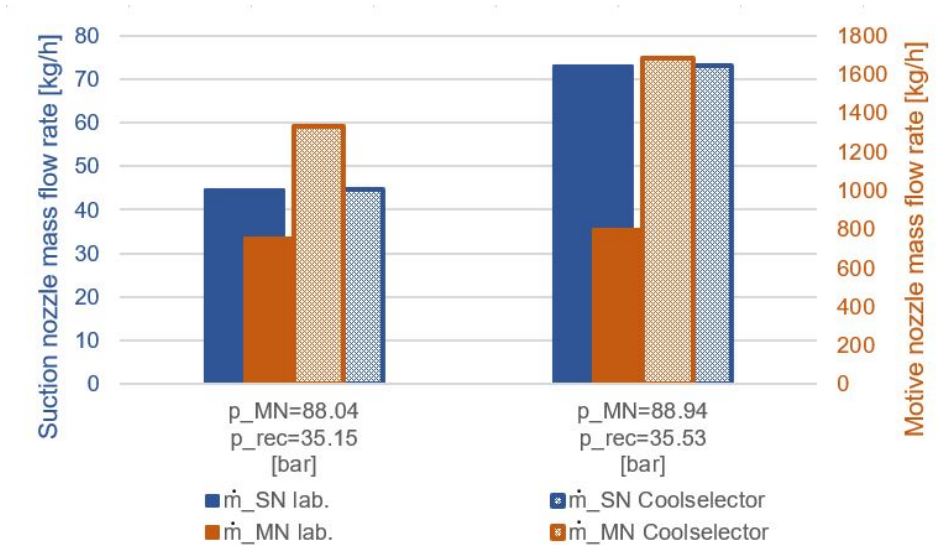


**Figure 4.9:** Motive nozzle mass flow rate for low pressure lift ejector performance comparison at equal suction nozzle mass flow rate and receiver pressure (Case 3, Test A and B).

To sum up for all three comparisons in this section, the advanced multi-ejector have higher suction mass flow rates than LP 935 in Case 1, where the same tendency follows for the receiver pressure in Case 2. In Case 3, the LP 1435 and LP 1935 had higher motive mass flow rates than the advanced multi-ejector.

## 4.2.2 Advanced multi-ejector compared to LP multi-ejector – efficiency, entrainment ratio and pressure lift

In this subsection the advanced multi-ejector is compared to LP multi-ejectors in Coolselector on the basis of ejector efficiency, entrainment ratio and pressure lift, see Table 4.3. The following three figures in this section show the difference in ejector efficiency, entrainment ratio and pressure lift based on the difference in suction nozzle mass flow rate (Case 1), the difference in receiver pressure (Case 2) and the difference in motive nozzle mass flow rate (Case 3). An overview of the cases are illustrated in Table 4.4. The test conditions with constant motive nozzle pressure of 88.04 bar (Test A) , 88.94 bar (Test B), 90.04 bar (Test C) and 90.30 bar (Test D) found in Table 4.2, are the same as in the last subsection. The entrainment ratio is coloured red, the ejector efficiency is blue and the pressure lift is green. The full coloured graphs are values from the laboratory, whereas the patterned graphs are from Coolselector.

### Case 1

The results in Figure 4.10 show the entrainment and ejector efficiency results of the comparison between the advanced multi-ejector and LP 935 from Coolselector with the difference in suction nozzle mass flow rate (Case 1).

The first group of columns (Test A) from the left have a constant motive nozzle pressure of 88.04 and a constant pressure lift of 8.05 bar. The entrainment ratio for LP 935 is 0.04 and for the advanced multi-ejector 0.06, while the ejector efficiency is 3.35% for LP 935 and 5.04% for the advanced multi-ejector. The entrainment ratio and the ejector efficiency have both an increase by 49% from the LP 935 to the advanced multi-ejector.

The second group of columns (Test B), the constant motive nozzle pressure is 88.94 bar and the pressure lift of 7.93 bar is constant. The entrainment ratio is 0.06 for LP 935 and 0.09 for the advanced multi-ejector. The ejector efficiency is 5.0% for LP 935 and 7.58% for the advanced multi-ejector. The results give a 50% increase in both entrainment ratio and ejector efficiency from the LP 935 to the advanced multi-ejector.

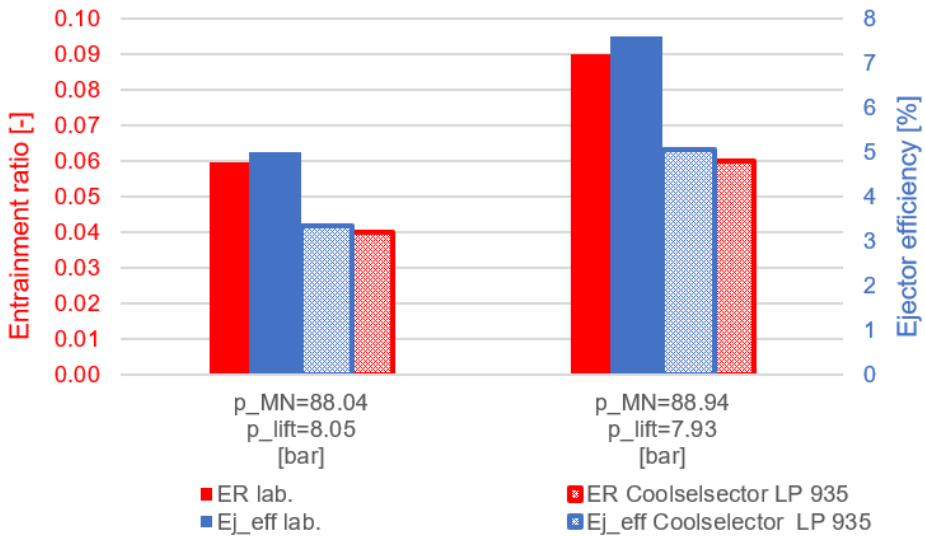


**Figure 4.10:** Entrainment ratio and ejector efficiency for lower pressure ejector performance comparison at equal motive nozzle pressure and pressure lift (Case 1 like Figure 4.7).

## Case 2

The results in Figure 4.11 show the pressure lift and the ejector efficiency results of the comparison between the advanced multi-ejector and LP 935 from Coolselector with the difference in receiver pressure (Case 2). The four groups of columns plotted in this figures, present one after another a constant motive nozzle pressure and a constant entrainment ratio of respectively 88.09 bar and 0.06 for Test A, next 88.94 bar and 0.09 for Test B, further 90.04 bar and 0.08 for Test C and at last a motive pressure of 90.30 bar and entrainment ratio of 0.08 for Test D. The results from Coolselector concluded that the low pressure lift multi-ejector LP 935 is the most fitted for these test conditions.

The results from first group of columns from the left (Test A) reveals that the pressure lift is 7.93 bar for LP 935 and 8.05 bar for the advanced multi-ejector, which for the multi-ejector is an increase by 1%. The ejector efficiency is 4.89% for LP 935 and 5.00% for the advanced multi-ejector, which for the latter is an increase by 2%.

The second group of columns shown from the left (Test B) reveals that the pressure lift is 7.70 bar for LP 935 and 7.90 bar for the advanced multi-ejector, which is an increase by 3% for the advanced multi-ejector. The LP 935 achieved an ejector efficiency of 7.30%, whereas the the advanced multi-ejector achieved 7.58%. That is an increase by 4% from the Coolselector option to the advanced multi-ejector.

In the third group of columns (Test C) from the left, the pressure lift of the LP 935 is 7.66 bar and 8.2 bar for the advanced multi-ejector, which is an increase of 6%. The ejector efficiency with 7.11% for the advanced multi-ejector is approximately 2 times higher

than the result from Coolselector with 3.53%.

For the last group of columns (Test D) from the left, the pressure lift of the LP 935 is 7.56 bar and 8.2 bar for the advanced multi-ejector, which is an increase by 8%. The ejector efficiency for the advanced ejector with 7.32% is an increase by 11.52% from the LP 935 with 6.56%.

In summary, the advanced multi-ejector achieved higher results from the pressure lift and the ejector efficiency when compared with the LP 935 in Coolselector. The highest increase in ejector efficiency from the Coolselector to the laboratory results was found in Test C with an increase by 101%. The highest increase by pressure lift from the Coolselector to the laboratory results was found in Test D with an increase by 7.97%.

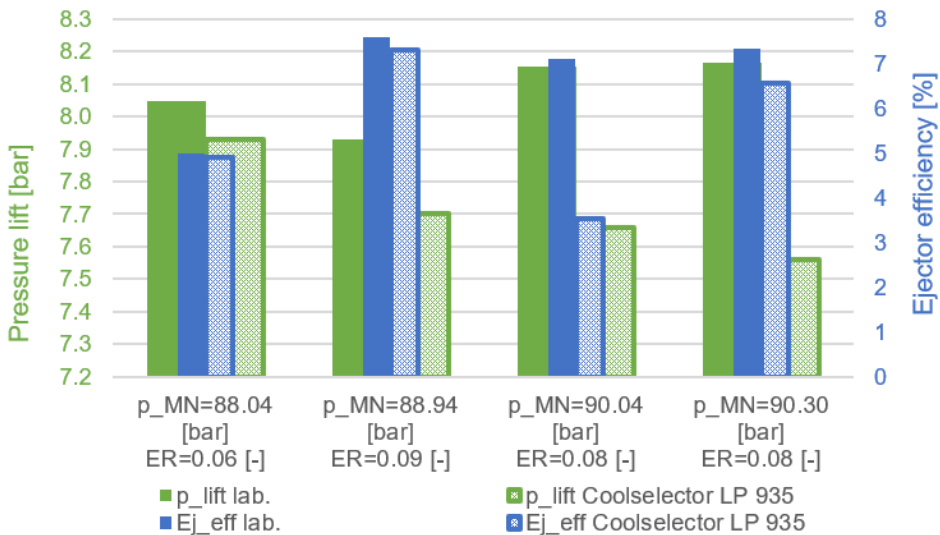


**Figure 4.11:** Pressure lift and ejector efficiency for lower pressure lift ejector performance comparison at equal motive nozzle pressure and entrainment ratio (Case 2 like Figure 4.8).

### Case 3

The results in Figure 4.12 show the entrainment ratio and ejector efficiency for the comparison between the multi-ejectors in the laboratory and the Coolselector with the difference in motive nozzle mass flow rate (Case 3) and constant receiver pressure and suction nozzle mass flow rate, which is shown in 4.9.

For the first group of columns (Test A), the pressure lift is constant at 8.05 bar and the motive nozzle pressure is constant at 88.04 bar for both multi-ejectors. The entrainment ratio for the advanced multi-ejector with 0.06 in Test A is an increase by 98% from the multi-ejector LP 1435 from Coolselector with 0.03 entrainment ratio. The ejector efficiency is 5.00% for the advanced multi-ejector, which is an increase by 99% from ejector

efficiency of 2.51% for LP 1435.

For the second group of columns (Test B), the pressure lift is constant at 7.93 bar and the motive nozzle pressure is constant at 88.94 bar for both multi-ejectors. The increase in entrainment ratio and the ejector efficiency are approximately by 125% from the selected LP 1935 to the advanced multi-ejector. The entrainment ratio values are 0.09 and 0.04 and the ejector efficiencies are 8% and 3.36%, where the highest values present the advanced multi-ejector.

Comparing the advanced multi-ejector with LP 1435 in Test A and LP 1935 in Test B, the largest entrainment and ejector efficiency difference is found in Test B. The advanced multi-ejector has a higher efficiency than LP 1435 and LP 1935 and are therefore a better choice of multi-ejector under these refrigeration conditions.

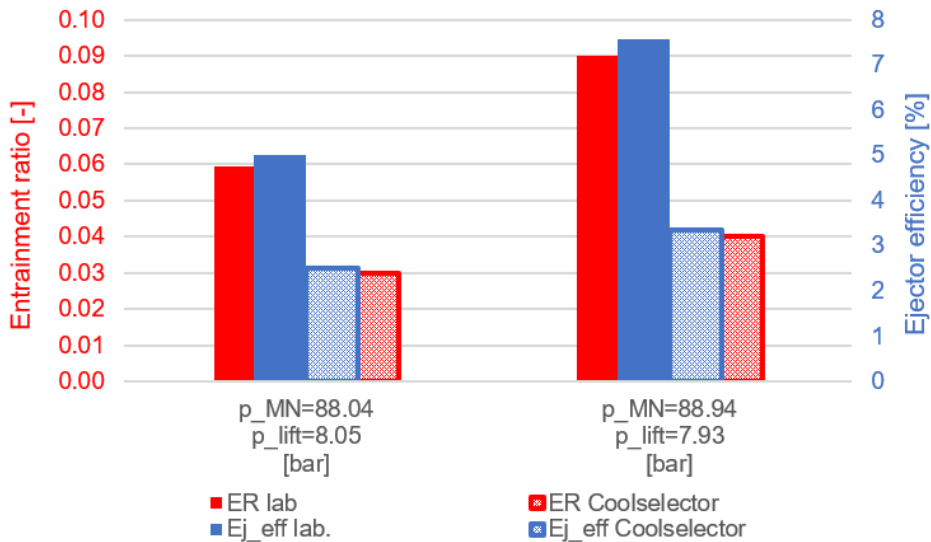


**Figure 4.12:** Entrainment ratio and ejector efficiency for lower pressure ejector performance comparison at equal motive nozzle pressure and pressure lift (Case 3 like Figure 4.9).

Comparing the results for the ejector prototype and the low pressure lift multi-ejectors, they both have relative low ejector efficiencies in range from approximately 2% to 8%. However, the ejector prototype has better efficiencies and entrainment ratios than the LP 935, LP 1435 and LP 1935 multi-ejectors from Danfoss for the operating conditions in Test A, B, C and D with motive pressure nozzle conditions around 88-90 bar.

### 4.2.3 Advanced multi-ejector compared to HP multi-ejector from Coolselector

The results present the comparison between the advanced multi-ejector operating in the laboratory and selected high pressure lift (HP) multi-ejectors with the same refrigeration conditions in Coolselector. As previously in Section 4.2.1, the three figures present the difference in suction nozzle mass flow rate (Case 1), the difference in receiver pressure (Case 2) and the difference in motive nozzle mass flow rate (Case 3). Except, in this section the comparison is between the advanced multi-ejector and a selected HP multi-ejector. An overview of the three different cases can be found in Table 4.4. Each case is a function of constant motive nozzle pressures of 88.04 bar (Test A), 88.94 bar (Test B), 90.04 bar (Test C) and 90.30 bar (Test D). An overview of the constant parameters for the individual tests is found in Table 4.2.

#### Case 1

Figure 4.13 illustrates the difference in suction nozzle mass flow rate (Case 1) between the advanced multi-ejector and the selected multi-ejector HP 1875 in Coolselector.

For the constant motive nozzle pressure of 88.04 bar (Test A), receiver pressure of 35.15 bar and constant motive nozzle mass flow rate of 758 kg/h, the suction nozzle mass flow rate is 45 kg/h for the advanced multi-ejector and 315 kg/h for HP 1875. This is an increase by 603% in suction mass flow rate from the advanced multi-ejector to the HP 1875.

Next, the motive nozzle pressure is constant at 88.94 bar (Test B), the receiver pressure is constant at 35.53 bar and the motive nozzle mass flow rate is constant at 799 kg/h for both multi-ejectors. The suction motive mass flow rate is 325 kg/h for the multi-ejector in Coolselector, which is an increase by 391.46% from the advanced multi-ejector with 73 kg/h.

Next, where both multi-ejectors have a constant motive nozzle pressure of 90.04 bar (Test C), a constant receiver pressure of 35.29 bar and a constant motive nozzle mass flow rate of 788 kg/h, the suction mass flow rate in Coolselector increases by 345.55% from the laboratory measurement, with respectively 328 kg/h and 63 kg/h.

At last, the constant motive nozzle pressure of 90.30 bar (Test D), constant receiver pressure of 35.20 bar and motive nozzle mass flow rate of 807 kg/h gives an increase by 420.08% in suction mass flow rate from the laboratory to the selected multi-ejector in Coolselector. The range is 68 kg/h and 334 kg/h.

Summarised for Case 1 under HP conditions, all suction mass flow rates for HP 1875 are higher than the advanced multi-ejector. The highest suction nozzle mass flow rate difference between the two multi-ejectors is 270 kg/h, which is an increase by 602.78% from the advanced multi-ejector found in Test A, meanwhile Test C has the lowest difference with 252 kg/h, which is an increase by 345.55% from the advanced multi-ejector to the HP 1875 multi-ejector.



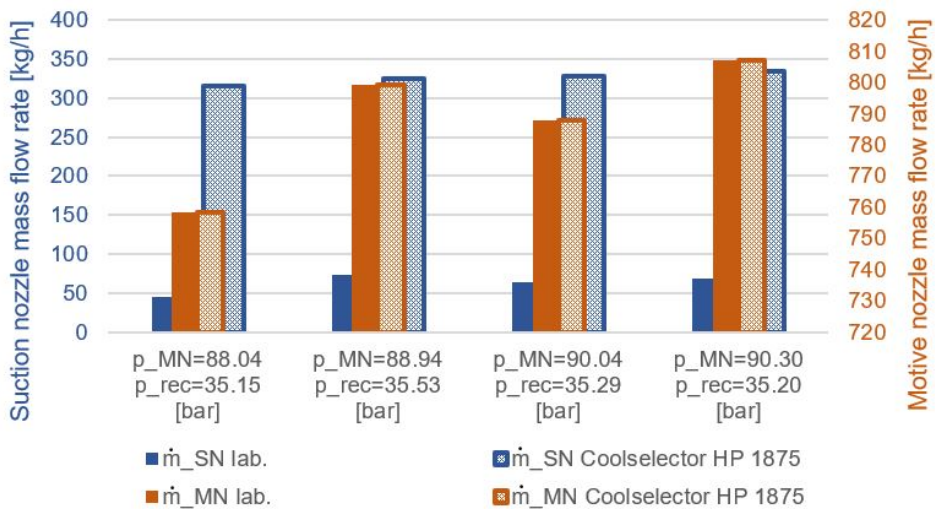


**Figure 4.13:** Suction nozzle mass flow rate for high pressure lift ejector performance comparison at equal motive nozzle mass flow rate and receiver pressure (Case 1).

## Case 2

Figure 4.14 illustrates the difference in receiver pressure (Case 2) between the advanced multi-ejector and the selected multi-ejector HP 1875 in Coolselector.

For the first group of columns (Test A) the motive nozzle pressure is constant at 88.04 bar, the suction mass flow rate is constant at 44.78 kg/h and motive nozzle mass flow rate is constant at 758 kg/h for both multi-ejectors. The receiver pressure achieved 40.46 bar in Coolselector, which is an increase by 15.12% from the advanced multi-ejector that achieved 35.15 bar.

For the second group of columns (Test B) the constant motive nozzle pressure is 88.94 bar, the constant suction mass flow rate is 72.94 kg/h and the constant motive nozzle mass flow rate is 799 kg/h for both multi-ejectors. The receiver pressure achieved 40.38 bar in Coolselector, which is an increase by 13.66% from the advanced multi-ejector that achieved 35.53 bar.

For the third group of columns (Test C) the constant motive nozzle pressure is 90.04 bar, suction mass flow rate of 63.13 kg/h and motive nozzle mass flow rate of 788 kg/h for both multi-ejectors. The receiver pressure achieved 40.16 bar in Coolselector, which is an increase by 13.80% from the advanced multi-ejector that achieved 35.29 bar.

For the fourth and last group of columns (Test D) the constant motive nozzle pressure is 90.04 bar, the suction mass flow rate is 67.96 kg/h and the motive nozzle mass flow rate is 807 kg/h for both multi-ejectors. The receiver pressure achieved 40.07 bar in Coolselector.

tor, which is an increase by 13.83% from the advanced multi-ejector that achieved 35.20 bar.

In summary for Case 2, the receiver pressure for HP 1875 is higher than the advanced multi-ejector. The maximum receiver pressure level difference between the two multi-ejectors is 5.31 bar found in Test A, which illustrates an increase in receiver pressure of 15.12%. The minimum receiver pressure level difference between the two multi-ejectors is 4.85 bar found in Test B shows an increase of 13.66% compared to the advanced multi-ejector.

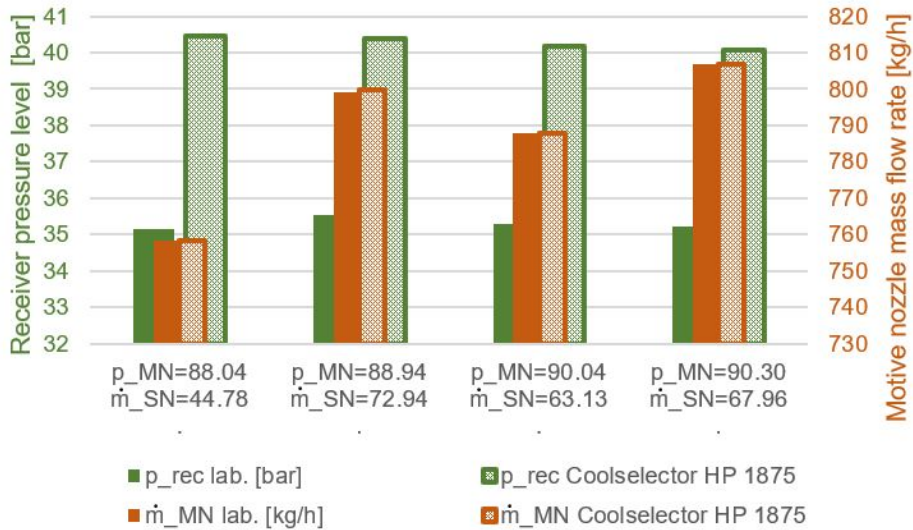


**Figure 4.14:** Receiver pressure level for higher pressure lift ejector performance comparison at equal motive- and suction nozzle mass flow rate (Case 2).

### Case 3

Figure 4.15 illustrates the difference in motive nozzle mass flow rate (Case 3) between the advanced multi-ejector used in the laboratory and the multi-ejector HP 1875 recommended in Coolselector.

For the constant motive nozzle pressure of 88.04 bar (Test A) and the constant receiver pressure of 35.15 bar and the constant suction mass flow rate of 45 bar, the reduction in motive nozzle mass flow rate is by 86% compared to the advanced multi-ejector. The advanced multi-ejector has a motive mass flow rate of 758 kg/h, meanwhile the HP 1875 multi-ejector achieves 108 kg/h.

For the constant motive nozzle pressure of 88.94 bar (Test B) and the constant receiver pressure of 35.53 bar and the constant suction mass flow rate of 73 bar, the reduction in

motive nozzle mass flow rate is by 78% compared to the advanced multi-ejector. The motive nozzle mass flow rates for the advanced multi-ejector and the HP 1875 are 799 kg/h and 179 kg/h, respectively.

For the constant motive nozzle pressure of 90.04 bar (Test C) and the constant receiver pressure of 35.29 bar and the constant suction mass flow rate of 63 bar, the reduction in motive nozzle mass flow rate is by 81% compared to the advanced multi-ejector. The advanced multi-ejector has a motive mass flow rate of 788 kg/h, meanwhile the HP 1875 multi-ejector achieves 152 kg/h.

For the constant motive nozzle pressure of 90.30 bar (Test D) and the constant receiver pressure of 35.20 bar and the constant suction mass flow rate of 68 kg/h, the reduction in motive nozzle mass flow rate is by 85% compared to the advanced multi-ejector. The advanced multi-ejector has a motive mass flow rate of 807 kg/h, meanwhile the HP 1875 multi-ejector achieves 164 kg/h.

Summarised, the advanced multi-ejector has higher motive mass flow than the multi-ejector in Coolselector. The maximum motive nozzle mass flow rate difference between the two multi-ejectors is 651 kg/h, found in Test A. This corresponds to a reduction by 86% for the HP 1875 compared to the advanced multi-ejector.

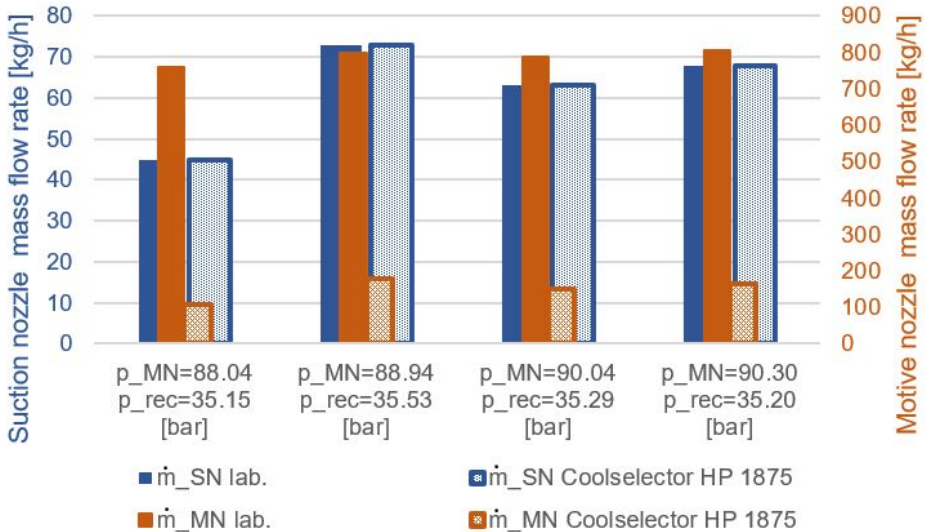


**Figure 4.15:** Motive nozzle mass flow rate for higher pressure lift ejector performance comparison at equal suction mass flow rate and pressure lift (Case 3).

To sum up for all three comparisons in this section, the Coolselector recommended multi-ejector HP 1875 had higher suction mass flow rates (Case 1) and higher receiver pressure levels (Case 2) than the advanced multi-ejector. The motive nozzle mass flow rates (Case

3) were lower for HP 1875 than the advanced multi-ejector.

#### **4.2.4 Advanced multi-ejector compared to HP multi-ejector – entrainment ratio, ejector efficiency and pressure lift**

In this subsection the advanced multi-ejector is compared to high pressure lift multi-ejectors from Danfoss on the basis of ejector efficiency, entrainment ratio and pressure lift. The refrigeration conditions Test A, B, C and D, found in Figure 4.2, are the same as in the last section and present the conditions with constant motive nozzle pressure of 88.04 bar, 88.94 bar, 90.04 bar and 90.30 bar. The following three figures in this subsection reveal the difference in suction nozzle mass flow rate (Case 1), the difference in receiver pressure (Case 2) and the difference in motive nozzle mass flow rate (Case 3), exactly as the subsection before, but now the adjoined efficiency, entrainment ratio and pressure lift are visualised. An overview of the cases are as mentioned before illustrated in Figure 4.4. The entrainment ratio is coloured red, the ejector efficiency is blue and the pressure lift is green. The full coloured column graph are values from the laboratory, whereas the patterned column graphs are from Coolselector.

##### **Case 1**

Figure 4.16 shows the entrainment and ejector efficiency results of the comparison between the advanced multi-ejector and HP 1875 from Coolselector with the difference in suction nozzle mass flow rate illustrated in Figure 4.13 (Case 1).

The constant motive nozzle pressure of 88.04 and a constant pressure lift of 8.05 bar for both multi-ejectors illustrate Test A. The entrainment ratio is 0.06 for the advanced multi-ejector and 0.41 for HP 1875. This is an increase by 589% compared to the advanced multi-ejector. The ejector efficiency is 5.00% and 34.32%, which is an increase by 587% compared to the advanced multi-ejector.

The constant motive nozzle pressure of 88.94 bar and the constant pressure lift of 7.93 bar for both multi-ejectors illustrate Test B. The entrainment ratio is 0.09 and 0.41, an increase by 335.6%, and the ejector efficiency is 7.58% and 34.45%, an increase by 354.4%, for respectively the advanced multi-ejector in the laboratory and the HP 1875 multi-ejector from the Coolselector results.

For Test C, where both multi-ejectors have a motive nozzle pressure of 90.04 bar, a pressure lift of 8.15 bar, the HP 1875 multi-ejector's increase in entrainment ratio is 420.9% compared to the advanced multi-ejector. The same pattern follows for the HP 1875, where the increase in ejector efficiency is 424.3% from the the advanced multi-ejector. The absolute values for the entrainment ratio is 0.08 and 0.42, where the latter is for the HP 1875. The ejector efficiency 7.11% for the advanced multi-ejector and 37.27% for HP 1875.

At the last columns from the left, the constant motive nozzle pressure is 90.30 bar and constant pressure lift is 8.16 bar (Test D). The HP 1875 multi-ejector's increase in entrainment ratio is 384% compared with the advanced multi-ejector. The same pattern follows

where HP 1875 has an increase by 375% in ejector efficiency from the advanced multi-ejector. The absolute values for the entrainment ratios are 0.08 and 0.41, where the latter is the selected multi-ejector in Coolselector. The ejector efficiencies are 7.32% and 34.78%, where the advanced multi-ejector achieved the lowest value.

The high ejector efficiency for the recommended HP 1875 multi-ejector in Coolselector is due to the high suction nozzle mass flow rate illustrated in Figure 4.13. The ejector efficiency for the HP 1875 multi-ejector has a significant higher efficiency than the ejector prototype. Test A has the maximum increase of 587% in ejector efficiency from the advanced multi-ejector. The lowest increase from the advanced multi-ejector to the Coolselector option was 354% in Test B. The same tendency was found for the entrainment ratio, where the maximum increase was also found in Test A with 589%. The minimum increase of entrainment ratio was also found in Test B with 356% from the advanced multi-ejector.

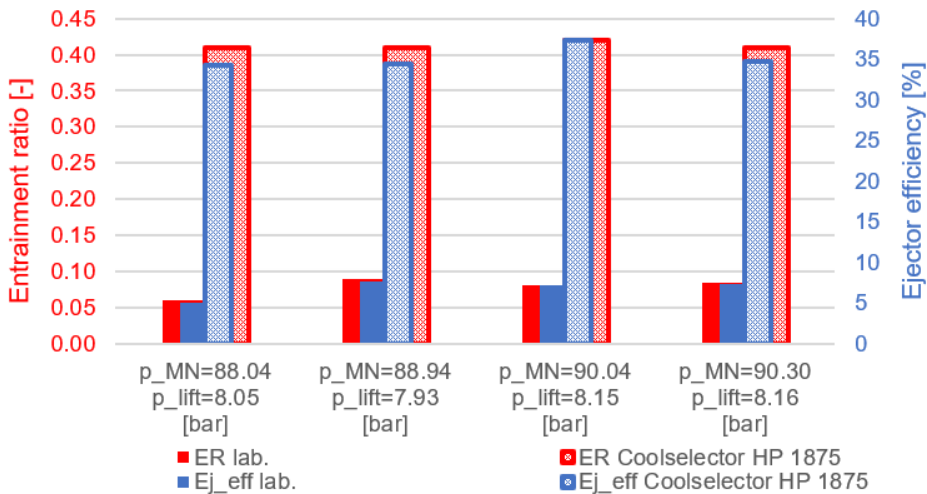


**Figure 4.16:** Entrainment ratio and ejector efficiency for higher pressure lift ejector performance comparison at equal motive nozzle pressure and pressure lift (Case 1 like Figure 4.13).

## Case 2

Figure 4.17 illustrates the difference in pressure lift and ejector efficiency with the difference in receiver pressure (Case 2, see Figure 4.14) between the advanced multi-ejector and the multi-ejector HP 1875 in Coolselector.

For the first group of columns the constant motive nozzle pressure is 88.04 bar (Test A) and entrainment ratio is 0.06. The pressure lift is 8.05 bar for the advanced multi-ejector and 13.36 bar in Coolselector, which is an increase by 66.0% in pressure lift. The ejector efficiency is 5.00% for the advanced multi-ejector, meanwhile the ejector efficiency is 9.42% in Coolselector, which corresponds to an increase by 88.5% compared to the advanced multi-ejector.

For the second group of columns the constant motive nozzle pressure is 88.94 bar (Test B) and entrainment ratio 0.09 for both multi-ejectors. The pressure lift with 12.78 bar in Coolselector is an increase by 61.2% compared to the advanced multi-ejector with 7.93 bar. The ejector efficiency for the advanced multi-ejector is 7.58% and 13.67% for HP 1875, which corresponds to an increase by 80.4% in ejector efficiency.

For the third group of columns the constant motive nozzle pressure is 90.04 bar (Test C) and the entrainment ratio 0.08 for both multi-ejectors. The pressure lift with 13.02 bar in Coolselector is an increase by 59.7% compared to the advanced multi-ejector at 8.15 bar. For the ejector efficiency of 12.77% in Coolselector, the increase is by 79.7% compared to the advanced multi-ejector which has a ejector efficiency of 7.11%.

For the fourth and last group of columns the constant motive nozzle pressure is 90.04 bar (Test D) and the entrainment ratio is 0.08 for both multi-ejectors. The pressure lifts are 8.15 bar and 13.03 bar, which is an increase by 59.6% from the advanced multi-ejector to HP 1875. The ejector efficiency of 12.92% in Coolselector is an increase by 76.5% compared with the advanced multi-ejector at 7.32%.

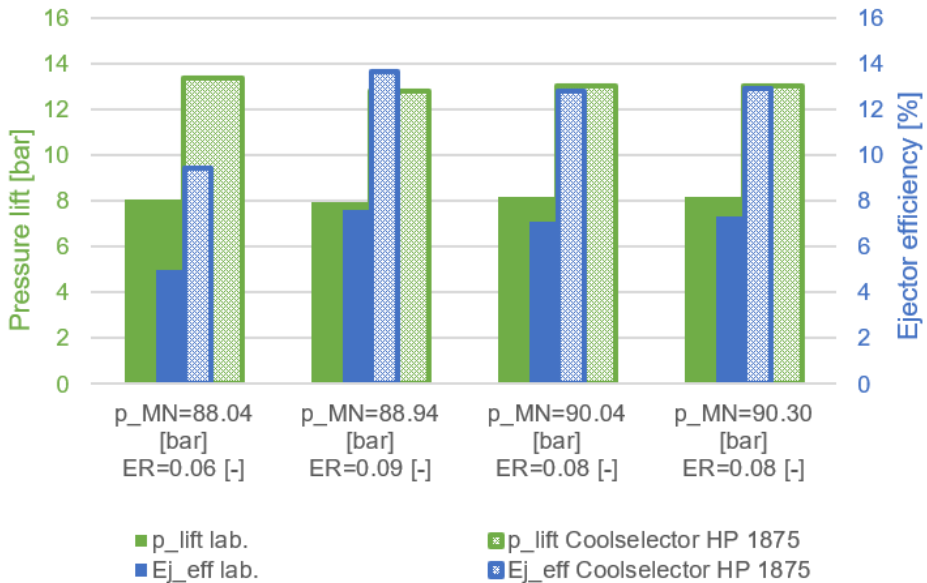


**Figure 4.17:** Pressure lift and ejector efficiency for higher pressure lift ejector performance comparison at equal motive nozzle pressure and entrainment ratio (Case 2 like Figure 4.14).

### Case 3

Figure 4.18 illustrates the difference in entrainment ratio and ejector efficiency with the difference in motive nozzle mass flow rate (Case 3 shown in Figure 4.15) between the advanced multi-ejector and the multi-ejector HP 1875 in Coolselector.

Figure 4.18 are identical to the results in Figure 4.16 with the difference in suction mass flow rate (Case 1). This is due to the same entrainment ratios values for Case 1 and Case 3, even though the values of the motive- and suction mass flow rates are different.

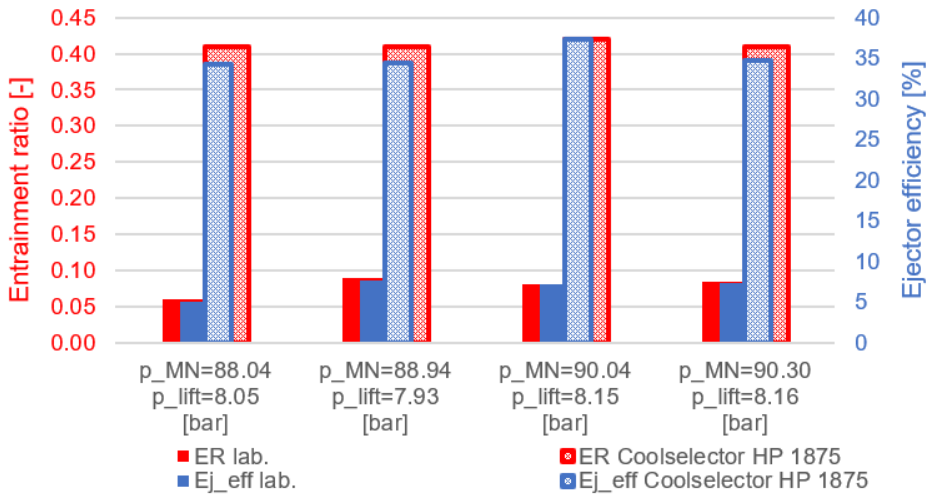


**Figure 4.18:** Entrainment ratio and ejector efficiency for higher pressure lift ejector performance comparison at equal motive nozzle pressure and pressure lift (Case 3 like Figure 4.15).

To sum up, the advanced multi-ejector has a lower ejector efficiency and a lower entrainment ratio as the HP 1875 multi-ejector for all cases. This is because, the values for the multi-ejector is lower for the suction mass flow rate and the receiver pressure and higher for the motive mass flow rate as illustrated in Section 4.2.3.

The HP 1875 multi-ejector from Coolselector has higher efficiencies than the advanced multi-ejector under the same conditions. The efficiency is based on a simulation that would recreate the optimal process for the laboratory multi-ejector. The suction mass flow rate is only 44.78 kg/h for  $p_{MN}=88.04$  (Test A), however the HP 1875 achieved a higher suction mass flow rate of 314.7 kg/h. The difference in suction mass flow rate (Case 1) is found in Figure 4.13. Due to the low suction mass flow rate at the laboratory, the advanced multi-ejector has a relatively very low efficiency of 5.0%, found in Figure 4.16. It can be assumed that the problem is caused by a non-optimised geometry which leads to very low entrainment ratios. The suction mass flow rate, entrainment ratio and the ejector efficiency are proportional. Here the entrainment ratio reached a value of only 0.06 due to a low suction mass flow rate. In contrast, the HP multi-ejector from Coolselector had a high suction

mass flow rate, a high entrainment ratio value of 0.41 and therefore the output of the high ejector efficiency of 34.32%.

The highest performed ejector efficiency for HP 1875 in Coolselector was 37%, which is excellent for a multi-ejector. As mentioned in the Methodology in Section 3.4, the equations are calculated from real laboratory tests. The ejector efficiency is on the limit on how high the ejector efficiency can be. This is close to the design point of the multi-ejector, since the ejector efficiency is very high.



## Discussion

In this chapter the values from the laboratory, the uncertainty analysis and the comparison between the advanced multi-ejector and multi-ejectors from Coolselector are discussed.

### 5.1 Laboratory measurements

The measurements from the CO<sub>2</sub> rig derived from the test conditions in Table 3.3 by Danfoss. It was difficult to control and manage all parameters in the test facility at once. It would have taken a disproportionate amount of time to find and adjust everything perfectly.

The test conditions, given in Table 3.3, were motive pressure and temperature, suction pressure and temperature, receiver pressure (ejector outlet pressure) and pressure lift. The measured tests were grouped after these conditions. Due to the many parameters that had to be controlled simultaneously at the rig, some parameters were chosen as more important than others. In this thesis the above mentioned parameters had all the attention excluding the suction temperature. Due to the difficult circumstances of handling all the parameters simultaneously in the rig, the suction temperature was given no attention. This can be seen from the overview table in the appendix, where the suction temperature changes from -7.01°C to 10.75°C, when it should have been approximately around the set point of -4°C. For the rest of the parameters with some exceptions, most of the measured points were in the deviation area between  $\pm 0$  and 3% from the set points. More tests could have been performed to decrease the deviation within the groups of the test conditions, but due to the corona pandemic it was not feasible.

## 5.2 Uncertainty analysis

### 5.2.1 Change of temperature and pressure uncertainties

By comparing Type A, based on the standard deviation, with Type B based on the equipment, as a function of ejector efficiency. Figure 5.1 shows that Type B has a higher uncertainty than Type A. The potential for further improvements on the uncertainty will be discussed.

Type A is the standard deviation of the mean, which shows how far away from the individual values in a measurement lies from the mean value. Indirectly, the standard deviation can be affected, if it depends on an input signal that has a large spread which is not accurate. The time steps between the measured values must be also considered. If the time steps are too large, it can overlook important signals. Other factors like unstable compressors affects the standard deviation as well.

In Figure 5.1 the relative uncertainties for Type B for the ejector efficiency is under 3.5%. The relative uncertainty is highest for the highest ejector efficiencies, due to the mean values dependency in the temperature uncertainty. The uncertainties for the pressures are constant for all measurements.

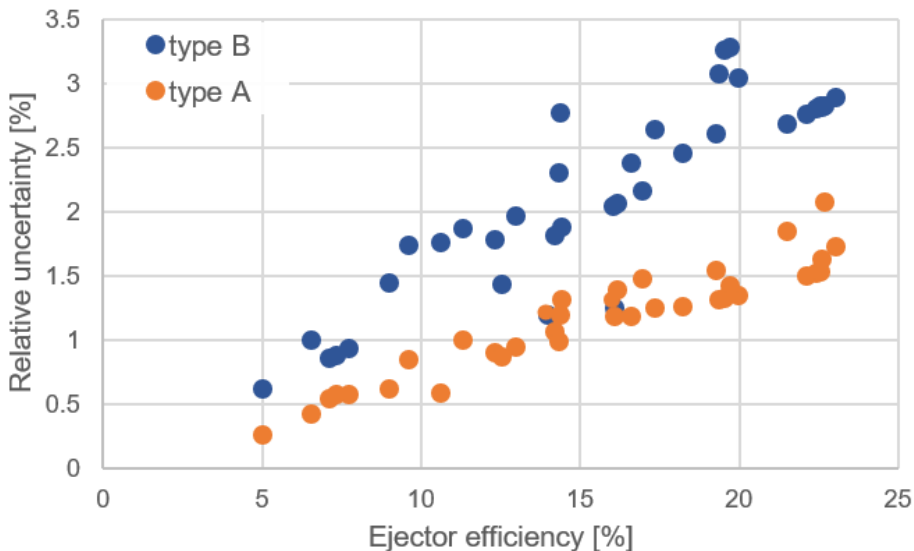


**Figure 5.1:** Type A versus Type B uncertainty as a function of ejector efficiency.

The Type B uncertainty for the temperatures and pressures are higher than Type A, however the opposite for the mass flow rates. The mass flow meter in this thesis has a very low Type B uncertainty, namely 0.12% of the reading. As an example Test 1 with a motive mass flow rate of 785.01 kg/h has a Type A uncertainty of 47.39 kg/h and Type B uncer-

tainty of only 0.94 kg/h. The latter is 50 times better than Type A. The highest Type A uncertainty for the motive mass flows is 48.68 kg/h found in Test 2 with 770 kg/h. The lowest Type A uncertainty is 23.15 kg/h found in Test 27 with 618.28 kg/h. The latter Type A uncertainty is almost half (48%) of the highest Type A uncertainty. A reason for the high Type A uncertainties for the mass flow rate is that it was difficult to keep it stable during the test run. The mass flow in test 2 with the highest Type A uncertainty fluctuated between 755.46 kg/h and 793.65 kg/h, which was shown as 12.5 kg/min and 13.2 kg/min in the mass flow meter. The fluctuation lead to a high standard deviation value, which is probably the main reason for the relative high Type A uncertainty for the mass flow rate.

The Type A uncertainty pressures for the motive, suction and outlet are between 0.00 bar and 0.06 bar. Conversely, the pressure transmitter has a relative high uncertainty (Type B).

The pressure uncertainty is 0.46 bar for all pressure transmitters in the test facility. Using Test 1 as an example again the motive pressure is 60.87 bar with a Type B uncertainty of 0.46 bar, which is 9.2 times higher than Type A that is only 0.05 bar.

The pressure transmitters that are used in the test facility today are intended for industrial processes that is known for stable conditions over a long period of time. The sensors used today are cheap enough to control a system, but the accuracy has its price. The more accurate, the more expensive is the product. The test facility is not an industrial system that should keep the same stable condition, but an experimental rig where tests under different conditions occur. Therefore, the quality of the sensors should be better than the standard.

In order to improve the uncertainty, only Type B which includes the equipment data can be examined for further investigation. The discussion focuses further on three scenarios, where i) the pressure accuracy improves, ii) the temperature accuracy improves and at last iii) where both sensors improves. As mentioned before, the Type B uncertainty equals the accuracy when divided by square root of 3, as defined in Equation 3.14.

#### **i) Change of the pressure accuracy from 0.5% to 0.2%**

A change in accuracy from 0.5%FS to 0.2%FS, where the full scale is still 160 bar, means that the Type B uncertainty reduces by 60.9% from 0.46 bar to 0.18 bar.

To the best of the authors knowledge, the best pressure transmitters on the market can have an accuracy of 0.01% and are used for test stands (TE connectivity (2020)). The uncertainty would be 0.009 bar with the best pressure transmitter, but also more expensive.

#### **ii) Change of the temperature accuracy from class A to class AA**

According to the standard of thermometers IEC 60751:2008, the best class is AA which has the accuracy of  $\pm 0.1 + 0.0017(t)$ . The class A that is used today, has the accuracy of  $\pm 0.15 + 0.002(t)$ .

For the motive nozzle temperature in Test 1, found in Table 4.1, with 19.54°C, the Type B

uncertainty will be reduced from  $0.19^{\circ}\text{C}$  to  $0.08^{\circ}\text{C}$ . That is a reduction of 57.9%. Test 1 has an ejector efficiency of 13.96%. With the change in uncertainty in temperatures, the uncertainty for the ejector efficiency decreases by 31.1% from the absolute value of 1.19% to 0.82%.

### iii) Combining the change of pressure and temperature from i) and ii)

The uncertainty for the ejector efficiency explained in Section 3.3.2 is affected by the improved pressure and temperature uncertainties. Figure 5.2 shows the relative uncertainty as a function of ejector efficiency for all tests performed in the laboratory. The blue dots are the original uncertainties, where the green dots are the possible uncertainties with the more precise pressure and temperature sensors. The latter achieves a more accurate ejector efficiency. The accuracies for the pressure and the temperature sensors for both original and new are described in the left upper corner of the figure.

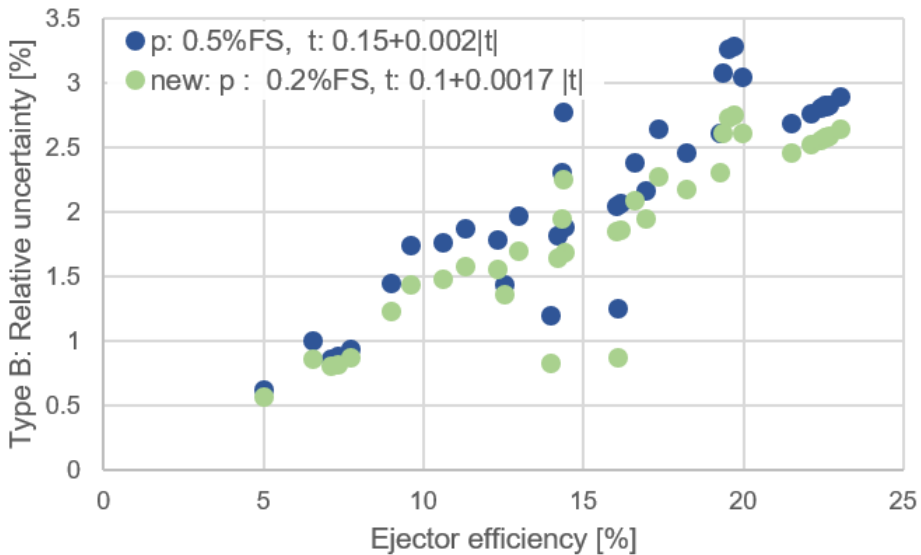


**Figure 5.2:** Type B uncertainty as a function of ejector efficiency with original (blue) and new improved (green) temperature and pressure sensors. The accuracies for pressure (p) and temperature (t) sensors used in the uncertainty calculations are found in the upper left corner. Full scale (FS) is 160 bar.

As indicated in the figure by the green dots, the uncertainties reduces for the ejector efficiencies, when equipment with lower accuracy are installed.

To summarise, the present mass flow meter has an uncertainty of 0.12% of the reading. The uncertainty is 0.46 for the pressure transmitters, which means that the pressure transmitters for the ejector motive, suction and outlet are between 0.51% and 1.83% of the reading depending on the mean pressure. The mass flow meter uncertainty of the reading is at least 4.3 times lower than than the pressure transmitters of the reading. Due to this

fact, pressure transmitters with a lower uncertainty should be installed in the test facility.

### **5.2.2 Change of differential pressure uncertainties**

The superheat and the pressure lift uncertainties were calculated with the use of two sensors. The uncertainty for the superheat was calculated by a pressure and a temperature sensor. The uncertainty for the pressure lift was calculated from two pressure sensors. By installing a differential temperature sensor and a differential pressure sensor, the uncertainty will be reduced. Differential pressure transmitters will be further discussed.

To the best of the authors knowledge, there are differential pressure transmitters with a measurement accuracy up to 0.025% (ABB (2020)). Endress+Hauser (2020) has a differential pressure lift sensor with a standard accuracy of 0.05% and a "platinum" with  $\pm 0.035\%$  accuracy.

The Type B uncertainty for all the pressure lifts are 0.65 bar in this thesis. If the uncertainty of the pressure lift changes to  $0.5\% * FS / \sqrt{3}$ , where full scale (FS) is 160 bar, then the Type B is 0.045 bar. Changing full scale (FS) to 10 bar, the uncertainty is only 0.003 bar. This is a reduction by respectively 93% and 99.5%, which is a relative large and positive influence.

There is no doubt that the uncertainty is lower by inserting a differential pressure transmitter than inserting two separate pressure transmitters. A differential pressure transmitter should be installed.

## 5.3 Coolselector

According to the website of Danfoss (2020a) a disclaimer for using the application Coolselector2 is that the results and information cannot be relied on as accurate data or analysis. Anyway, the results give an important view on how the ejector prototype is compared to current transcritical ejectors on the market. Due to closed laboratory under the corona pandemic, where the advanced multi-ejector could not physically be compared to other multi-ejectors, the comparison was made using the digital solution Coolselector.

### 5.3.1 Refrigeration conditions outside the ejectors envelope in Coolselector

When comparing the multi-ejector prototype with the LP and the HP transcritical multi-ejectors from Danfoss with data from Coolselector, it is obvious that that the full picture is missing when the comparison only includes 4 measured tests. The significant cause for the comparison was to show the principle for the conditions that was analysed. The principle was shown and a conclusion from those values could be drawn.

The LP and HP multi-ejector comparison were both performed for only four tests, despite having 35 laboratory tests from the multi-ejector prototype. The other 31 laboratory tests were omitted in Coolselector, due to error in the compilation. For some tests, no multi-ejectors were found for these conditions, for others the suction conditions or the motive conditions were outside the valid operating envelope of the selected multi-ejectors available.

For the transcritical HP system, only HP 1875 was selected with the operational conditions from the laboratory test that were successful. The other tests did not compile, due to the operational conditions being outside the envelope. The motive envelope for HP 1875 is shown in Figure 5.3, and the suction envelope in 5.4. Both envelopes show the compilation for Test 28 from Table 4.1.

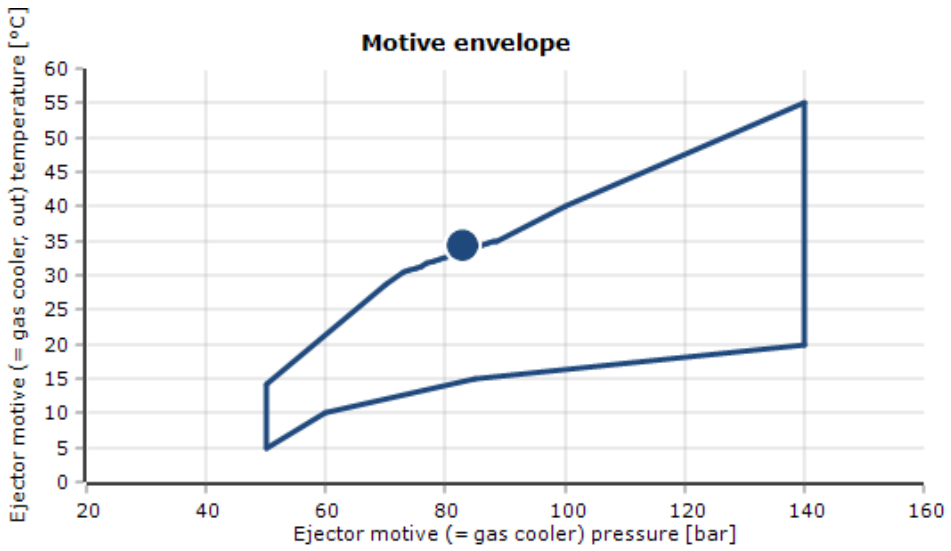


**Figure 5.3:** Motive envelope for HP 1875 adapted from Coolselector

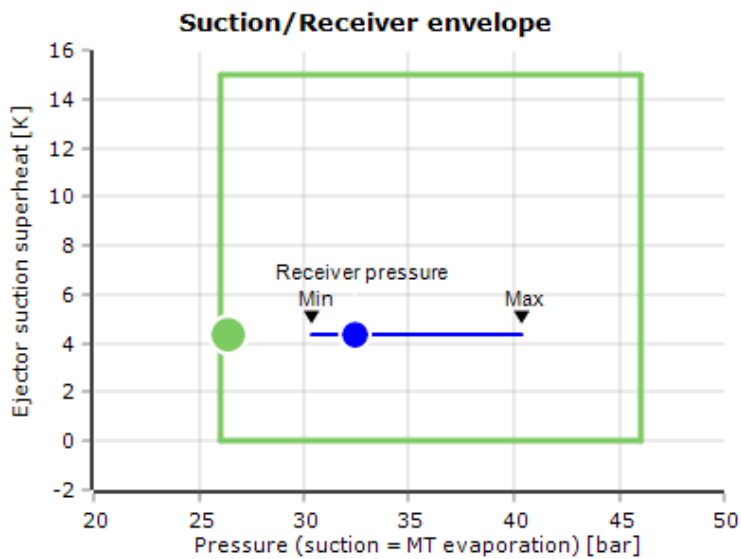


**Figure 5.4:** Suction/receiver envelope for HP 1875 adapted from Coolselector

The blue dot in Figure 5.3, illustrates the motive nozzle pressure for Test 28 that is 82.80 bar and the motive temperature that is 34.4°C. The dot is outside the motive envelope, which is defined as the area inside the blue lines.

Figure 5.4 illustrates the superheat as a function of suction pressure. The suction and receiver envelope is the area inside the green line. The superheat has a range from 0 K to 15 K, which includes the superheat of 4.43 K from Test 28. The suction pressure varies between 26 and 46 bar. The green dot inside the envelope illustrates the suction pressure for Test 28, which is 26.39 bar. The receiver pressure ranges from 31 bar to 41 bar and is illustrated by the blue line. The blue dot is the receiver pressure of 32.39 bar from the test. The suction conditions are all within the limits, but due to test's motive conditions being outside the motive envelope, the multi-ejector could not be selected.

### **5.3.2 Is the advanced multi-ejector prototype a LP or a HP multi-ejector?**

Since the other Danfoss' transcritical multi-ejectors on the commercial market are divided in low pressure lift and high pressure lift multi-ejectors, it can be interesting to discuss what indications the results have given regarding whether it is more a LP or a HP multi-ejector.

For the comparison with different suction mass flow rate (Case 1), the prototype had a higher suction mass nozzle flow rate than the LP ejector, but a lower suction mass flow than the HP multi-ejector in Coolselector. Case 2, the difference in receiver pressure, showed that the receiver pressure for the prototype is higher than the LP multi-ejector, but lower than the HP multi-ejector. For the difference in motive mass flow rate (Case 3), the opposite tendency compared to Case 1 and Case 2 were found, since the motive mass flow for the prototype was lower than the LP multi-ejector, but higher than the HP multi-ejector. The corresponding entrainment ratio and ejector efficiency for the prototype was higher than the LP multi-ejectors, but simultaneously lower than the HP multi-ejector for all cases.

Since the comparison only regard the upper motive pressures between 88.04 bar and 90.30 bar, it can be concluded that in this area the advanced multi-ejector is more a LP than a HP multi-ejector. Taking all the measurements from the laboratory into the account, the best ejector efficiency was found at the lower pressure lifts between 3 and 4 bar. This also suggests that the prototype is more a LP than a HP multi-ejector.



## Conclusion

Experimental investigation of the R744 multi-ejector prototype from the Danish company Danfoss was performed under different operational conditions in a test facility. The refrigeration system was operated in subcritical and transcritical mode.

The experiments at the laboratory investigated motive nozzle pressures from 59.3 until 90.3 bar with increasing pressure lifts from 2.17 bar until 8.16 bar. The experimental results revealed that the advanced multi-ejector achieved a maximum ejector efficiency of 23.02% with the motive nozzle pressure of 70.7 bar and pressure lift of 3.8 bar. The multi-ejector efficiency decreased for higher motive nozzle pressures with higher pressure lifts due to drop of suction nozzle mass flow rates and entrainment ratios.

The test rig functioned and performed well, but there were some challenges with the measurement precision for certain sensors. Due to the corona pandemic, the test facility was closed and further measurements could not be performed.

The uncertainty of the independent parameters were found by standard deviation (Type A) and equipment data (Type B). The pressure transmitters have a relatively higher uncertainty than the mass flow sensor. The mass flow meter had an uncertainty of 0.12% of reading, whereas the pressure transmitters for the ejector motive, suction and outlet were between 0.51% and 1.83% of reading depending on the mean pressure. The mass flow meter uncertainty were at least 4.23 times lower than than the pressure transmitters.

In order to investigate the performance of the advanced multi-ejector compared to other multi-ejectors from Danfoss on the commercial market, the operational conditions from the laboratory measurements were inserted into the selection software Coolselector. The software results were obtained for low pressure system and high pressure system. The four laboratory measurements with the highest motive pressures (88.04 bar - 90.30 bar) and highest pressure lifts (7.93 bar - 8.16 bar) compiled with the high pressure (HP) and low pressure (LP) multi-ejectors. The rest of the laboratory measurements were outside

the motive and or suction envelopes of the LP and HP multi-ejectors available in Coolselector. The comparison based on varying suction mass flow rate (Case 1), inlet receiver pressure (Case 2) and motive mass flow rate (Case 3).

The advanced multi-ejector had higher suction mass flow rates, higher receiver pressures than the recommended LP 9325 and lower motive mass flow rates than the recommended LP 1435 and LP 1935 multi-ejectors. This resulted into higher ejector efficiencies and higher entrainment ratios for the advanced multi-ejector than the recommended low pressure lift multi-ejectors. The highest efficiency of the compared laboratory measurements was 7.58%, whereas the highest efficiency of the LP multi-ejectors was 7.30%, which is an decrease of 3.6% in ejector efficiency.

On the contrary, the advanced multi-ejector had lower suction mass flow rates, lower receiver pressures and higher motive mass flow rates than the recommended HP 1875 multi-ejector. The highest efficiency from the compared laboratory tests was 7.58%, whereas the highest efficiency from the HP 1875 relieved 37.27%, which is around 4 times higher than the advanced multi-ejector.

Since the comparison only regarded the upper motive pressures between 88.04 bar and 90.30 bar, it can be concluded that in this area the advanced multi-ejector is more a LP than a HP multi-ejector. The ejector prototype had low efficiencies for all values compared with Coolselector, which means that those values are probably off-design points. Taking all the measurements from the laboratory into account, the best ejector efficiency was found at the lower pressure lifts between 3 and 4 bar. This also suggests that the prototype is more a LP than a HP ejector.

The suction mass flow rates were low for the higher pressure lifts in the laboratory measurements, which resulted in low ejector efficiencies. This indicates, that the low ejector efficiencies is due to a non-optimal geometry in the advanced ejector for the highest motive pressures between approximately 83 bar and 90 bar. The suction nozzle mass flow rates was much higher for the HP ejectors than for what was possible in the laboratory for the conditions with motive pressures around 90 bar.

The advanced multi-ejector has still a potential to achieve higher ejector efficiencies. In this Master Thesis the maximum overall ejector efficiency was 23.02%, which is far away from the highest ever measured vapour ejector cartridge efficiency of 36.8%. However, compared with the overall efficiency of 22.8% in the literature, the result is acceptable.

The work of this Master Thesis has thus produced measurements for the advanced multi-ejector, which may simplify further research of improving the prototype.

## Suggestions for further work

For future tests at the test facility, the pressure transmitters should be replaced with pressure transmitters that have a lower uncertainty. In addition, differential pressure transmitters should be installed to decrease the pressure lift uncertainty.

Due to the corona pandemic, the operational conditions could not be performed for other multi-ejectors, which later could have been compared with the advanced multi-ejector. A further work is needed to finish the comparison.

Since the advanced multi-ejector still is a prototype, more tests can be performed and more investigation can be made in order to improve the performance of the prototype. Moreover, multi-ejectors in general still have a potential to be improved.



# Bibliography

- ABB, 2020. Differential pressure transmitter with multisensor technology, model 266mst. <https://new.abb.com/products/measurement-products/pressure/differential-pressure-transmitters/266mst-differential-pressure-transmitter-with-multisensor-technology>, accessed: 2020-07-12.
- Banasiak, K., Hafner, A., Andresen, T., 2012. Experimental and numerical investigation of the influence of the two-phase ejector geometry on the performance of the r744 heat pump. *International journal of Refrigeration* 35, 1617–1625.
- Banasiak, K., Hafner, A., Kriezi, E.E., Madsen, K.B., Birkelund, M., Fredslund, K., Olsson, R., 2015a. Development and performance mapping of a multi-ejector expansion work recovery pack for r744 vapour compression units. *International Journal of Refrigeration* 57, 265–276.
- Banasiak, K., Hafner, A., Kriezi, E.E., Madsen, K.B., Birkelund, M., Fredslund, K., Olsson, R., 2015b. Development and performance mapping of a multi-ejector expansion work recovery pack for r744 vapour compression units. *International Journal of Refrigeration* 57, 265–276.
- Banasiak, K., Pardiñas, A., 2019. Sheccobase webinar: zero net energy supermarkets: towards a sustainable future. [https://www.youtube.com/watch?v=mpbWQbk18\\_g#t=20m15s](https://www.youtube.com/watch?v=mpbWQbk18_g#t=20m15s), accessed: 2020-07-01.
- Boccardi, G., Botticella, F., Lillo, G., Mastrullo, R., Mauro, A., Trinchieri, R., 2017. Experimental investigation on the performance of a transcritical co2 heat pump with multi-ejector expansion system. *International Journal of Refrigeration* 82, 389–400.
- Bodys, J., Smolka, J., Palacz, M., Haida, M., Banasiak, K., Nowak, A.J., Hafner, A., 2016. Performance of fixed geometry ejectors with a swirl motion installed in a multi-ejector module of a co2 refrigeration system. *Energy* 117, 620–631.
- Chunnanond, K., Aphornratana, S., 2004. Ejectors: applications in refrigeration technology. *Renewable and sustainable energy reviews* 8, 129–155.

- 
- Ciconkov, R., 2018. Refrigerants: There is still no vision for sustainable solutions. *International Journal of Refrigeration* 86, 441–448.
- Commission, E., 2014. Regulation (eu) no 517/2014 of the european parliament and of the council of 16th april 2014 on fluorinated greenhouse gases and repealing regulation (ec) no 842/2006.
- Daneshmand, S., Aghanajafi, C., Bahrami, A., 2009. Analytical and experimental methods of design for supersonic two-stage ejectors. *World Academy of Science, Engineering and Technology* 50, 201–204.
- Danfoss, 2018a. Co2 in lebensmitteleinzelhandel. <https://www.danfoss.com/en-gb/service-and-support/case-studies/dcs/the-danfoss-multi-ejector-range-for-co2-refrigeration/>, accessed: 2020-02-10.
- Danfoss, 2018b. The danfoss multi ejector range for co2 refrigeration: design, applications and benefits. <https://www.danfoss.com/en/service-and-support/case-studies/dcs/the-danfoss-multi-ejector-range-for-co2-refrigeration/>, accessed: 2020-02-01.
- Danfoss, 2020a. Coolselector 2. <https://www.danfoss.com/en/service-and-support/downloads/dcs/coolselector-2/#tab-overview>, accessed: 2020-04-15.
- Danfoss, 2020b. Pressure transmitter, mbs 8250. <https://store.danfoss.com/en/search/?text=MBS+8250>, accessed: 2020-02-10.
- Eikevik, T.M., 2017. Compendium for heat pumping processes and systems (TEP4255).
- Elbel, S., Hrnjak, P., 2008. Experimental validation of a prototype ejector designed to reduce throttling losses encountered in transcritical r744 system operation. *International Journal of Refrigeration* 31, 411–422.
- Endress+Hauser, 2020. Differential pressure deltabar pmd75. <https://www.no.endress.com/no/skreddersom-tilpasset-felt-instrumentering/trykk-differensialtrykk-absolutt-overtrykk-/Differential-Pressure-Deltabar-PMD75>, accessed: 2020-07-31.
- Gay, N.H., 1931. Refrigerating system. US Patent 1,836,318.
- Ge, Y., Tassou, S., 2011. Thermodynamic analysis of transcritical co2 booster refrigeration systems in supermarket. *Energy Conversion and Management* 52, 1868–1875.
- Giffard, H., 1860. Improved feed-water apparatus for steam-boilers. US Patent 27,979.
- Graham Corporation, 2017. A mystery solved. [https://www.graham-mfg.com/usr/pdf/TechLibVacuum/Article\\_-\\_A\\_Mystery\\_Solved\\_2017\\_Hydrocarbon\\_Engineering.pdf?fbclid=IwAR08t7f3wiVrMSrk7NEtjcK\\_etWVlyj584fyi8AI6ydGiPh5xkaFZvIMQNC](https://www.graham-mfg.com/usr/pdf/TechLibVacuum/Article_-_A_Mystery_Solved_2017_Hydrocarbon_Engineering.pdf?fbclid=IwAR08t7f3wiVrMSrk7NEtjcK_etWVlyj584fyi8AI6ydGiPh5xkaFZvIMQNC), accessed: 2020-04-01.

- 
- Gullo, P., 2019. Innovative fully integrated transcritical r744 refrigeration systems for a hfc-free future of supermarkets in warm and hot climates. *International Journal of Refrigeration* 108, 283–310.
- Gullo, P., Hafner, A., Banasiak, K., Minetto, S., Kriezi, E.E., 2019. Multi-ejector concept: A comprehensive review on its latest technological developments. *Energies* 12, 406.
- Gullo, P., Hafner, A., Cortella, G., 2017a. Multi-ejector r744 booster refrigerating plant and air conditioning system integration—a theoretical evaluation of energy benefits for supermarket applications. *international journal of refrigeration* 75, 164–176.
- Gullo, P., Kærn, M.R., Haida, M., Smolka, J., Elbel, S., 2020. A review on current status of capacity control techniques for two-phase ejectors. *International Journal of Refrigeration* .
- Gullo, P., Tsamos, K., Hafner, A., Ge, Y., Tassou, S.A., 2017b. State-of-the-art technologies for transcritical r744 refrigeration systems—a theoretical assessment of energy advantages for european food retail industry. *Energy Procedia* 123, 46–53.
- Gullo, P., Tsamos, K.M., Hafner, A., Banasiak, K., Yunting, T.G., Tassou, S.A., 2018. Crossing co2 equator with the aid of multi-ejector concept: A comprehensive energy and environmental comparative study. *Energy* 164, 236–263.
- Hafner, A., Banasiak, K., 2016. Full scale supermarket laboratory r744 ejector supported and ac integrated parallel compression unit, in: *Proceedings of the 12th IIR Gustav Lorentzen Natural Working Fluids Conference*, Edinburgh, UK, pp. 21–24.
- Hafner, A., Eikevik, T., 2019. *Lecture notes in TEP4255 Heat pumping processes and systems*, NTNU.
- Hafner, A., Försterling, S., Banasiak, K., 2014. Multi-ejector concept for r-744 supermarket refrigeration. *International Journal of Refrigeration* 43, 1–13.
- Hafner, A., Poppi, S., Neksa, P., Minetto, S., Eikevik, T., 2012. Development of commercial refrigeration systems with heat recovery for supermarket building, in: *Proceedings of the 10th IIR Gustav Lorentzen Conference on Natural Refrigerants*, Delft, The Netherlands, pp. 25–27.
- Haida, M., Banasiak, K., Smolka, J., Hafner, A., Eikevik, T.M., 2016. Experimental analysis of the r744 vapour compression rack equipped with the multi-ejector expansion work recovery module. *international journal of refrigeration* 64, 93–107.
- Haida, M.P., 2015. Experimental analysis of the r744 vapour compression rack equipped with the multi-ejector expansion work recovery module. <https://ntnuopen.ntnu.no/ntnu-xmlui/handle/11250/2350181>, pages=31-40, accessed: 2020-05-10.
- Haukås, Stene, R.N.H.E., 2016. *Kompendium CO2 (R744) som kuldemedium*. Norsk kjøleteknisk forening.

- 
- JCGM, 2008. Evaluation of measurement data — guide to the expression of uncertainty in measurement. [https://www.bipm.org/utils/common/documents/jcgm/JCGM\\_100\\_2008\\_E.pdf](https://www.bipm.org/utils/common/documents/jcgm/JCGM_100_2008_E.pdf), accessed: 2020-02-7.
- Karampour, M., Sawalha, S., Arias, J., 2016. Eco-friendly supermarket—an overview, public report 2 for supersmart project (project number: 696076). <http://www.supersmart-supermarket.info/downloads/>, accessed: 2020-07-18.
- Kim, M.H., Pettersen, J., Bullard, C.W., 2004. Fundamental process and system design issues in co2 vapor compression systems. *Progress in energy and combustion science* 30, 119–174.
- Lawrence, N., Elbel, S., 2015. Analysis of two-phase ejector performance metrics and comparison of r134a and co2 ejector performance. *Science and Technology for the Built Environment* 21, 515–525.
- Liu, F., Groll, E.A., Li, D., 2012. Modeling study of an ejector expansion residential co2 air conditioning system. *Energy and buildings* 53, 127–136.
- Ma, Z., Bao, H., Roskilly, A.P., 2017. Thermodynamic modelling and parameter determination of ejector for ejection refrigeration systems. *international journal of refrigeration* 75, 117–128.
- Moffat, R.J., 1988. Describing the uncertainties in experimental results. *Experimental thermal and fluid science* 1, 3–17.
- Nordtvedt, T., Hafner, A., 2012. Integration of refrigeration and hvac supermarkets, in: *Proceedings of 10th IIR Gustav Lorentzen Conference, International Institute of Refrigeration*. Delft, the Netherlands.
- Purohit, N., Gullo, P., Dasgupta, M.S., 2017. Comparative assessment of low-gwp based refrigerating plants operating in hot climates. *Energy Procedia* 109, 138–145.
- Rheonik, 2019a. Pressure transmitter, mbs 8250. [https://www.rheonik.com/wp-content/uploads/pdf/Rheonik\\_Coriolis\\_RHM06\\_Datasheet.pdf](https://www.rheonik.com/wp-content/uploads/pdf/Rheonik_Coriolis_RHM06_Datasheet.pdf), accessed: 2020-02-10.
- Rheonik, 2019b. Pressure transmitter, mbs 8250. [https://www.rheonik.com/wp-content/uploads/pdf/Rheonik\\_Coriolis\\_RHM08\\_Datasheet.pdf](https://www.rheonik.com/wp-content/uploads/pdf/Rheonik_Coriolis_RHM08_Datasheet.pdf), accessed: 2020-02-10.
- Sag, N.B., Ersoy, H., Hepbasli, A., Halkaci, H., 2015. Energetic and exergetic comparison of basic and ejector expander refrigeration systems operating under the same external conditions and cooling capacities. *Energy conversion and management* 90, 184–194.
- Sarkar, J., 2012. Ejector enhanced vapor compression refrigeration and heat pump systems—a review. *Renewable and Sustainable Energy Reviews* 16, 6647–6659.
- Sawalha, S., 2008. Theoretical evaluation of trans-critical co2 systems in supermarket refrigeration. part i: Modeling, simulation and optimization of two system solutions. *international journal of refrigeration* 31, 516–524.



- 
- Sawalha, S., 2013. Investigation of heat recovery in co2 trans-critical solution for supermarket refrigeration. *International journal of refrigeration* 36, 145–156.
- Sawalha, S., Piscopiello, S., Karampour, M., Manickam, L., Rogstam, J., 2017. Field measurements of supermarket refrigeration systems. part ii: Analysis of hfc refrigeration systems and comparison to co2 trans-critical. *Applied Thermal Engineering* 111, 170–182.
- Schröder, W., 2014. *Fluidmechanik. Aachener Beiträge zur Strömungsmechanik.* pp. 220–223.
- Shecco, 2020. World guide to transcritical co2 refrigeration - part 2. <http://shecco.com/articles/2020-06-18-shecco-guide-puts-global-transcritical-co2-installations-at-35000/>, pages=20, accessed: 2020-07-23.
- Tassou, S., Ge, Y., Hadawey, A., Marriott, D., 2011. Energy consumption and conservation in food retailing. *Applied Thermal Engineering* 31, 147–156.
- Taylor, B.N., Kuyatt, C.E., 1994. Guidelines for evaluating and expressing the uncertainty of nist measurement results .
- TE connectivity, 2020. 0.1% accuracy pressure transducer. <https://www.te.com/global-en/product-CAT-PTT0037.html>, pages=31-40, accessed: 2020-08-02.
- Testo industrial services GmbH, 2020. Praxisgerechte Bestimmung von Messunsicherheiten nach GUM (bei Kalibrierungen), Messunsicherheitsfibel. [https://www.testotis.de/fileadmin/testotis.de/downloads/fibeln/Testo\\_Industrial\\_Services\\_GmbH\\_Messunsicherheitsfibel.pdf?fbclid=IwAR0wQYmINsM83knFokzJxRrPTVmUdi2PHD3C3TkhZtn2Y1fWZjn7XSRHa0A](https://www.testotis.de/fileadmin/testotis.de/downloads/fibeln/Testo_Industrial_Services_GmbH_Messunsicherheitsfibel.pdf?fbclid=IwAR0wQYmINsM83knFokzJxRrPTVmUdi2PHD3C3TkhZtn2Y1fWZjn7XSRHa0A), accessed: 2020-07-01.
- Zhu, J., Elbel, S., 2016. A new control mechanism for two-phase ejector in vapor compression cycles using adjustable motive nozzle inlet vortex .
- Zhu, J., Elbel, S., 2020. Experimental investigation into the influence of vortex control on transcritical r744 ejector and cycle performance. *Applied Thermal Engineering* 164, 114418.



# Appendix

---

# Appendix A

## Abstract for article

### EXPERIMENTAL ANALYSIS OF AN ADVANCED R744 MULTI-EJECTOR

**Merethe Leksen Selnes, Armin Hafner, Krzysztof Banasiak**

Norwegian University of Science and Technology

Kolbjørn Hejes Ved 1D, 7491 Trondheim, Norway

merethels@hotmail.com, armin.hafner@ntnu.no, krzysztof.banasiak@ntnu.no

#### ABSTRACT

The increasing interest in energy efficient solutions, and working towards a more sustainable future, give rise to the importance of saving energy. Present supermarket refrigeration systems, with carbon dioxide, have a large potential to limit power consumption. Multi-ejectors are a part of the solution and have already been installed in throughout Europe, but further improvements are necessary.

A new prototype of an multi-ejector is set for experimental investigation in a test facility under vapour conditions. The experimental tests, based on motive nozzle inlet temperature, suction nozzle temperature, pressure lift of the multi-ejector, resulted in measured entrainment ratios and ejector efficiencies. The experimental results indicated a ejector efficiency up to 23.2% and entrainment ratio up to 0.52.

Moreover, a comparison analysis was performed between the advanced multi-ejector and commercial multi-ejectors from Danfoss. The experimental results were implemented into the calculation tool Coolselector, were transcritical low pressure and high pressure multi-ejectors from Danfoss under the same operational conditions as the advanced multi-ejector were recommended. Three cases were investigated based on the difference in motive and suction nozzle mass flow rates and receiver pressures. Additionally, the corresponding entrainment ratios, ejector efficiencies and pressure lifts were compared. The conducted simulations confirmed that the advanced multi-ejector has low efficiencies for higher motive nozzle pressures around 90 bar. The simulations also suggested that the multi-ejector is more similar to a low pressure multi-ejector than a high pressure multi-ejector.

**Keywords:** multi-ejector, R744, ejector efficiency

---

## NOMENCLATURE

### List of abbreviations

CFC	=	Chlorofluorocarbons
GWP	=	Global warming potential
HFC	=	Hydrofluorocarbons
HP	=	High pressure level
HPV	=	high pressure electronic expansion valve
LEJ	=	Liquid ejector cartridge
LP	=	Low pressure level
MN	=	Ejector motive nozzle flow inlet
OUT	=	Ejector flow outlet
SN	=	Ejector suction nozzle flow inlet
VEJ	=	Vapour ejector cartridge

### List of symbols

$C_P$	=	Heat capacity	[kJ/K]
$h$	=	Specific enthalpy	[kJ/kg]
$\dot{m}$	=	Mass flow rate	[kg/h]
$\eta$	=	Efficiency	[%]
$p$	=	Pressure	[bar]
$\Delta p$	=	Pressure lift	[bar]
$t$	=	Temperature	[°C]

---

## 1. INTRODUCTION

Global warming and climate change have led researchers to search for sustainable solutions to reduce emission of greenhouse gases. The implementation of the EU F-Gas regulation 517/2014 on fluorinated greenhouse gases has made the industry substitute harmful refrigerants by environmental friendly alternatives. The goal is to decrease HFC emissions by about 80% by 2030, which will favour low GWP refrigerants in the refrigeration sector (Commission (2014)).

Supermarkets are energy-intensive users, accounting for between 3% and 4% of the annual electricity consumption in industrialized countries. Refrigeration systems account for 30-60 percent of the total energy use in supermarkets, making them the highest consuming system in the store. The energy use varies due to non-technical barriers such as climate and social habits (Tassou et al. (2011)). Hence, supermarkets has also one of the highest specific energy consumption per  $m^2$  of all commercial buildings. The specific energy demand, regards the refrigeration system, is between  $300 \text{ kWh/m}^2$  and  $600 \text{ kWh/m}^2$ . Meanwhile, an office building consumes between  $150 \text{ kWh/m}^2$  and  $200 \text{ kWh/m}^2$  (Nordtvedt and Hafner (2012)). Today, there are more than 35 500 transcritical  $\text{CO}_2$  installations globally. In May 2020 there was 29 000 transcritical  $\text{CO}_2$  installations in Europe, which is a growth of 81% since 2018, when there were approximately 16 000 installations. Gullo et al. (2019) estimated for new supermarkets in 2020 the market share of ejector supported parallel systems is supposed to be in the range from 50% to 80%. Moreover, the commercial refrigeration applications can go HFC-free all over Europe, due to the great energy efficiency in any European climate context by adapting the system layout for R744. The “ $\text{CO}_2$  only” concept can be installed world-wide (Gullo et al. (2018)).

$\text{CO}_2$  is widely used as a refrigerant, mainly in marine systems as well as in air conditioning and stationary refrigeration systems such as in supermarkets.  $\text{CO}_2$  is non-flammable and non-toxic and is also inexpensive and available (Gullo et al. (2017b)). Professor Gustav Lorentzen from NTNU reintroduced  $\text{CO}_2$  as a working fluid, and in 1989 he patented a transcritical  $\text{CO}_2$  cycle system, where the throttling valve controlled the high pressure.

$\text{CO}_2$  is the most promising natural refrigerant for commercial refrigeration.  $\text{CO}_2$  has a high operating pressure and a low critical temperature.  $\text{CO}_2$  has favourable thermo-physical properties. These include higher specific heat, density, latent heat, thermal conductivity and volumetric cooling capacity than HFC refrigerants. Since  $\text{CO}_2$  has a relatively low viscosity in the liquid phase, this leads to a lower pumping performance for systems with large pipelines. Together with the low surface tension,  $\text{CO}_2$  has excellent heat transfer properties especially in the nucleate boiling regime (Eikevik (2017)).

The combination of the multi-ejector and “ $\text{CO}_2$  only” concept can grow and develop around the world. Gullo (2019) results have revealed that “ $\text{CO}_2$  only” compared to HFC-based refrigeration systems in selected high ambient temperature locations have an annual energy saving of 32.1% and reduction of environmental impact of 75.8%. The “ $\text{CO}_2$  only” refrigeration system relies on both multi-ejector concept and direct space heating.

---

## CO<sub>2</sub> transcritical installations in the world

sheccoBase



Figure 1: Transcritical CO<sub>2</sub> supermarkets globally in 2020. Adopted from Shecco (2020)

## 2. TEST FACILITY

The R744 multi-ejector refrigeration test rig is located at Varmeteknisk at NTNU Trondheim. The prototype of the advanced multi-ejector from Danfoss was installed in 2019. A censored picture of the advanced multi-ejector installed in the test facility is shown in Figure 2.

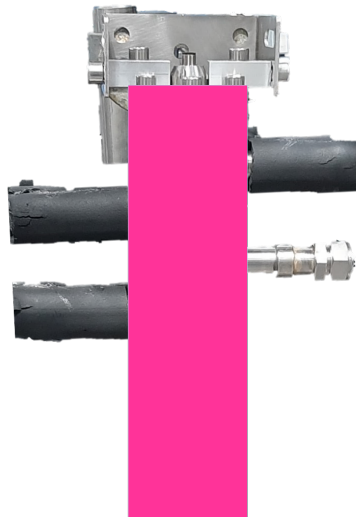


Figure 2: A closer look at the advanced multi-ejector developed by Danfoss.

---

The pipeline and instrumental diagram of the of the CO<sub>2</sub> test rig with the installed advanced multi-ejector in addition to the main components are included in Figure 3.

The working fluid CO<sub>2</sub> flows from the outlet of the multi-ejector at medium pressure level into the liquid receiver. The liquid exit the liquid receiver at the bottom and the vapour escape at the top. The pressure level in the liquid receiver can be regulated, because CO<sub>2</sub> has a constant density, which means the liquid level depends on the pressure level. The liquid receiver can be controlled by the flash gas valve. The evaporator receives saturated liquid from the liquid receiver. The number of evaporators activated depends on the required capacity. The working fluid continues to flow into the suction accumulator. If the testing requires liquid suction conditions, the level of liquid in the suction accumulator should be between 40% and 60%, to avoid damage on the compressor. This is regulated by the expansion valve. The peak-load evaporator should have no superheat, to get more liquid into the suction accumulator.

From the suction accumulator saturated or superheated vapour enters the compressors and the suction side of the vapour ejector. The suction side of the liquid ejector can be supplied by the liquid phase of the CO<sub>2</sub>. This makes it possible to utilize the evaporator in flooded mode. In this master thesis only vapour flows into the suction inlet of the advanced multi-ejector. One vapour ejector is illustrated, because number of vapour ejectors in this thesis is secret. The vapour from the liquid receiver is compressed by the compressor rack, which consist of a medium temperature compressor (base-load compressor) and two parallel compressors. When the parallel compressors are not in operation, the vapour from the liquid receiver is throttled by the flash gas bypass valve connected to the medium temperature compressor (base-load compressor). Depending on the operating mode, the pressure level in the liquid receiver is determined by the degree of opening of the flash gas bypass valve, the suction pressure of the base load compressor or the ejector capacity. There are two manual valves on the suction side, respectively for vapour and liquid.

The pressure level in the liquid receiver is regulated by the flash valve or the parallel compressors. The vapour phase from both receivers flows through the internal heat exchangers, and thereby absorbing the heat from the high-pressure CO<sub>2</sub> downstream of the gas cooler section. After the compression, the high pressure flow passes through the gas cooler stages. It flows into the multi-ejector and the high-pressure valve. The gas cooler outlet temperature is equal to the inlet motive temperature of the multi-ejector.

The test facility has a glycol loop that is connected to the first gas cooler and the evaporators. The purpose of the glycol loop is to absorb heat from the first stage gas cooler and transfer the heat to the evaporators. The evaporator temperature (and the pressure) is proportional to the glycol temperature in the heat exchanger. The evaporator pressure is equal to the multi-ejector suction pressure. A water loop is connected to the second stage gas cooler. The outlet temperature of the gas cooler is regulated by the mass flow rate of the cooling water since the water loop absorbs heat from the second stage gas cooler. The ejector motive temperature increases proportionally with the water temperature in the gas cooler.



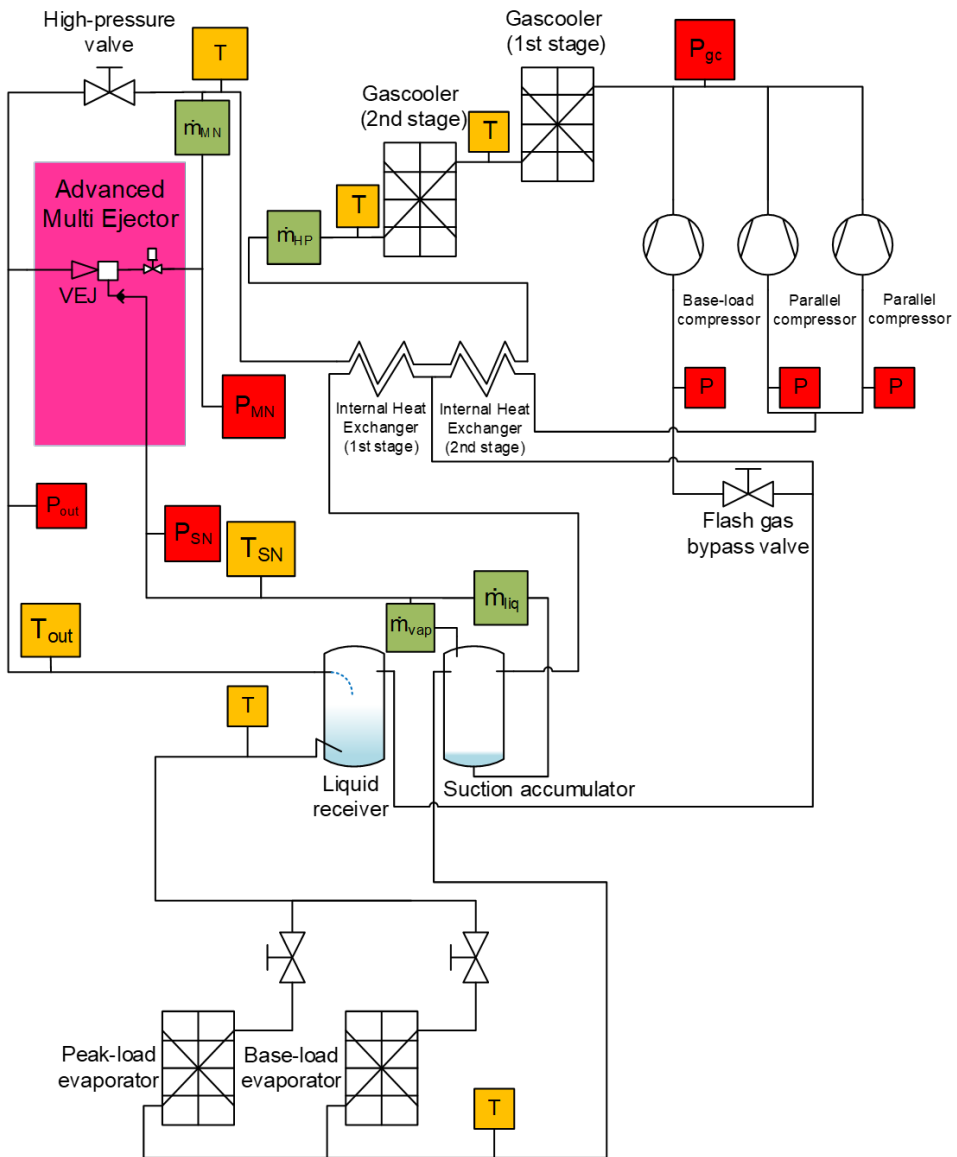


**Figure 3: Illustrates the pipeline and instrumental diagram of the CO<sub>2</sub> test rig, where all main components are included. The water loop and glycol loop are excluded.**

The main components in the test rig is listed in Table 1 and the accuracy for the pressure and temperature sensors and the uncertainty for the mass flow meters are listed in Table 2.

**Table 1: Set of main components in the R744 multi-ejector test rig**

System Component	Model	Type
Base-load compressor	Dorin CD 1400H	Semi-hermetic reciprocating
Parallel compressor #1	Dorin CD 1000H	Semi-hermetic reciprocating
Parallel compressor #2	Dorin CD 380H	Semi-hermetic reciprocating
First-stage gas cooler	SWEP B18Hx100	Brazed plates heat exchanger
Second-stage gas cooler	KAORI K095C-30C-NP8M	Brazed plates heat exchanger
Base-load evaporator	SWEP B16DWHx100	Brazed plates heat exchanger
Liquid receiver tank	Frigomec 39-litre	Pressure vessel
Liquid separator tank		
Oil accumulator tank	Frigomec 21-litre	Pressure vessel
Cold glycol tank	IMA 200-litre	Thermal storage tank
High-pressure valve	Danfoss CCMT8	Electronic expansion valve
Flash valve		
Base-load evaporator - metering valve	Danfoss CCM20	Electronic expansion valve

**Table 2: Sensor specifications at the test facility. FS means full scale (range).**

Variable	Transducer	Accuracy	Range
Pressure	Piezoelectric transmitter MBS8250 064G1136	$\pm 0.5\%$ FS (FS= 160 bar)	-1 – 159 bar
Temperature	Resistance thermometer PT1000 (PR21A31000-A-M6-0150-M12)	$\pm(0.15 + 0.002 t )$ (Class A, t in °C)	-30°C – +300 °C
Uncertainty			
Mass flow rate	Coriolis type RHM 06	$\pm 0.12\% \dot{m}$ (Goldline calibration)	0.5 – 20 kg/min
Mass flow rate	Coriolis type RHM 08	$\pm 0.12\% \dot{m}$ (Goldline calibration)	1.0 – 50 kg/min

---

### 3. EJECTOR PARAMETERS

The performance of two-phase ejector can be described by the entrainment ratio, pressure ratio, the pressure lift and ejector efficiency. In this master thesis the performance is described for the multi-ejector, and not for a single ejector. The objective of using an ejector is to both entrain a fluid and to increase its pressure.

Pressure ratio is the quotient of pressure level of the outlet to the inlet suction pressure.

$$\Pi = \frac{p_{outlet}}{p_{suction}} [-] \quad (1)$$

The pressure lift is determined by the geometry of the ejector, operational conditions and system control. It is defined as the difference between the the ejector outlet pressure and the ejector inlet suction pressure. Whereby the outlet pressure of the ejector corresponds to the inlet pressure of the receiver in a refrigeration system and the inlet suction pressure corresponds to the evaporator pressure. The definition of pressure lift is shown in Equation 2.

$$p_{lift} = \Delta p = p_{outlet} - p_{suction} [bar] \quad (2)$$

To evaluate the ejector work and ability to pump the low-pressure stream from the evaporator, it is necessary to know the mass flow rate of the motive and suction fluids. The low-pressure fluid can be entrained by the ejector until the pressure in the mixing chamber is lower than the pressure of the suction fluid. The mass entrainment ratio, Equation 3, is the quotient of the mass flow rate of the entrainment fluid and the mass flow rate of the motive fluid. Rising evaporator pressure helps increasing the entrainment ratio (Chunnanond and Aphornratana (2004)).

$$\Phi = \frac{\dot{m}_{suction}}{\dot{m}_{motive}} [-] \quad (3)$$

Elbel and Hrnjak (2008) define ejector efficiency on the basis of standard measured pressure, temperature, and mass flow rate. The ejector efficiency compares the amount of expansion work rate recovered by the ejector with the maximum possible expansion work rate recovery potential, see Equation 4.

$$\eta_{ejector} = \frac{\dot{W}_{rec}}{\dot{W}_{max,rec}} [-] \quad (4)$$

can be expressed as

$$\eta_{ejector} = \frac{\dot{m}_{SN}(h_C - h_D)}{\dot{m}_{MN}(h_A - h_B)} = \Phi \frac{(h_C - h_D)}{(h_A - h_B)} [-] \quad (5)$$

In the equation above the  $\dot{m}_{SN}$  the suction mass flow rate and the  $\dot{m}_{MN}$  is the mass flow rate of the ejector motive nozzle. The enthalpies at point A, B, C and D are respectively identified by  $h_A, h_B, h_C, h_D$  in Figure 4.

Furthermore, the enthalpy for point A presents the enthalpy for the ejector motive inlet flow. The enthalpy for point B found on the motive isentropic line crossing the outlet pressure line in the two-phase area of the pressure and specific enthalpy diagram. The enthalpy of point D is the enthalpy of the inlet suction flow. Whereas point C is found on the suction flow isentropic line, which crosses the constant outlet pressure line. The ejector efficiency increases when entrainment ratio increases or the pressure lift decreases.

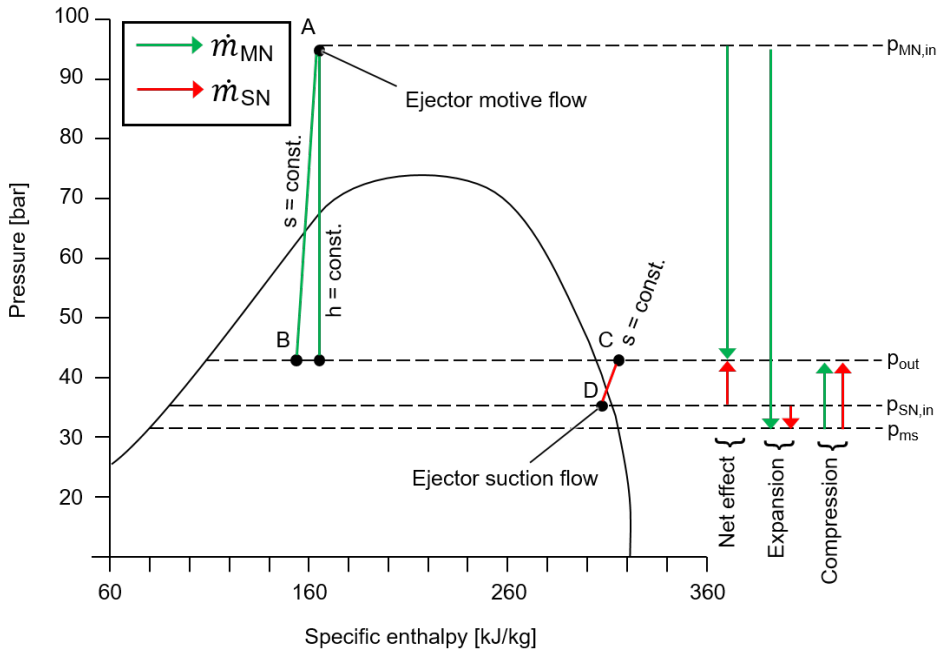


**Figure 4: Pressure and specific enthalpy diagram to recognize the enthalpies A, B, C, D that are included in the equation of the ejector efficiency of a two-phase ejector.**

---

## 4. RESULTS

### 4.1 Laboratory results

The results of the multi-ejector efficiency and the entrainment ratio as a function of pressure lift is shown in Figure 5. The motive pressures ranges from 59.26 bar to 90.30 bar with an overall uncertainty of  $\pm 0.46$  bar. The motive temperature ( $t_{MN}$ ) varies from 18.40°C to 35.21°C and the overall uncertainty is between  $\pm 0.11$ °C and  $\pm 0.14$ °C. The suction nozzle pressure varies from 25.15 bar to 28.25 bar. The suction temperature ranges from -8.7°C to 10.75°C with an overall uncertainty ranging between  $\pm 0.09$  °C and  $\pm 0.11$  °C.

At the lowest pressure lift of 2 bar the ejector efficiency is 14%. The ejector efficiency increases until it reaches its maximum value at 23.02% at 3.8 bar. The belonging motive nozzle pressure is 70.7 bar. The highest efficiencies are found in the light blue and green group . Hence, the efficiencies are at maximum where the motive nozzle pressure range from 68.4 bar until 71.1 bar with motive temperatures from 25.50 °C until 25.93°C and the ejector outlet pressures are from 28.5 bar until 29.7 bar.

From the pressure lift of 4 bar and higher, the ejector efficiency decreases simultaneously as the motive nozzle pressure and the pressure lift increases. The lowest ejector efficiency is 5.0% with a pressure lift of 8.05 bar. Belonging motive nozzle pressure is 88.09 bar. The lowest efficiencies are all found in the test numbers 31 to 35 (brown and purple coloured dots) at 82.69 bar until 90.3 bar.

The highest entrainment ratio is 0.53 found at the pressure lift of 2.65 bar and it has a motive nozzle pressure of 69.24 bar (yellow group). The lowest entrainment ratio with 0.06 has a motive nozzle pressure of 88.04 bar and has a pressure lift of 8.05 bar (purple group).

The lowest pressure lift at 2.2 bar shows a entrainment ratio of 0.31, then the entrainment ratio increases with a higher pressure lift until the turning point where the entrainment ratio decreases at motive pressure at 81 bar (dark red group) at the pressure lift of 5 bar. After the turning point, the higher the motive pressure of the measurement gets, the lower is the suction mass flow rate.

The suction mass flow rate varies between 193 kg/h (3.22 kg/min) and 343 kg/min (5.7 kg/min) from the pressure lift from 2 bar until 5 bar. The decrease in entrainment ratio from the pressure lift of 6 bar, is due to the decrease in suction mass flow rate between 185 kg/h (3.08 kg/min) and 45 kg/h (0.75 kg/min). The entrainment ratio and ejector efficiency for the blue points between the motive pressure of 80.8 and 83.3 bar are rapidly decreasing due to the decrease of suction mass flow rate. The suction mass flow rate is the basis for the entrainment ratio and ejector efficiency.

The yellow dots at motive pressure around 70 bar and the orange dots at motive pressure around 59 bar, have both a pressure lift of approximately 2.5 bar. However, they have a difference in entrainment ratio of 0.28, with the values 0.53 and 0.25, respectively. The

yellow group has a superheat of 1.9 K, whereas the the orange has a superheat between 17 and 22 K. The yellow points have the highest entrainment ratio, due to the highest suction mass flow of 328 kg/h (5.4 kg/min) and 342 kg/h (5.7 kg/min), respectively.

When comparing both the entrainment ratio and the ejector efficiency as functions of pressure lift, the highest ejector efficiency (green dot) do not have the highest entrainment ratio (yellow dot). The definition of the ejector efficiency, given in Equation 5, shows that it is proportional to entrainment ratio and enthalpy difference. This means that the enthalpy difference overrules the entrainment ratio in this situation. Anyway, both the highest entrainment ratio and ejector efficiency are found at 69.24 bar and 70.7 bar respectively, with pressure lift of 2.65 bar (entrainment ratio) and 3.8 bar (ejector efficiency).

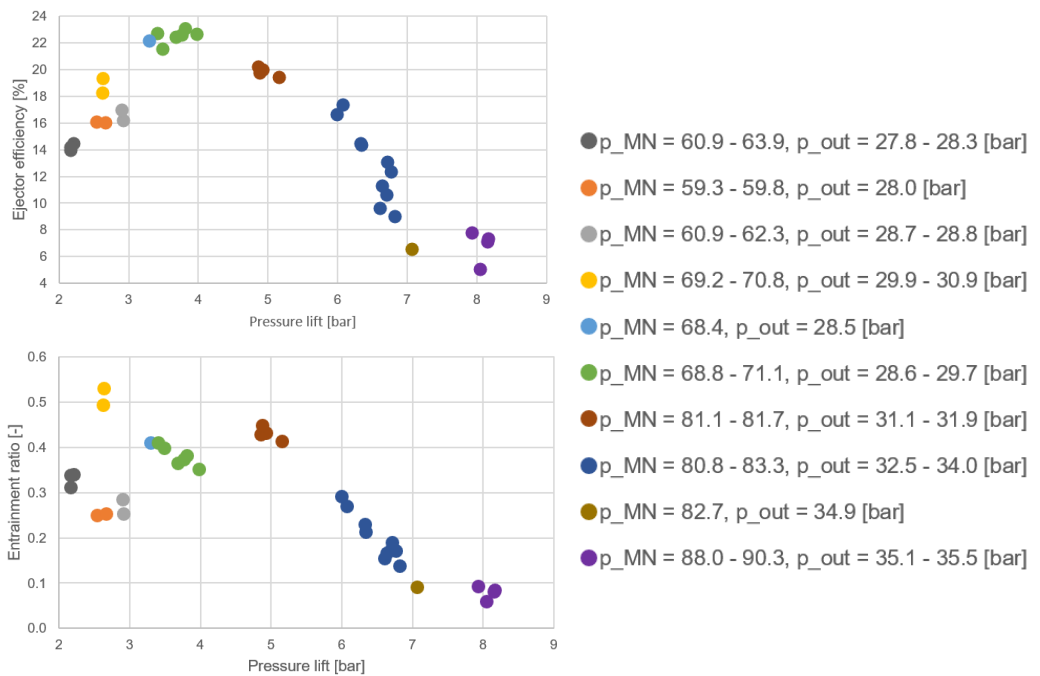


**Figure 5: Ejector efficiency and entrainment ratio as functions of pressure lift for all the measurements recorded. The coloured are grouped after increasing motive nozzle pressure and pressure lift.**

---

## 4.2 Comparing laboratory tests with LP and HP multi-ejectors in Coolselector

The calculation software Coolselector developed by Danfoss was used to find comparable transcritical R744 Danfoss low pressure (LP) and high pressure (HP) multi-ejectors for the advanced multi-ejector. The same refrigeration conditions as in the test facility were obtained. Four measurements from the laboratory tests were successfully adopted in Coolselector, in which the ejector parameters matched with a Danfoss multi-ejector from the commercial market.

The suitable tests were  $p_{MN}= 88.04$  bar,  $p_{MN}= 88.94$  bar,  $p_{MN}= 90.04$  bar and  $p_{MN}= 90.30$  bar from the laboratory results. The tests in question are named as Test A, B, C and D in Table 3 and Table 4. The tests comply with the purple dots in Figure 5.

**Table 3:** Test conditions from the advanced multi-ejector inserted into Coolselector

Test	$p_{MN}$ [bar]	$\dot{m}_{MN}$ [kg/h]	$\dot{m}_{SN,liq.}$ [kg/h]	$p_{SN}$ [bar]	$T_{Superheat}$ [°C]	$T_{MN}$ [°C]	$p_{Rec}$ [bar]
A	88.04	758.40	44.78	27.10	4.95	34.67	35.15
B	88.94	799.08	72.94	27.60	4.76	34.29	35.53
C	90.04	787.86	63.13	27.14	11.61	35.21	35.29
D	90.30	807.00	67.96	27.04	7.35	34.96	35.20

**Table 4:** Test conditions from the advanced multi-ejector inserted into Coolselector

Test	$p_{MN}$ [bar]	$\eta_{EJ}$ [%]	$\Delta p$ [bar]	$ER$ [-]
A	88.04	5	8.05	0.06
B	88.94	8	7.93	0.09
C	90.04	7	8.15	0.08
D	90.30	7	8.16	0.08

Three independent cases, illustrated in Table 5 were performed for the parameters above in Table 3 for the LP multi-ejector system and the HP multi-ejector system. Each of these cases concentrated successively on the manipulation of the mass flow rate of the suction nozzle (Case 1), the receiver pressure (Case 2) and the mass flow rate of the motive nozzle (Case 3). Each case includes three parameters where two are maintained constant and one is the variable in question.

---

**Table 5: Three cases for comparison in Coolselector**

	Case 1	Case 2	Case 3
Find	$\dot{m}_{suction}$	$p_{receiver}$	$\dot{m}_{motive}$
Constant value	$p_{receiver}$	$\dot{m}_{suction}$	$p_{receiver}$
Constant value	$\dot{m}_{motive}$	$\dot{m}_{motive}$	$\dot{m}_{suction}$

The results from the comparison between the advanced multi-ejector and low pressure multi-ejector are first presented and afterwards the results from the comparison with the high pressure multi-ejector are presented.

#### 4.2.1 Advanced multi-ejector compared with low pressure multi-ejectors from Danfoss

##### LP Case 1

Figure 6 shows motive nozzle pressure ( $p_{MN}$ ) equal to 88.04 bar (test A) with a constant receiver pressure ( $p_{rec}$ ) of 35.15 bar and a motive nozzle pressure equal to 88.94 bar (test B) with a constant receiver pressure of 35.53 bar for both the difference in suction mass flow rate (Case 1). For both multi-ejectors, the motive nozzle mass flow rate is constant for both Test A with 758.40 kg/h and Test B with 799.1 kg/h. The selected Danfoss multi-ejector under these test conditions is the transcritical low pressure lift multi-ejector LP 935. It is observed, that the second group of columns (Test B) has the highest difference in suction nozzle mass flow rate compared with the first group of columns (Test A).

For the first group of columns (Test A), the suction mass flow rate is 44.78 kg/h for the advanced multi-ejector, which is an increase by 41% from the LP 935 with 31.80 kg/h.

For the second group of columns (Test B), the suction mass flow is 72.94 kg/h for the advanced multi-ejector which is an increase by 62% from the LP 935 with 45.03 kg/h.



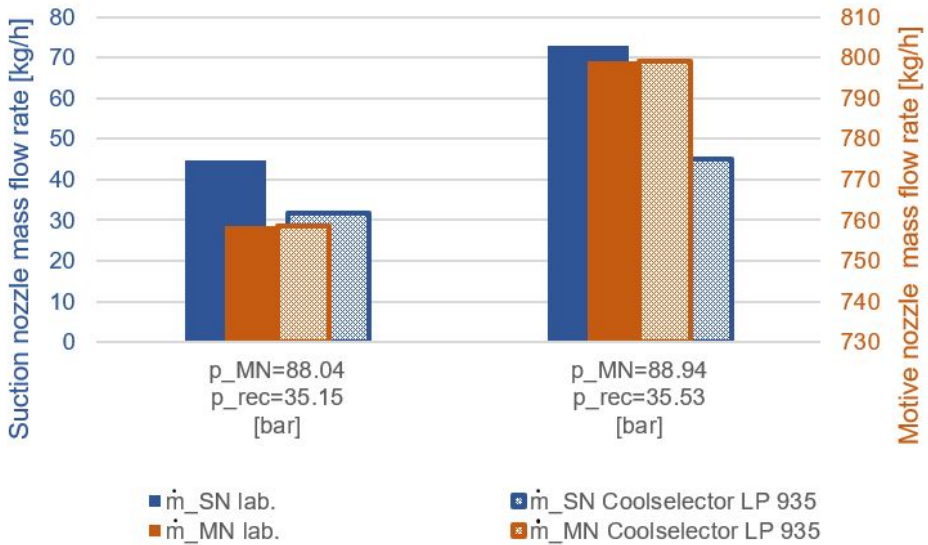


Figure 6: Suction nozzle mass flow rate at Test A and Test B for low pressure lift ejector performance comparison at equal motive nozzle mass flow rate and receiver pressure (Case 1).

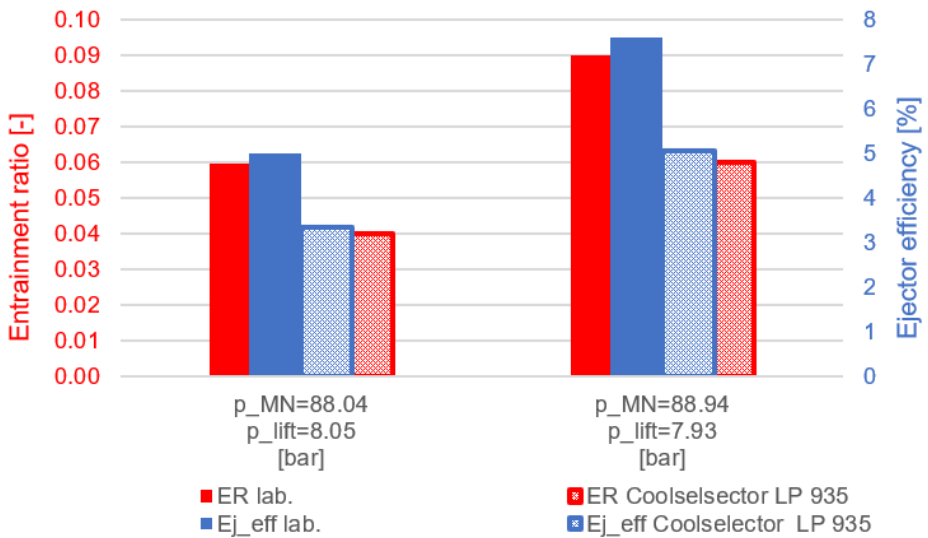


Figure 7: Entrainment ratio and ejector efficiency for lower pressure ejector performance comparison at equal motive nozzle pressure and pressure lift (Case 1).

Figure 7 shows the entrainment and ejector efficiency results of the comparison between the advanced multi-ejector and LP 935 from Coolselector with the difference in suction nozzle mass flow rate (Case 1).

---

The first group of columns (Test A) from the left have a constant motive nozzle pressure of 88.04 and a constant pressure lift of 8.05 bar. The entrainment ratio for LP 935 is 0.04 and for the advanced multi-ejector 0.06, while the ejector efficiency is 3.35% for LP 935 and 5% for the advanced multi-ejector. The increase in entrainment ratio and the ejector efficiency are both by 49% from the LP 935 to the advanced multi-ejector.

The second group of columns (Test B), the constant motive nozzle pressure is 88.94 bar and the pressure lift of 7.93 bar is constant. The entrainment ratio is 0.06 for LP 935 and 0.09 for the advanced multi-ejector. The ejector efficiency is 5.0% for LP 935 and 7.58% for the advanced multi-ejector. The results give a 50% increase in both entrainment ratio and ejector efficiency from the LP 935 to the multi-ejector.

## LP Case 2

Figure 8 presents the difference in receiver pressure (Case 2) between the advanced multi-ejector and the recommended multi-ejector LP 935 in Coolselector for a constant motive pressure of 88.04 bar (Test A), 88.94 bar (Test B), 90.04 bar (Test C) and 90.30 bar (Test D). The motive nozzle mass flow rates and the suction mass flow rates are constant for each individual test.

For the first group of columns from the left (Test A), the suction nozzle mass flow rate is 44.78 kg/h and the motive nozzle mass flow rate is 758.40 kg/h for both the advanced multi-ejector and the multi-ejector LP 935. The receiver pressure for the advanced multi-ejector with 35.15 bar is an 0.33% increase from LP 935 with 35.03 bar. The pressure difference is only 0.12 bar.

For the second group of columns from the left (Test B), the receiver pressure for the advanced pressure multi-ejector is 35.53 bar which is an increase by 0.63% from 35.30 bar at the multi-ejector LP 935. This gives a pressure difference 0.23 bar. The constant motive- and suction nozzle mass flow rates are respectively 799.10 kg/h and 72.94 kg/h.

The third group of columns (Test C) from the left, the suction nozzle mass flow rate is 63.13 kg/h and the motive nozzle mass flow rate is 787.9 kg/h are constant for both the advanced multi-ejector and LP 935. The receiver pressure is 35.29 bar for the advanced multi-ejector which is an increase by 1.41% from 34.80 bar at the multi-ejector LP 935. This gives a pressure difference of 0.49 bar.

The fourth group of columns (Test D) from the left, the receiver pressure for the advanced pressure multi-ejector is 35.20 bar which is an 1.74% increase from LP 935 with 34.60 bar. The difference is 0.60 bar. The constant motive- and suction nozzle mass flow rates are respectively 807.00 kg/h and 67.96 kg/h.

In summary, the receiver pressure is higher for the advanced multi-ejector at the laboratory than LP 935 in Coolselector for all the test conditions in Case 2. The largest receiver pressure difference between the multi-ejector and LP 935 is 0.60 bar, an increase by 1.74%

found in Test D, meanwhile the minimum difference in receiver pressure is 0.12 bar, an increase by 0.33% found in Test A.

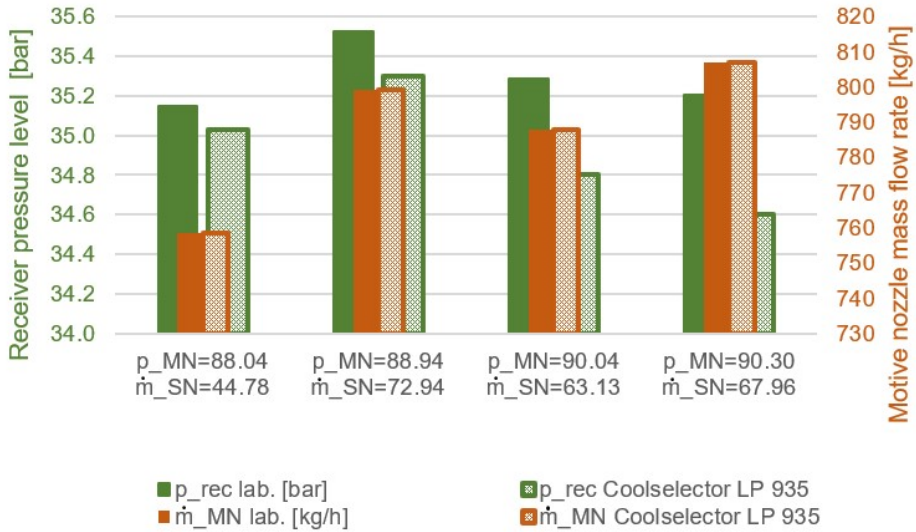


Figure 8: Receiver pressure level for low pressure lift ejector performance comparison at equal motive- and suction nozzle mass flow rate (Case 2).

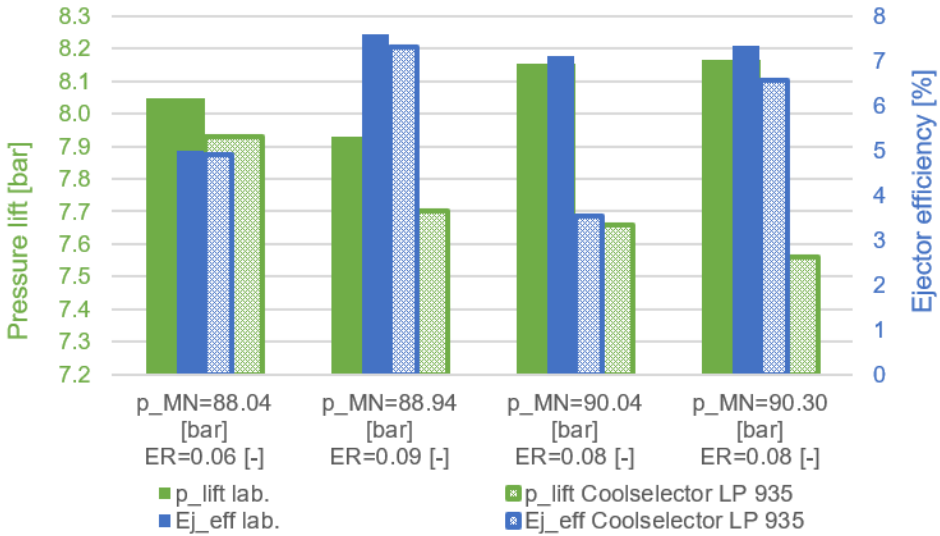


Figure 9: Pressure lift and ejector efficiency for lower pressure lift ejector performance comparison at equal motive nozzle pressure and entrainment ratio (Case 2).

---

Figure 9 shows the pressure lift and the ejector efficiency results of the comparison between the advanced multi-ejector and LP 935 from Coolselector with the difference in receiver pressure (Case 2). The four groups of columns plotted in this figures, present one after another a constant motive nozzle pressure and a constant entrainment ratio of respectively 88.09 bar and 0.06 for Test A, next 88.94 bar and 0.09 for Test B, further 90.04 bar and 0.08 for Test C and at last a motive pressure of 90.30 bar and entrainment ratio of 0.08 for Test D. The results from Coolselector concluded that the low pressure lift multi-ejector LP 935 is the most fitted for these test conditions.

The results from first group of columns from the left (Test A) reveals that the pressure lift is 7.93 bar for LP 935 and 8.05 bar for the advanced multi-ejector, which for the multi-ejector is an increase by 1%. The ejector efficiency is 4.89% for LP 935 and 5.00% for the multi-ejector, which for the latter is an increase by 2%.

The second group of columns shown from the left (Test B) reveals that the pressure lift is 7.70 bar for LP 935 and 7.90 bar for the advanced multi-ejector, which is an increase by 3% for the advanced multi-ejector. The LP 935 achieved an ejector efficiency of 7.30%, whereas the the multi-ejector achieved 7.58%. That is an increase by 4% from the Coolselector option to the advanced multi-ejector.

In the third group of columns (Test C) from the left, the pressure lift of the LP 935 is 7.66 bar and 8.2 bar for the advanced multi-ejector, which is an increase of 6%. The ejector efficiency with 7.11% for the advanced multi-ejector is approximately 2 times higher than the result from Coolselector with 3.53%.

For the last group of columns (Test D) from the left, the pressure lift of the LP 935 is 7.56 bar and 8.2 bar for the advanced multi-ejector, which is an increase by 8%. The ejector efficiency for the advanced ejector with 7.32% is an increase by 11.52% from the LP 935 with 6.56%.

In summary, the advanced multi-ejector achieved higher results from the pressure lift and the ejector efficiency when compared with the LP 935 in Coolselector. The highest increase in ejector efficiency from the Coolselector to the laboratory results was found in Test C with an increase by 101%. The highest increase by pressure lift from the Coolselector to the laboratory results was found in Test D with an increase by 7.97%.

### **LP Case 3**

Figure 10 presents the difference in motive nozzle mass flow rate (Case 3) for a constant motive nozzle pressure of 88.04 bar (Test A) and 88.94 bar (Test B). The most suited multi-ejector recommended from Coolselector is LP 1435 under the conditions at Test A. For Test B however, the most suitable multi-ejector is the LP 1935.

For the first group of columns (Test A), the suction nozzle mass flow rate at 44.78 kg/h and the receiver pressure at 35.15 bar are constant for both multi-ejectors. The motive nozzle

mass flow rate is 758.60 kg/h for the advanced multi-ejector, which is a reduction by 43% from the LP 1435 with 1333 kg/h. This is a difference in motive nozzle mass flow rate of 574.60 kg/h.

For the second group of columns (Test B), the receiver pressure is constant at 35.53 bar and the suction nozzle mass flow rate is constant at 72.94 kg/h for both multi-ejectors. The motive nozzle mass flow is 799.04 kg/h for the advanced multi-ejector, which is a reduction by 53% from the LP 1935 with 1683 kg/h. This is a difference in motive nozzle mass flow rate of 885 kg/h.

In summary, the multi-ejectors in Coolselector have a higher motive nozzle mass flow rate than the advanced multi-ejector in the laboratory. Test B shows the largest motive nozzle flow rate reduction of 53% from Coolselector which is 884.92 kg/h, whereas the Test A shows a reduction of 43% from Coolselector, which is a difference of 574.60 kg/h.

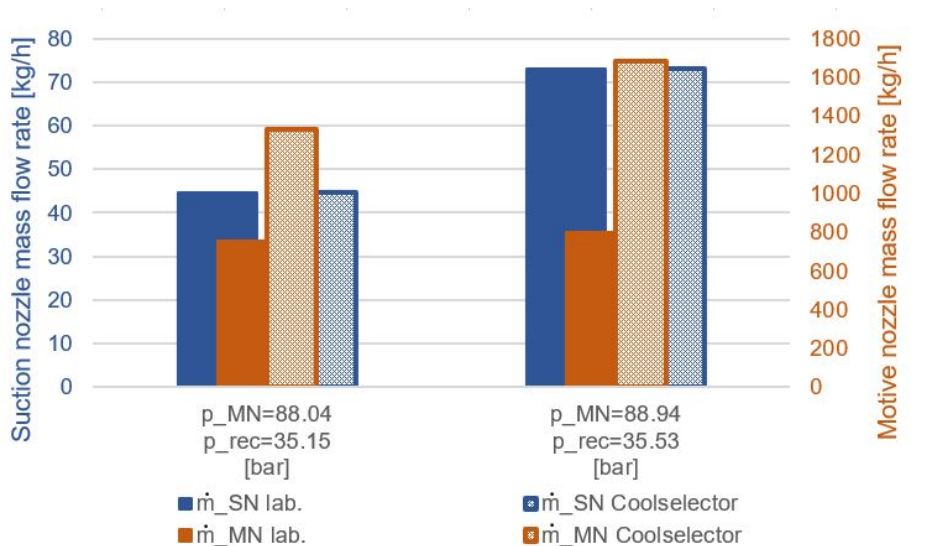


**Figure 10: Motive nozzle mass flow rate for Test A and B for low pressure lift ejector performance comparison at equal suction nozzle mass flow rate and receiver pressure (Case 3).**

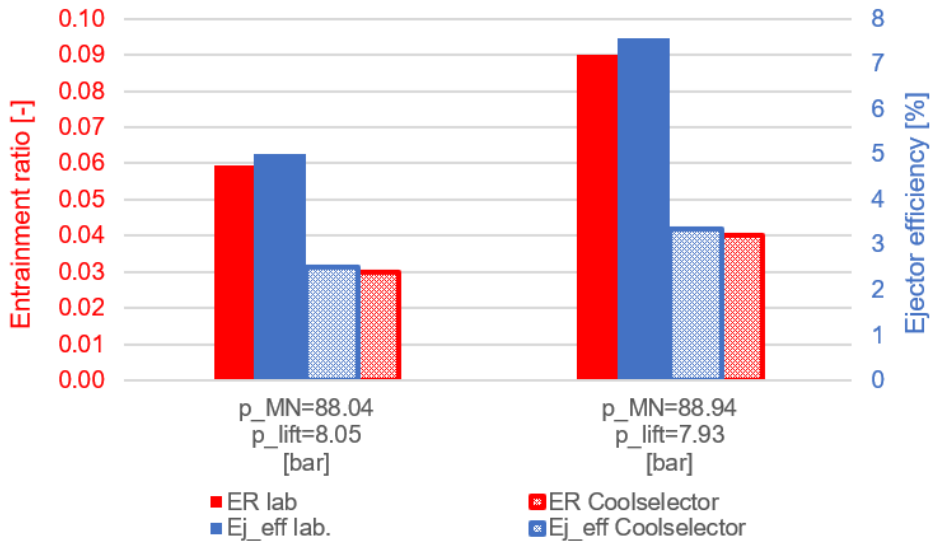


**Figure 11: Entrainment ratio and ejector efficiency for lower pressure ejector performance comparison at equal motive nozzle pressure and pressure lift (Case 3).**

Figure 11 shows the entrainment ratio and the ejector efficiency as a function of motive nozzle pressures and pressure lifts. The results show the comparison between the multi-ejectors in the laboratory and the Coolselector with the difference in motive nozzle mass flow rate (Case 3) and constant receiver pressure and suction nozzle mass flow rate.

For the first group of columns (Test A), the pressure lift is constant at 8.05 bar and the motive nozzle pressure is constant at 88.04 bar for both multi-ejectors. The entrainment ratio for the advanced multi-ejector with 0.06 in Test A is an increase by 98% from the multi-ejector LP 1435 from Coolselector with 0.03 entrainment ratio. The ejector efficiency is 5% for the advanced multi-ejector, which is an increase by 99% from ejector efficiency of 2.51% for LP 1435.

For the second group of columns (Test B), the pressure lift is constant at 7.93 bar and the motive nozzle pressure is constant at 88.94 bar for both multi-ejectors. The percentage increase in entrainment ratio and the ejector efficiency are approximately by 125% from the selected LP 1935 to the advanced multi-ejector. The entrainment ratio values are 0.09 and 0.04 and the ejector efficiencies are 8% and 3.36%, where the highest values present the advanced multi-ejector.

Comparing the advanced multi-ejector with LP 1435 in Test A and LP 1935 in Test B, the largest entrainment and ejector efficiency difference is found in Test B. The advanced multi-ejector has a higher efficiency than LP 1435 and LP 1935 and are therefore a better choice of multi-ejector under these refrigeration conditions.

---

## 4.2.2 Advanced multi-ejector compared with high pressure multi-ejectors from Danfoss

### HP Case 1

Figure 12 illustrates the difference in suction nozzle mass flow rate (Case 1) between the advanced multi-ejector and the selected multi-ejector HP 1875 in Coolselector.

For the constant motive nozzle pressure of 88.04 bar (Test A), receiver pressure of 35.15 bar and constant motive nozzle mass flow rate of 758 kg/h, the suction nozzle mass flow rate is 45 kg/h for the advanced multi-ejector and 315 kg/h for HP 1875. This is an increase by 603% in suction mass flow rate from the advanced multi-ejector to the HP 1875.

Next, the motive nozzle pressure is constant at 88.94 bar (Test B), the receiver pressure is constant at 35.53 bar and the motive nozzle mass flow rate is constant at 799 kg/h for both multi-ejectors. The suction motive mass flow rate is 325 kg/h for the multi-ejector in Coolselector, which is an increase by 391.46% from the advanced multi-ejector with 73 kg/h.

Next, where both multi-ejectors have a constant motive nozzle pressure of 90.04 bar (Test C), a constant receiver pressure of 35.29 bar and a constant motive nozzle mass flow rate of 788 kg/h, the suction mass flow rate in Coolselector increases by 345.55% from the laboratory measurement, with respectively 328 kg/h and 63 kg/h.

At last, the constant motive nozzle pressure of 90.30 bar (Test D), constant receiver pressure of 35.20 bar and motive nozzle mass flow rate of 807 kg/h gives an increase by 420.08% in suction mass flow rate from the laboratory to the selected multi-ejector in Coolselector. The range is 68 kg/h and 334 kg/h.

Summarised for Case 1 under HP conditions, all suction mass flow rates for HP 1875 are higher than the advanced multi-ejector. The highest suction nozzle mass flow rate difference between the two multi-ejectors is 270 kg/h, which is an increase by 602.78% from the advanced multi-ejector found in Test A, meanwhile Test C has the lowest difference with 252 kg/h, which is an increase by 345.55% from the advanced multi-ejector to the HP 1875 multi-ejector.

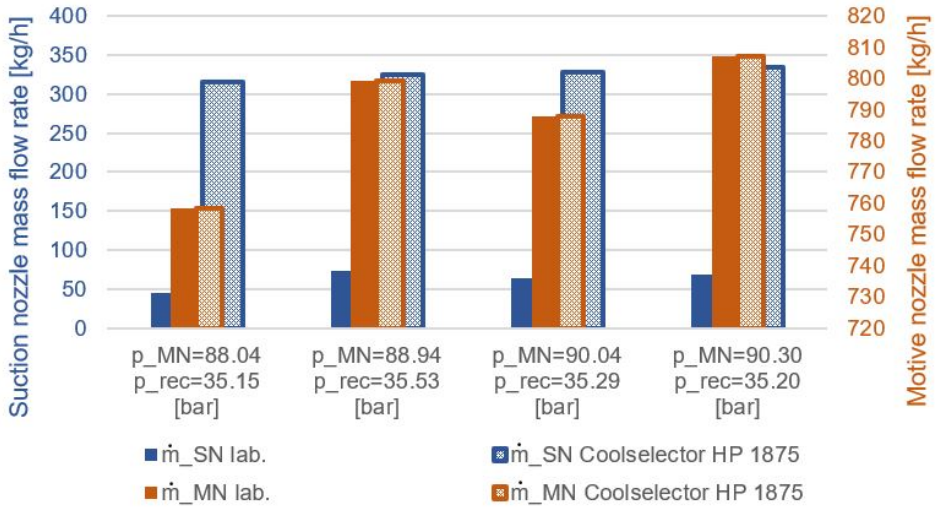


Figure 12: Suction nozzle mass flow rate for high pressure lift ejector performance comparison at equal motive nozzle mass flow rate and receiver pressure (Case 1).

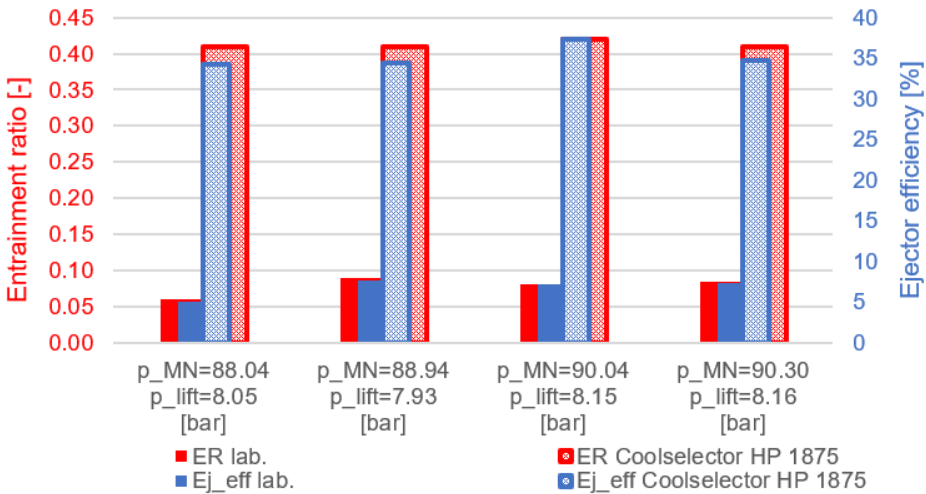


Figure 13: Entrainment ratio and ejector efficiency for higher pressure lift ejector performance comparison at equal motive nozzle pressure and pressure lift (Case 1).

Figure 13 shows the entrainment and ejector efficiency results of the comparison between the advanced multi-ejector and HP 1875 from Coolselector with the difference in suction nozzle mass flow rate illustrated in Figure 4.13 (Case 1).

The constant motive nozzle pressure of 88.04 and a constant pressure lift of 8.05 bar for



---

both multi-ejectors illustrate Test A. The entrainment ratio is 0.06 for the advanced multi-ejector and 0.41 for HP 1875. This is an increase by 589% compared to the multi-ejector. The ejector efficiency is 5.00% and 34.32%, which is an increase by 587% compared to the advanced multi-ejector.

The constant motive nozzle pressure of 88.94 bar and the constant pressure lift of 7.93 bar for both multi-ejectors illustrate Test B. The entrainment ratio is 0.09 and 0.41, an increase by 335.6%, and the ejector efficiency is 7.58% and 34.45%, an increase by 354.4%, for respectively the advanced multi-ejector in the laboratory and the HP 1875 multi-ejector from the Coolselector results.

For Test C, where both multi-ejectors have a motive nozzle pressure of 90.04 bar, a pressure lift of 8.15 bar, the HP 1875 multi-ejector's increase in entrainment ratio is 420.9% compared to the advanced multi-ejector. The same pattern follows for the HP 1875, where the increase in ejector efficiency is 424.3% from the the advanced multi-ejector. The absolute values for the entrainment ratio is 0.08 and 0.42, where the latter is for the HP 1875. The ejector efficiency 7.11% for the advanced multi-ejector and 37.27% for HP 1875.

At the last columns from the left, the constant motive nozzle pressure is 90.30 bar and constant pressure lift is 8.16 bar (Test D). The HP 1875 multi-ejector's increase in entrainment ratio is 384% compared with the advanced multi-ejector. The same pattern follows where HP 1875 has an increase by 375% in ejector efficiency from the advanced multi-ejector. The absolute values for the entrainment ratios are 0.08 and 0.41, where the latter is the selected multi-ejector. The ejector efficiencies are 7.32% and 34.78%, where the advanced multi-ejector achieved the lowest value.

The high ejector efficiency for the recommended HP 1875 multi-ejector in Coolselector is due to the high suction nozzle mass flow rate illustrated in 4.13. The ejector efficiency for the HP 1875 multi-ejector has a significant higher efficiency than the ejector prototype. Test A has the maximum increase of 587% in ejector efficiency from the advanced multi-ejector. The lowest increase from the advanced multi-ejector to the Coolselector option was 354% in Test B. The same tendency was found for the entrainment ratio, where the maximum increase was also found in Test A with 589%. The minimum increase of entrainment ratio was also found in Test B with 356%.

## **HP Case 2**

Figure 14 illustrates the difference in receiver pressure (Case 2) between the advanced multi-ejector and the selected multi-ejector HP 1875 in Coolselector.

For the first group of columns (Test A) the motive nozzle pressure is constant at 88.04 bar, the suction mass flow rate is constant at 44.78 kg/h and motive nozzle mass flow rate is constant at 758 kg/h for both multi-ejectors. The receiver pressure achieved 40.46 bar in Coolselector, which is an increase by 15.12% from the advanced multi-ejector that achieved 35.15 bar.

For the second group of columns (Test B) the constant motive nozzle pressure is 88.94 bar, the constant suction mass flow rate is 72.94 kg/h and the constant motive nozzle mass flow rate is 799 kg/h for both multi-ejectors. The receiver pressure achieved 40.38 bar in Coolselector, which is an increase by 13.66% from the advanced multi-ejector that achieved 35.53 bar.

For the third group of columns (Test C) the constant motive nozzle pressure is 90.04 bar, suction mass flow rate of 63.13 kg/h and motive nozzle mass flow rate of 788 kg/h for both multi-ejectors. The receiver pressure achieved 40.16 bar in Coolselector, which is an increase by 13.80% from the advanced multi-ejector that achieved 35.29 bar.

For the fourth and last group of columns (Test D) the constant motive nozzle pressure is 90.04 bar, the suction mass flow rate is 67.96 kg/h and the motive nozzle mass flow rate is 807 kg/h for both multi-ejectors. The receiver pressure achieved 40.07 bar in Coolselector, which is an increase by 13.83% from the advanced multi-ejector that achieved 35.20 bar.

In summary for Case 2, the receiver pressure for HP 1875 is higher than the advanced multi-ejector. The maximum receiver pressure level difference between the two multi-ejectors is 5.31 bar found in Test A, which illustrates an increase in receiver pressure of 15.12%. The minimum receiver pressure level difference between the two multi-ejectors is 4.85 bar found in Test B shows an increase of 13.66% compared to the advanced multi-ejector.

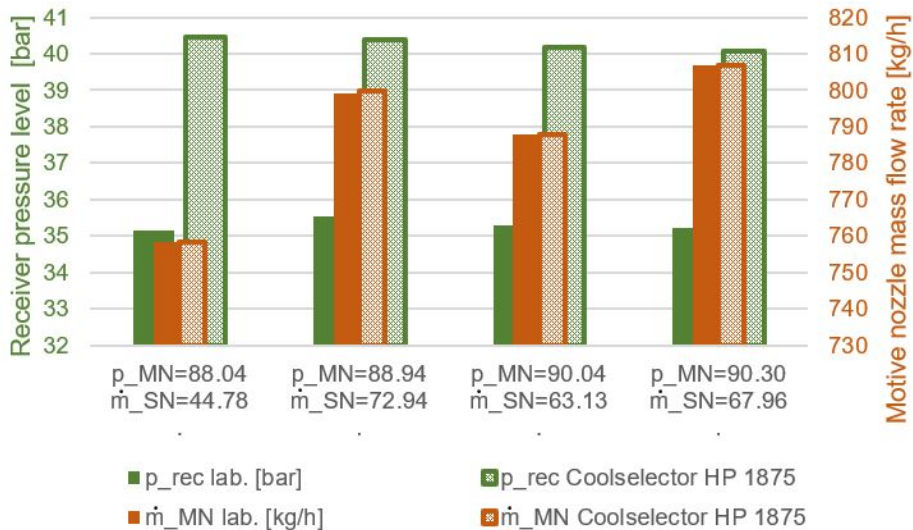


**Figure 14: Receiver pressure level for higher pressure lift ejector performance comparison at equal motive- and suction nozzle mass flow rate (Case 2).**

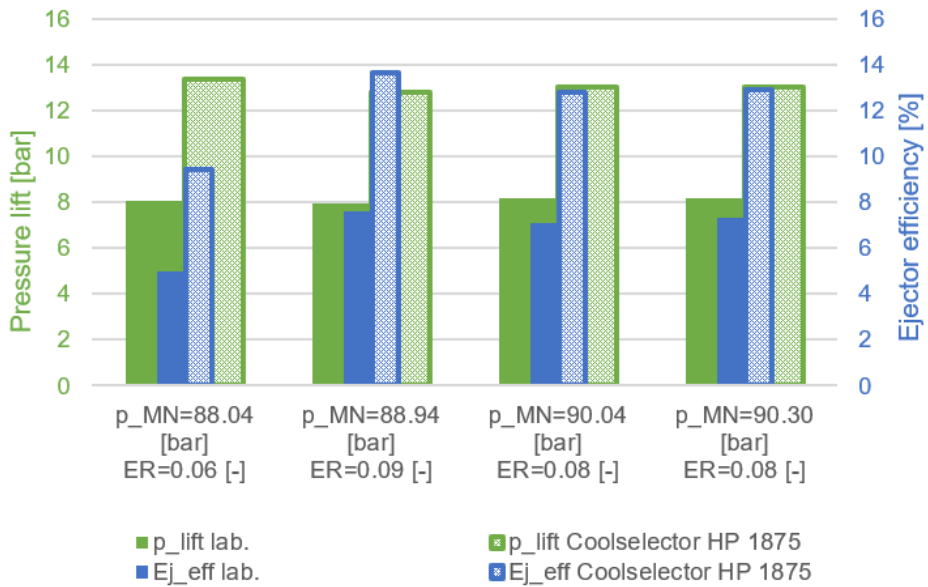


**Figure 15: Pressure lift and ejector efficiency for higher pressure lift ejector performance comparison at equal motive nozzle pressure and entrainment ratio (Case 2).**

Figure 15 illustrates the difference in pressure lift and ejector efficiency with the difference in receiver pressure (Case 2, see figure 4.14) between the advanced multi-ejector and the multi-ejector HP 1875 in Coolselector.

For the first group of columns the constant motive nozzle pressure is 88.04 bar (Test A) and entrainment ratio is 0.06. The pressure lift with 13.36 bar in Coolselector, is an increase by 66.0% compared to the advanced multi-ejector at 8.05 bar. The ejector efficiency of 9.42% in Coolselector, is an increase by 88.5% compared to the advanced multi-ejector at 5.00%.

For the second group of columns the constant motive nozzle pressure is 88.94 bar (Test B) and entrainment ratio 0.09 for both multi-ejectors. The pressure lift with 12.78 bar in Coolselector, is an increase by 61.2% compared to the advanced multi-ejector at 7.93 bar. The ejector efficiency of 13.67% in Coolselector, is an increase by 80.4% compared to the advanced multi-ejector at 7.58%.

For the third group of columns the constant motive nozzle pressure is 90.04 bar (Test C) and the entrainment ratio 0.08 for both multi-ejectors. The pressure lift with 13.02 bar in Coolselector, is an increase by 59.7% compared to the advanced multi-ejector at 8.15 bar. The ejector efficiency of 12.77% in Coolselector, is an increase by 79.7% compared with the advanced multi-ejector at 7.11%.

For the fourth and last group of columns the constant motive nozzle pressure is 90.04

---

bar (Test D) and the entrainment ratio 0.08 for both multi-ejectors. The pressure lifts are 8.15 bar and 13.03 bar, which is an increase by 59.6% from the advanced multi-ejector to HP 1875. The ejector efficiency of 12.92% in Coolselector, is an increase by 76.5% compared with the advanced multi-ejector at 7.32%.

### **HP Case 3**

Figure 16 illustrates the difference in motive nozzle mass flow rate (Case 3) between the advanced multi-ejector used in the laboratory and the multi-ejector HP 1875 recommended in Coolselector.

For the constant motive nozzle pressure of 88.04 bar (Test A) and the constant receiver pressure of 35.15 bar and the constant suction mass flow rate of 45 bar, the reduction in motive nozzle mass flow rate is by 86% compared to the advanced multi-ejector. The advanced multi-ejector has a motive mass flow rate of 758 kg/h, meanwhile the HP 1875 multi-ejector achieves 108 kg/h.

For the constant motive nozzle pressure of 88.94 bar (Test B) and the constant receiver pressure of 35.53 bar and the constant suction mass flow rate of 73 bar, the reduction in motive nozzle mass flow rate is by 78% compared to the advanced multi-ejector. The motive nozzle mass flow rates for the advanced multi-ejector and the HP 1875 are 799 kg/h and 179 kg/h, respectively.

For the constant motive nozzle pressure of 90.04 bar (Test C) and the constant receiver pressure of 35.29 bar and the constant suction mass flow rate of 63 bar, the reduction in motive nozzle mass flow rate is by 81% compared to the advanced multi-ejector. The advanced multi-ejector has a motive mass flow rate of 788 kg/h, meanwhile the HP 1875 multi-ejector achieves 152 kg/h.

For the constant motive nozzle pressure of 90.30 bar (Test D) and the constant receiver pressure of 35.20 bar and the constant suction mass flow rate of 68 kg/h, the reduction in motive nozzle mass flow rate is by 85% compared to the advanced multi-ejector. The advanced multi-ejector has a motive mass flow rate of 807 kg/h, meanwhile the HP 1875 multi-ejector achieves 164 kg/h.

Summarised, the advanced multi-ejector has higher motive mass flow than the multi-ejector in Coolselector. The maximum motive nozzle mass flow rate difference between the two multi-ejectors is 651 kg/h, found in Test A. This corresponds to a reduction by 86% for the HP 1875 compared to the advanced multi-ejector.

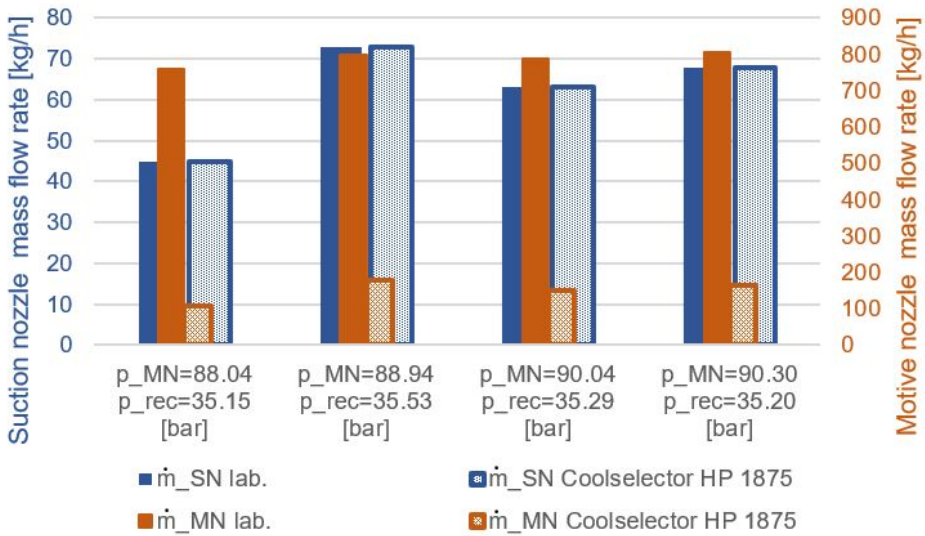


**Figure 16: Motive nozzle mass flow rate for higher pressure lift ejector performance comparison at equal suction mass flow rate and pressure lift (Case 3).**

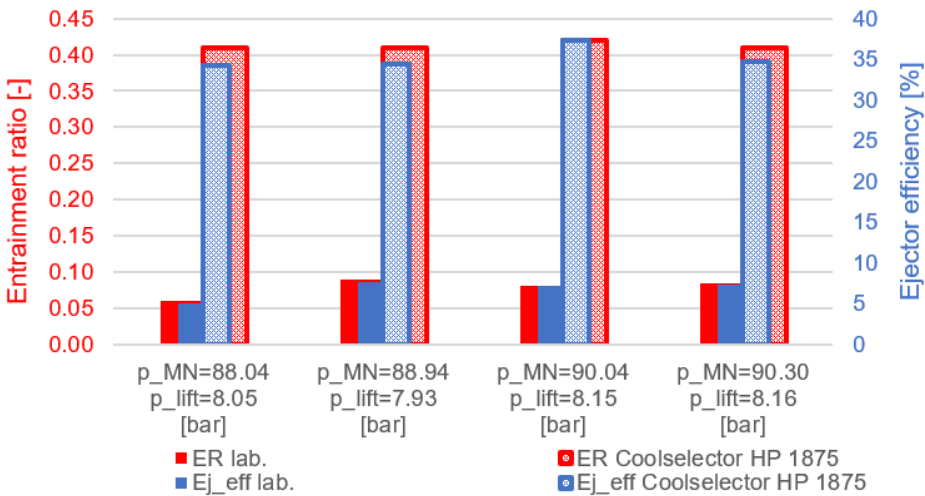


**Figure 17: Entrainment ratio and ejector efficiency for higher pressure lift ejector performance comparison at equal motive nozzle pressure and pressure lift (Case 3).**

Figure 17 illustrates the difference in entrainment ratio and ejector efficiency with the difference in motive nozzle mass flow rate (Case 3 shown in figure 4.15) between the advanced multi-ejector and the multi-ejector HP 1875 in Coolselector.

---

Figure 17 are identical to the results in Figure 4.16 with the difference in suction mass flow rate (Case 1). This is ought to the same entrainment ratios values for Case 1 and Case 3, even though the values of the motive- and suction mass flow rates are different.

---

## 5. CONCLUSION

Experimental investigation of the R744 multi-ejector prototype from the Danish company Danfoss was performed under different operational conditions in a test facility.

The experiments at the laboratory investigated motive nozzle pressures from 59.3 until 90.3 bar with increasing pressure lifts from 2.17 bar until 8.16 bar. The experimental results revealed that the advanced multi-ejector achieved a maximum ejector efficiency of 23.02% with the motive nozzle pressure of 70.7 bar and pressure lift of 3.8 bar. The multi-ejector efficiency decreased for higher motive nozzle pressures with higher pressure lifts due to drop of suction nozzle mass flow rates and entrainment ratios.

The test rig functioned and performed well, but there were some challenges with the measurement precision for certain sensors. Due to the corona pandemic, the test facility was closed and further measurements could not be performed.

The uncertainty of the independent parameters were found by standard deviation (type A) and equipment data (type B). The pressure transmitters have a relatively higher uncertainty than the mass flow sensor. The mass flow meter had an uncertainty of 0.12% of reading, whereas the pressure transmitters for the ejector motive, suction and outlet were between 0.51% and 1.83% of reading depending on the mean pressure. The mass flow meter uncertainty were at least 4.23 times lower than than the pressure transmitters.

The advanced multi-ejector had higher suction mass flow rates, higher receiver pressures than the recommended LP 9325 and lower motive mass flow rates than the recommended LP 1435 and LP 1935 multi-ejectors. This resulted into higher ejector efficiencies and higher entrainment ratios for the advanced multi-ejector than the recommended low pressure lift multi-ejectors. The highest efficiency of the compared laboratory measurements was 7.58%, whereas the highest efficiency of the LP multi-ejectors was 7.30%, which is an decrease of 3.6% in ejector efficiency.

On the contrary, the advanced multi-ejector had lower suction mass flow rates, lower receiver pressures and higher motive mass flow rates than the recommended HP 1875 multi-ejector. The highest efficiency from the compared laboratory measurements was 7.58%, whereas the highest efficiency from the HP 1875 relieved 37.27%, which is around 4 times higher.

Since the comparison only regarded the upper motive pressures between 88.04 bar and 90.30 bar, it can be concluded that in this area the advanced multi-ejector is more a LP than a HP multi-ejector. The ejector prototype had low efficiencies for all values compared with Coolselector, which means that those values are probably off-design points. Taking all the measurements from the laboratory into account, the best ejector efficiency was found at the lower pressure lifts between 3 and 4 bar. This also suggests that the prototype is more a LP than a HP ejector.

The suction mass flow rates were low for the higher pressure lifts in the laboratory mea-

---

surements. There is something with the geometry in the advanced multi-ejector which is not working for the highest motive nozzle pressures. The suction nozzle mass flow rate in Coolselector was much higher for the HP ejectors than for what was possible in the laboratory for the conditions with motive pressures around 90 bar.

The advanced multi-ejector has still a potential regards archiving higher ejector efficiencies. In this Master Thesis the maximum ejector efficiency was 23.02%, which is still far away from the highest ever measured vapour ejector efficiency 36.8%.

## REFERENCES

Commission, E., 2014. Regulation (eu) no 517/2014 of the european parliament and of the council of 16th april 2014 on fluorinated greenhouse gases and repealing regulation (ec) no 842/2006.

Eikevik, T.M., 2017. Compendium for heat pumping processes and systems (TEP4255).

Gullo, P., Hafner, A., Banasiak, K., Minetto, S., Kriezi, E.E., 2019. Multi-ejector concept: A comprehensive review on its latest technological developments. *Energies* 12, 406.

Gullo, P., Tsamos, K., Hafner, A., Ge, Y., Tassou, S.A., 2017. State-of-the-art technologies for transcritical r744 refrigeration systems—a theoretical assessment of energy advantages for european food retail industry. *Energy Procedia* 123, 46–53.

Nordtvedt, T., Hafner, A., 2012. Integration of refrigeration and hvac supermarkets, in: *Proceedings of 10th IIR Gustav Lorentzen Conference, International Institute of Refrigeration*. Delft, the Netherlands.

Shecco, 2020. World guide to transcritical co2 refrigeration - part 2. <http://shecco.com/articles/2020-06-18-shecco-guide-puts-global-transcritical-co2-installations-at-pages=20>, accessed: 2020-07-23.

Tassou, S., Ge, Y., Hadaway, A., Marriott, D., 2011. Energy consumption and conservation in food retailing. *Applied Thermal Engineering* 31, 147–156.



---

# **Appendix B**

## **Risk assessment**

NTNU	Kartlegging av risikofylt aktivitet	Utarbeidet av	Nummer	Dato	
		HMS-avd.	HMSRV2601	22.03.2011	
HMS		Godkjent av		Erstatter	
		Rektor		01.12.2006	

Enhet: EPT

Dato: 09.05.2019

Linjeleder:

Deltakere ved kartleggingen (m/ funksjon): **Helen Langeng, Krzysztof Banasiak, Merethe Leksen Selnes**

(Ansv. veileder, student, evt. medveiledere, evt. andre m. kompetanse)

**Kort beskrivelse av hovedaktivitet/hovedprosess:** Masteroppgave student Merethe Leksen Selnes. Experimental analysis of a R744 multi-ejector.

**Er oppgaven rent teoretisk? (JA/NEI):** NEI

krever risikovurdering.

Dersom «JA»: Beskriv kort aktiviteten i kartleggingskjemaet under. Risikovurdering trenger ikke å fylles ut.

«JA» betyr at veileder innestår for at oppgaven ikke inneholder noen aktiviteter som

**Signaturer:** Ansvarlig veileder:

Student:



CB

NTNU	Kartlegging av risikofylt aktivitet	Utarbeidet av	Nummer	Dato	
		HMS-avd.	HMSRV2601	22.03.2011	
HMS		Godkjent av		Erstatter	
		Rektor		01.12.2006	

Id	Aktivitet	Mulig hendelse	Mulig konsekvens	Eksisterende barrierer	Risikoverdi med eksisterende tiltak			
					Menneske	Ytre miljø	Økonomi	Økonomi / materiell
	Lag en kort beskrivelse av hva som gjøres i denne fasen av forsøksgjennomføringen							
1	Ingen strømning/No flow	Ikke åpner isvannstilførsel	Kjører uten kjøling og da stiger glykol temperatur i tanken. Trykkoppbygging på kompressor utløpssiden.	Regulator slår av kompressor. Presostat slår av kompressor. Sikkerhetsventil åpner ved 120bar. Sjekklister for kjøring har med åpning av vanntilførsel	A1	A1	A1	A1
2	Reversert strømning/Reverse flow	Reversert strømning i CO2-kretsen kan skje på grunn av trykkdifferanse ved at ejetor yter for dårlig	Riggen får dårlig virkningsgrad	to trinn tilbakeslagsventil	A1	A1	A1	A1
3	For stor strømning/More flow	Alle kretser er dimensjonert slik at det ikke er mulig å få for stor strømning. I alle	Ingen fare		A1	A1	A1	A1

KB

NTNU	Kartlegging av risikofylt aktivitet	Utarbeidet av	Nummer	Dato	
		HMS-avd.	HMSRV2601	22.03.2011	
HMS		Godkjent av		Erstatter	
		Rektor		01.12.2006	

		kretser, vann, glykol og CO2. Ikke mulig						
4	For lav strømning/Less flow	Glykolpumper kan kjøres med lav massestrøm	Riggen fungerer ustabil. Får ikke stabile driftsforhold. Ingen fare	Sjekkliste inneholder info om innstillinger for å oppnå stabile driftsforhold.	A1	A1	A1	A1
5	Høyere nivå/More level	I glykol krets og CO2 krets kan få for høyt nivå av væske.	Glykol: spruter ut av kretsen ( er ikke en lukket krets) CO2: Tilfører for mye væske til kompressorer. De kan i verste fall ødelegges	Erfaren riggoperatør regulerer væsknivået i kretsene, for begge kretsene. Utføres kun av utstyrsansvarlig.	A2	B2	A2	A2
6	Lavere nivå/Less level	Glykol og CO2 krets kan ha for lavt nivå	Riggen fungerer ustabil. Får ikke stabile driftsforhold. Ingen fare		A1	A1	A1	A1
7	Høyere trykk/More pressure	Romstemperaturer over 32grader kan gi forhøyet trykk på CO2-kretsen og i flasken.	Trykkoppygging i kretsen helt til sikkerhetsventil utløses. Dette kan skje bare når riggen ikke er i bruk	Følge med på værvarsel og romtemperatur og ha kjølevannet på for riggen. Da vil ikke temperaturen stige. Vernebriller	A2	A2	A2	A2
8	Høyere trykk/More pressure	Forhøyet trykk på glykol-krets. Stenger ventiler mens pumpa er på	Trykkoppygging i krets	Sikkerhetsventiler og sjekkliste som beskriver at avstengingsventil skal være åpne	A1	A1	A1	A1
9	Lavere trykk/Less pressure	For lav trykk i CO2-kretsen. For liten mengde CO2 i systemet.	Ustabil drift; redusert kjøletelse.	Se-glass i medium- og lavtrykkbeholdere for visuell overvåking av væsknivå	A1	A1	A1	A1



KB

NTNU	Kartlegging av risikofylt aktivitet	Utarbeidet av	Nummer	Dato
		HMS-avd.	HMSRV2601	22.03.2011
HMS		Godkjent av Rektor		Erstatter 01.12.2006



10	Høyere temperatur/More temperature	Forhøyet temperatur i CO2-krets på kompressorutløp; forhøyet temperatur i glykolkretsen	Nedbryting av smøreolje i kompressoren og kompressorhavari; smelting av pakningspasta i glykolkretsen	Termisk bryter (termistor montert på elektrisk motoren til kompressoren); sjekklister som inneholder info om nødvendighet av isvannsirkulasjon og glykolsirkulasjon	B2	B2	A1	A2
11	Lavere temperatur/Less temperature	For lav temperatur i CO2 kretsen pga. for lav sugetrykk	tørrisdannelse i CO2-kretsen	Regulator slår av kompressor. Lavtrykkpresostat slår av kompressor.	A2	A2	A2	A2
12	Høyere viskositet/More viscosity	For høy viskositet til glykol (se: for lave temperaturer i CO2-kretsen)	Lav massestrøm i glykolkretsen	Regulator slår av kompressor. Lavtrykkpresostat slår av kompressor.	A2	A2	A2	A2
13	Lavere viskositet/Less viscosity	gjelder ikke	gjelder ikke	gjelder ikke	A1	A1	A1	A1
14	Endring i sammensetning/Composition Change	Oljenedbryting pga. for høy oljetemperatur	Kompressorhavari pga. friksjon	Termisk bryter (termistor montert på elektrisk motoren til kompressoren); sjekklister som inneholder info om nødvendighet av isvannsirkulasjon og glykolsirkulasjon	A2	A2	A2	A2
15	Forurensning/Contamination	Fuktighet i CO2-kretsen	dannelse av iskrystaller i CO2-kretsen	Filter-avfukter montert i CO2-kretsen	B2	B2	B2	B2

12/15

NTNU	<b>Kartlegging av risikofylt aktivitet</b>	Utarbeidet av	Nummer	Dato	
		HMS-avd.	HMSRV2601	22.03.2011	
HMS		Godkjent av		Erstatter	
		Rektor		01.12.2006	

16	Lekkasje/ leakage	CO2-lekasje; glykol-lekasje	tap av CO2 sammen med olje; tap av glykol	Begrenset antal skrutilkoblinger; hyppige testprøver og inspeksjoner av rør.	A3	A3	A3	A3
17	Instrumentering/Instrumentation	feilt signal; strømbrudd	Feilregulering; tap av registrert data;	Hyppige dataanalyser av måleutstyret for datakvalitet	A3	A3	A3	A3
18	Prøvetaking/Sampling	gjelder ikke	gjelder ikke	gjelder ikke	A1	A1	A1	A1
19	Korrosjon/Corrosion	korrosjon av rørmateriale	lekkasje/tap av glykol/CO2	rørmaterialer som ikke korroderer (rustfritt stål, plasmaterialer)	B2	B2	B2	B2
20	Erosjon/erosion	gjelder ikke	gjelder ikke	gjelder ikke	A1	A1	A1	A1
21	Driftsavvik/Abnormal operation	gjelder ikke	gjelder ikke	gjelder ikke	A1	A1	A1	A1
22	Vedlikehold/Maintenance	Vedlikehold ikke gjennomført	riggen klarer ikke å oppnå normale driftsforhold	Hyppige kontroller og vedlikehold aktiviteter	A1	A1	A1	A1
23	Antennelse/Ignition	CO2 er ikke brannbart; glykol tenes kun i høgere konsentrasjoner ved bruk av flamme	gjelder ikke	gjelder ikke	A1	A1	A1	A1
24	Reservedeler/Spare equipment	Havari av komponenter	rigg i ustand	kommunikasjon med riggleverandøren	A3	A3	A3	A3

ker

NTNU  HMS	Kartlegging av risikofylt aktivitet	Utarbeidet av	Nummer	Dato	
		HMS-avd.	HMSRV2601	22.03.2011	
		Godkjent av Rektor		Erstatter 01.12.2006	

25	Svikt i kritisk infrastruktur (strøm, vann, kjøling, ventilasjon)/ Failure of critical infrastructure	Ved svikt i isvanntilførsel når riggen er i drift stiger høytrykk (se 'høyere trykk')	Trykkoppbygging i kretsen helt til sikkerhetsventil utløses. Dette kan skje bare når riggen ikke er i bruk	Vernebriller	B2	B2	B2	B2
26	Sikkerhet/Safety	diverse ulykker	helseskader	ryddig arbeidsplass	B1	B1	B1	B1

CS

NTNU	Kartlegging av risikofylt aktivitet	Utarbeidet av	Nummer	Dato
		HMS-avd.	HMSRV2601	22.03.2011
HMS		Godkjent av		Erstatter
		Rektor		01.12.2006

### Sannsynlighet vurderes etter følgende kriterier:

Svært liten 1	Liten 2	Middels 3	Stor 4	Svært stor 5
1 gang pr 50 år eller sjeldnere	1 gang pr 10 år eller sjeldnere	1 gang pr år eller sjeldnere	1 gang pr måned eller sjeldnere	Skjer ukentlig

### Konsekvens vurderes etter følgende kriterier:

Gradering	Menneske	Ytre miljø Vann, jord og luft	Øk/materiell	Omdømme
<b>E</b> Svært Alvorlig	Død	Svært langvarig og ikke reversibel skade	Drifts- eller aktivitetsstans >1 år.	Troverdighet og respekt betydelig og varig svekket
<b>D</b> Alvorlig	Alvorlig personskade. Mulig uførhet.	Langvarig skade. Lang restitusjonstid	Driftsstans > ½ år Aktivitetsstans i opp til 1 år	Troverdighet og respekt betydelig svekket
<b>C</b> Moderat	Alvorlig personskade.	Mindre skade og lang restitusjonstid	Drifts- eller aktivitetsstans < 1 mnd	Troverdighet og respekt svekket
<b>B</b> Liten	Skade som krever medisinsk behandling	Mindre skade og kort restitusjonstid	Drifts- eller aktivitetsstans < 1uke	Negativ påvirkning på troverdighet og respekt
<b>A</b> Svært liten	Skade som krever førstehjelp	Ubetydelig skade og kort restitusjonstid	Drifts- eller aktivitetsstans < 1dag	Liten påvirkning på troverdighet og respekt

### Risikoverdi = Sannsynlighet x Konsekvens

Beregn risikoverdi for Menneske. Enheten vurderer selv om de i tillegg vil beregne risikoverdi for Ytre miljø, Økonomi/materiell og Omdømme. I så fall beregnes disse hver for seg.

### Til kolonnen "Kommentarer/status, forslag til forebyggende og korrigerende tiltak":

Tiltak kan påvirke både sannsynlighet og konsekvens. Prioriter tiltak som kan forhindre at hendelsen inntreffer, dvs. sannsynlighetsreducerende tiltak foran skjerpet beredskap, dvs. konsekvensreducerende tiltak.

KS



NTNU	Kartlegging av risikofylt aktivitet	Utarbeidet av	Nummer	Dato	
		HMS-avd.	HMSRV2601	22.03.2011	
HMS		Godkjent av		Erstatter	
		Rektor		01.12.2006	

## MATRISSE FOR RISIKOVURDERINGER ved NTNU

KONSEKVENNS	Svært alvorlig	E1	E2	E3	E4	E5
	Alvorlig	D1	D2	D3	D4	D5
	Moderat	C1	C2	C3	C4	C5
	Liten	B1	B2	B3	B4	B5
	Svært liten	A1	A2	A3	A4	A5
	Svært liten	Liten	Middels	Stor	Svært stor	
	SANNSYNLIGHET					

Prinsipp over akseptkriterium. Forklaring av fargene som er brukt i risikomatriksen.

Farge	Beskrivelse
Rød	Uakseptabel risiko. Tiltak skal gjennomføres for å redusere risikoen.
Gul	Vurderingsområde. Tiltak skal vurderes.
Grønn	Akseptabel risiko. Tiltak kan vurderes ut fra andre hensyn.

KB

---

# Appendix C

## Ejector performance

**Table C1:** Overview of the results of the experimental tests 1 to 35 for the advanced multi-ejector with the uncertainty for the standard deviation (type A) and the uncertainty from the equipment (type B). The table are 3 pages long.

Test	P <sub>in</sub>	T <sub>in</sub>	P <sub>sn</sub>	T <sub>sn</sub>	P <sub>out</sub>	m <sub>in</sub>	m <sub>sn</sub>	η <sub>e</sub>	P <sub>in</sub>	Φ <sub>ER</sub>	SH	
	[bar]	[°C]	[bar]	[°C]	[bar]	[kg/h]	[kg/h]	[-]	[bar]	[-]	[%]	
	Type A	Type B	Type A	Type B	Type A	Type B	Type A	Type B	Type A	Type B	Type A	Type B
1	60.87	19.54	26.11	-5.37	28.28	785.01	244.39	0.14	2.17	0.3114	5.14	
	0.05	0.46	0.02	0.11	0.01	0.46	47.39	0.94	14.75	0.29	0.01	0.01
2	62.94	20.71	25.82	-4.29	28.03	776.87	263.13	0.14	2.21	0.3388	6.61	
	0.03	0.46	0.01	0.11	0.01	0.46	48.66	0.93	16.48	0.32	0.01	0.02
3	63.86	21.03	25.64	-0.94	27.81	783.84	265.16	0.14	2.17	0.3383	10.19	
	0.03	0.46	0.02	0.11	0.01	0.46	39.37	0.94	13.31	0.32	0.01	0.02
4	59.26	18.40	25.48	10.75	28.03	802.20	199.91	0.16	2.55	0.2492	22.10	
	0.04	0.46	0.01	0.11	0.00	0.46	41.39	0.96	10.32	0.24	0.01	0.01
5	59.79	18.96	25.38	5.49	28.05	786.93	198.73	0.16	2.67	0.2526	16.99	
	0.03	0.46	0.03	0.11	0.01	0.46	41.68	0.94	10.52	0.24	0.01	0.02
6	60.93	19.76	25.74	-0.04	28.66	770.52	194.07	0.16	2.92	0.2519	10.97	
	0.02	0.46	0.02	0.11	0.01	0.46	46.51	0.92	11.71	0.23	0.01	0.02
7	62.26	20.85	25.92	0.16	28.82	741.09	210.19	0.17	2.90	0.2837	10.92	
	0.03	0.46	0.02	0.11	0.00	0.46	44.74	0.89	12.69	0.25	0.01	0.02
8	69.24	26.17	27.28	-7.01	29.92	620.78	328.58	0.19	2.64	0.5295	1.95	
	0.06	0.46	0.01	0.12	0.04	0.46	32.06	0.74	16.95	0.39	0.02	0.03
9	70.81	25.96	28.25	-5.75	30.88	694.53	342.89	0.18	2.62	0.4939	1.96	
	0.05	0.46	0.01	0.12	0.02	0.46	32.93	0.83	16.23	0.41	0.01	0.02
10	68.38	25.51	25.21	5.60	28.51	625.37	255.74	0.22	3.30	0.4091	17.33	
	0.03	0.46	0.01	0.12	0.00	0.46	29.63	0.75	12.11	0.31	0.01	0.03
11	68.80	25.50	25.71	6.54	29.39	641.53	233.73	0.22	3.68	0.3644	17.58	
	0.02	0.46	0.02	0.12	0.00	0.46	30.39	0.77	11.06	0.28	0.02	0.03
12	69.44	26.03	25.68	5.29	29.45	626.80	233.41	0.23	3.77	0.3725	16.38	
	0.04	0.46	0.01	0.12	0.00	0.46	29.69	0.75	11.05	0.28	0.02	0.03

Test	P <sub>MN</sub>		t <sub>MN</sub>		P <sub>SN</sub>		t <sub>SN</sub>		P <sub>out</sub>		t <sub>MN</sub>		t <sub>SN</sub>		T <sub>el</sub>		P <sub>lit</sub>		Φ <sub>ER</sub>		SH	
	Type A	Type B	Type A	Type B	Type A	Type B	Type A	Type B	Type A	Type B	Type A	Type B	Type A	Type B	Type A	Type B	Type A	Type B	Type A	Type B	Type A	Type B
13	69.96		26.25		25.54		10.17		28.95		629.71		257.93		0.23		3.41		0.4097		21.44	
	0.05	0.46	0.04	0.12	0.01	0.46	0.01	0.10	0.01	0.46	38.01	0.76	15.57	0.31	0.02	0.03	0.01	0.65	0.0350	0.0007	0.01	0.38
14	70.12		26.50		25.16		8.57		29.15		618.64		217.68		0.23		3.98		0.3519		20.36	
	0.03	0.46	0.01	0.12	0.01	0.46	0.01	0.10	0.01	0.46	31.07	0.74	10.93	0.26	0.02	0.03	0.01	0.65	0.0250	0.0006	0.01	0.38
15	70.70		26.68		25.93		8.17		29.74		628.14		239.42		0.23		3.82		0.3812		18.92	
	0.07	0.46	0.03	0.12	0.01	0.46	0.01	0.10	0.01	0.46	30.66	0.75	11.68	0.29	0.02	0.03	0.02	0.65	0.0263	0.0006	0.01	0.37
16	68.35		25.52		25.21		5.64		28.50		656.83		261.64		0.22		3.30		0.3984		17.36	
	0.03	0.46	0.01	0.12	0.00	0.46	0.01	0.09	0.01	0.46	39.64	0.79	15.79	0.31	0.02	0.03	0.01	0.65	0.0340	0.0007	0.01	0.38
17	81.28		34.28		26.45		-5.69		31.48		610.80		263.92		0.20		5.02		0.4322		4.36	
	0.02	0.46	0.00	0.13	0.02	0.46	0.03	0.09	0.04	0.46	28.92	0.73	12.53	0.32	0.01	0.03	0.04	0.65	0.0290	0.0007	0.03	0.37
18	81.14		33.84		26.74		-5.34		31.67		621.85		267.75		0.20		4.93		0.4306		4.32	
	0.02	0.46	0.01	0.13	0.01	0.46	0.01	0.09	0.01	0.46	29.44	0.75	12.67	0.32	0.01	0.03	0.01	0.65	0.0288	0.0007	0.01	0.36
19	81.18		34.23		26.22		-5.66		31.11		610.68		273.54		0.20		4.88		0.4479		4.69	
	0.02	0.46	0.01	0.13	0.01	0.46	0.01	0.09	0.01	0.46	30.67	0.73	13.74	0.33	0.01	0.03	0.02	0.65	0.0318	0.0008	0.02	0.37
20	81.74		34.34		26.74		-5.62		31.90		618.67		255.19		0.19		5.16		0.4125		4.04	
	0.05	0.46	0.01	0.13	0.02	0.46	0.02	0.09	0.02	0.46	29.29	0.74	12.08	0.31	0.01	0.03	0.02	0.65	0.0276	0.0007	0.03	0.36
21	80.83		34.09		27.28		-4.93		33.89		606.44		93.59		0.10		6.61		0.1543		4.03	
	0.02	0.46	0.01	0.13	0.00	0.46	0.00	0.09	0.00	0.46	37.29	0.73	5.76	0.11	0.01	0.02	0.01	0.65	0.0134	0.0003	0.01	0.36
22	81.17		34.02		26.32		7.66		32.66		612.38		129.81		0.14		6.34		0.2120		17.88	
	0.02	0.46	0.02	0.13	0.01	0.46	0.01	0.10	0.01	0.46	28.99	0.73	6.15	0.16	0.01	0.02	0.02	0.65	0.0142	0.0004	0.02	0.37
23	81.41		34.66		26.20		7.91		32.54		595.88		136.61		0.14		6.34		0.2293		18.28	
	0.02	0.46	0.04	0.13	0.02	0.46	0.02	0.10	0.02	0.46	28.23	0.72	6.47	0.16	0.01	0.03	0.03	0.65	0.0154	0.0004	0.03	0.37
24	81.75		34.39		27.04		5.74		33.68		612.09		101.23		0.11		6.64		0.1654		15.01	
	0.02	0.46	0.01	0.13	0.01	0.46	0.02	0.09	0.01	0.46	37.64	0.73	6.24	0.12	0.01	0.02	0.02	0.65	0.0144	0.0003	0.02	0.36

Test	PMN		tMN		PSN		tSN		Pout		tMN		tMN		T <sub>el</sub>		P <sub>lit</sub>		Φ <sub>ER</sub>		SH	
	Type A	Type B	Type A	Type B	Type A	Type B	Type A	Type B	Type A	Type B	Type A	Type B	Type A	Type B	Type A	Type B	Type A	Type B	Type A	Type B	Type A	Type B
25	82.14	34.44	27.17	-4.29	33.99	621.87	85.78	0.09	6.82	0.1379	4.81											
	0.05	0.46	0.01	0.13	0.01	0.46	0.02	0.09	0.01	0.46	0.08	0.10	0.01	0.01	0.02	0.65	0.00092	0.0002	0.02	0.36		
26	82.21	34.39	26.67	9.48	32.75	622.50	167.79	0.17	6.08	0.2695	19.23											
	0.03	0.46	0.01	0.13	0.01	0.46	0.01	0.10	0.01	0.46	8.43	0.20	0.01	0.03	0.01	0.65	0.0192	0.0005	0.01	0.37		
27	82.63	34.90	27.21	-5.32	33.92	618.28	107.33	0.11	6.71	0.1736	3.73											
	0.05	0.46	0.01	0.13	0.02	0.46	0.02	0.09	0.02	0.46	23.15	0.74	4.03	0.13	0.01	0.02	0.03	0.65	0.00092	0.0003	0.03	0.36
28	82.80	34.44	26.39	-5.71	32.39	636.57	185.31	0.17	6.00	0.2911	4.42											
	0.02	0.46	0.01	0.13	0.01	0.46	0.01	0.09	0.01	0.46	31.96	0.76	9.31	0.22	0.01	0.02	0.01	0.65	0.0207	0.0005	0.01	0.37
29	83.11	34.62	26.18	7.60	32.96	632.27	107.55	0.12	6.77	0.1701	18.00											
	0.06	0.46	0.03	0.13	0.03	0.46	0.03	0.10	0.03	0.46	30.86	0.76	5.29	0.13	0.01	0.02	0.04	0.65	0.0118	0.0003	0.04	0.37
30	83.32	35.02	26.30	7.63	33.02	624.21	116.91	0.13	6.72	0.1874	17.87											
	0.01	0.46	0.02	0.13	0.01	0.46	0.02	0.10	0.01	0.46	30.47	0.75	5.72	0.14	0.01	0.02	0.02	0.65	0.0129	0.0003	0.02	0.37
31	82.69	34.44	27.83	0.31	34.90	634.28	57.95	0.07	7.07	0.0913	8.56											
	0.01	0.46	0.01	0.13	0.01	0.46	0.01	0.09	0.01	0.46	28.09	0.76	2.59	0.07	0.00	0.01	0.01	0.65	0.0057	0.0002	0.02	0.35
32	88.04	34.67	27.10	-4.27	35.15	758.40	45.26	0.05	8.05	0.0595	4.92											
	0.04	0.46	0.02	0.13	0.01	0.46	0.02	0.09	0.01	0.46	23.82	0.91	1.63	0.05	0.00	0.01	0.02	0.65	0.0029	0.0001	0.02	0.36
33	88.94	34.29	27.60	-3.79	35.53	799.08	73.42	0.08	7.93	0.0918	4.76											
	0.02	0.46	0.02	0.13	0.03	0.46	0.04	0.09	0.02	0.46	40.13	0.96	3.82	0.09	0.01	0.01	0.04	0.65	0.0066	0.0002	0.05	0.35
34	90.04	35.21	27.14	2.46	35.29	787.86	63.61	0.07	8.15	0.0806	11.61											
	0.07	0.46	0.06	0.13	0.02	0.46	0.02	0.09	0.03	0.46	37.32	0.95	3.14	0.08	0.01	0.01	0.03	0.65	0.0055	0.0001	0.02	0.36
35	90.30	34.96	27.04	-1.92	35.20	807.00	68.44	0.07	8.16	0.0847	7.35											
	0.02	0.46	0.02	0.13	0.02	0.46	0.02	0.09	0.02	0.46	40.54	0.97	3.53	0.08	0.01	0.01	0.03	0.65	0.0061	0.0001	0.03	0.36

